Journal of Science & Technology in the Tropics

Volume 6 Number 1 June 2010

JOSTT

DEDICATED TO THE ADVANCEMENT OF SCIENCE AND TECHNOLOGY RELATED TO THE TROPICS

Journal of Science & Technology in the Tropics

Volume 6 Number 1
June 2010
ISSN 1823-5034

Journal of Science & Technology in the Tropics Volume 6 Number 1 Jun 2010

CONTENTS

Journal of Science and Technology in the Tropics (2010) **6**: 11-16

Effect of colchicine on tissue culture derived plants of *Zingiber officinale* Rosc. and *Zingiber officinale* var. *rubrum* Theilade

Lindayani[1], K. Norzulaani[2], H. Ibrahim[2] and Noorsaadah Abd Rahman[3]
[1]Department of Food Technology, Faculty of Agricultural Technology, Soegijapranata Catholic University, Pawiyatan Luhur IV/1 Bendan Duwur, Semarang 50234, Indonesia
[2]Institute of Biological Sciences, [3]Department of Chemistry, Faculty of Science, University of Malaya, Lembah Pantai, 50603 Kuala Lumpur, Malaysia
(Email: lindayani@unika.ac.id)

Received 04-01-2010; accepted 01-02-2010

Abstract The aim of this study was to assess the effect of colchicine on the morphology and histology of gingers in view of polyploidisation. Rhizomes of ginger were treated separately with three concentrations of colchicine (0.5%, 1.0% and 2.0% w/v) for 30, 60 and 120 minutes. For morphology study, the fresh weight of rhizome (FWRH), length of root (RLEN) and plant height (PH) were measured. Histological analysis was done on shoot buds and rhizomes. All the parameters tested gave significant result. An increasing trend was observed with colchicine concentration up to 1.0%, but decreased at 2.0%. Histological analysis showed that the cell size of the shoot tip of *Zingiber officinale* Rosc. treated with colchicine (2.0%) for 120 minutes was 1.5 times larger than the control. For *Zingiber officinale* var. *rubrum* Theilade, the cell size was similar for treated and control shoot tips. Over all this study showed that polyploidisation might occur with colchicine treatment of various concentration and incubation time.

Keywords plant morphology – histology – polyploidisation – ginger

INTRODUCTION

Ginger, *Zingiber officinale* Rosc (Zingiberaceae), has been used as a spice both in the East as well as in the West since time immemorial [1]. In Peninsular Malaysia there are at least three local races, namely *halia betul* (true ginger), *halia bara* (red ginger) or alternatively *halia padi*, and *halia udang* [2]. Both *halia bara* and *halia padi* are distinguished from *halia betul* from their small rhizomes. *Halia udang* is probably extinct but *halia bara* differs slightly from *halia padi* by its externally red rhizome. *Halia bara* and *halia padi* are more pungent than the normal ginger and are mainly used in traditional medicine [2,3]. Pharmacological studies have shown that ginger rhizomes are effective for the recovery of intestinal disorder [4] and salivary secretion [5], for stimulating the vasomotor and respiratory centres, and for lowering serum and hepatic cholesterol levels [6,7].

Apart from the normal mitotic processes, polyploidy can be induced by treatment with colchicine [8-10]. The *in vitro* induction of polyploids with colchicine has been reported in many plant species [11-15]. The increase in the ploidy level could occur relatively easily and may lead to an overall enlargement of plant organs, for example cells, stomata, leaves, flowers, fruits and seeds [8].

Tetraploid gingers (*Z. officinale*) strains "4x Kintoki", "4x Sanshu" and "4x Phillippine Cebu 1" have been produced by soaking shoot tip explants in a colchicine solution (0.2%, w/v). The induced tetraploid gingers were much bigger in plant and rhizome size than the diploids [14]. In addition, the tetraploid ginger had higher pollen fertility and germination rates than the diploids. However, seed settings in the tetraploid ginger have not yet been reported [16].

Colchicine prevents spindle formation at prophase, precludes a nuclear mitosis, delays chromosomal separation, inhibits daughter nuclei, and effectively blocks the cleavage processes. Hence, when root tips

or other growing plant parts were placed in appropriate concentration of colchicine, the chromosomes of the treated cells duplicated without spindle formation and the cytoplasmic phase of cell division would not occur [17].

In general, colchicine is used as an antimitotic agent in plants. It influences the duplication of the number of chromosome. The effect of colchicine could be determined through the plant morphology. The present study was carried out to examine the effect of colchicine on the morphology and histology on tissue culture derived ginger plants *Zingiber officinale* and *Zingiber officinale* var. *rubrum*.

MATERIALS AND METHODS

Plant Material

The rhizomes of *Z. officinale* and *Z. officinale* var. *rubrum* used in this study were obtained from the local wet market. The specimens were authenticated by Halijah Ibrahim from the Institute of Biological Sciences, University of Malaya.

Application of colchicine

Colchicine solutions were cooled after autoclaving and were freshly prepared before use. Fourteen to sixteen shoot bud pieces were used for each treatment combination (Table 1). These buds were soaked in sterile distilled water (control), 0.5% (w/v), 1.0% (w/v) or 2.0% (w/v) aqueous colchicine solution in a 250-mL Erlenmeyer flask placed on an orbital shaker (90 rpm) at 24±2°C. The shoot buds were incubated according to the selected time (Table 1). Following that, each bud was dried on sterile filter paper and subsequently placed in MS semisolid initiation media under a 16 hours photoperiod at 3500 lx using white fluorescent tubes. The temperature was maintained at 24±2°C in the growth room. After about five months (5th subculture), the surviving colchicine-treated plantlets were transferred to sterile vermiculite placed in plastic polybags (3″ x 6″) and kept in a growth room under a 16:8-h light:dark photoperiod at 24±2°C for 4 months before transferring to the nursery.

Table 1. Combinations of treatment with colchicines concentration (C) and incubation time (T) used for *in vitro* derived shoot buds of ginger.

Concentration of Colchicines (%)	Incubation time (minutes)	Number of Shoot bud
CO (0.0)	TO (0)	16
	T1 (30)	16
	T2 (60)	16
	T3 (120)	16
C1 (0.5)	T0 (0)	14
	T1 (30)	14
	T2 (60)	14
	T3 (120)	14
C2 (1.0)	T0 (0)	14
	T1 (30)	14
	T2 (60)	14
	T3 (120)	14
C3 (2.0)	T0 (0)	14
	T1 (30)	14
	T2 (60)	14
	T3 (120)	14

Growth maintenance of colchicine treated plants

After the plantlets had rooted and reached 3-5 cm in height with well expanded leaves, they were transplanted into pots filled with soil mix consisting of sand:peat:top soil (3:2:1), vermiculite and fertilizer (N:P:K at the ratio of 15:15:15) after washing off the agar with tap water. To avoid fungal infection, the soil mix in the pot was drained with 1% (w/v) Thiram® over night before planting. For pest control, plants were sprayed with 1.0 mL of Plusbon 250® diluted with 5 L water. Plants were irrigated daily and 1.0 g of foliar fertilizer (Agrospray 63®) diluted in 5 L tap water was sprayed monthly for supplement.

Measurement of plant morphology

The plants were monitored every month. They were maintained in the nursery for one year before harvesting and analysis. For each treatment, fresh weight of rhizome (FWRH) and plant height (PH) were measured. Length of the root (RLEN) was measured randomly by using Image-Pro® Express Version 4.5 (Media Cybernetics).

Histological analysis

The shoot buds were fixed in FAA (formalin, acetic acid glacial, ethyl alcohol: 5:5:90), then progressively dehydrated in ethanol series, and finally infiltrated in paraffin. Longitudinal sections (10-20 µm thick) of paraffin-embedded materials were obtained using a

rotary microtome. The sections were stained with a mixture of 1% (v/v) safranine and 1% (v/v) fast green and mounted with Canada Balsam [18]. Size of cells was measured using a micrometer eyepiece where 0.01 mm equals to 5 mm (under x100 and x400 magnification). This work was done at the laboratory of plant histology, Biological Faculty, University of Gadjah Mada, Yogyakarta, Indonesia.

Statistical analysis

Analysis of variance (ANOVA), performed with the program SAS (SAS® proprietary software Release 6.02), of factorial design was used to test the effect of the concentrations of colchicine and incubation times. Duncan Multiple Range Test (DMRT) at $p<0.05$ was used to test for differences between the control and each of the treatment [19].

RESULTS AND DISCUSSION

Morphology of *ex vitro* derived treated plants during Hardening

In the nursery, plants that were unaffected by the treatments survived and grew vigorously as the control plants. No abnormal plants were found during hardening (Fig. 1). However, a few plants failed to survive in some concentrations of colchicine.

Treatment with increasing colchicine concentration produced decreasing measurement of the fresh weight of rhizome, plant height and root length (Table 2). For incubation time, T1 (30 minutes) produced higher measurement values compared to control ($p<0.05$). It can be concluded that T1 is the best incubation time for this experiment.

Based on the results (Table 3), the fresh weight of rhizome (FWRH) for *Zingiber officinale* did not show overlapping values from each concentration of colchicine and incubation time. The measurement values were higher at colchicine concentration of 2.0% (C3) and incubation time 60 minutes (T2), compared to colchicine concentration of 0.5% (C1) and incubation time 30 minutes (T1). For *Zingiber officinale* var. *rubrum* the rhizome weight was heavier at colchicine 1.0% (C2) and incubation time 30 minutes (T1) than colchicine 0.5% (C1) and 30 minutes incubation (T1) (Fig. 2).

Table 2. Fresh weight (g) of rhizome (FWRH), plant height (PH, cm) and length of root (RLEN, cm) of ginger after transferring to the nursery. Different alphabets show significant differences ($p<0.05$), based on Duncan's Multiple Range Test (DMRT). C, concentration of colchicine; T, incubation time.

Parameter	Treatment							
	C0	C1	C2	C3	T0	T1	T2	T3
FWRH	64.90a	42.36b	28.39c	23.52d	50.79b	55.24a	21.41d	31.72c
PH	35.67a	26.46b	14.30c	9.87d	24.46b	31.03a	9.82d	20.99c
RLEN	18.38a	13.60b	7.85c	3.75d	13.58b	15.91a	4.85d	9.23c

Figure 1. Vigorous growth of treated plants (C1T1) – *Zingiber officinale* (left) and *Zingiber officinale* var. *rubrum* (right) – after transferring to the nursery.

Plant height measured for *Z. officinale* (V1) showed the highest reading (48.24 cm) for treatment C1T1 compared to the other treatments. C1T1 treatment for *Z. officinale* var. *rubrum* (V2) exhibited similar result for the control (43.38 cm) and treated group (43.16 cm) (Table 3.). Roots for *Z. officinale* (V1) were shorter compared to *Z. officinale* var. *rubrum* (V2). The best result for *Z. officinale* was produced by treatment C1T1 while for *Z. officinale* var. *rubrum* the longest root measurement was obtained when the shoot bud was briefly dipped in treatment C1T0.

To date, there are no reports on the morphology of *ex vitro* colchicine treated plants as described at this study. Based on this study, an increasing trend for fresh

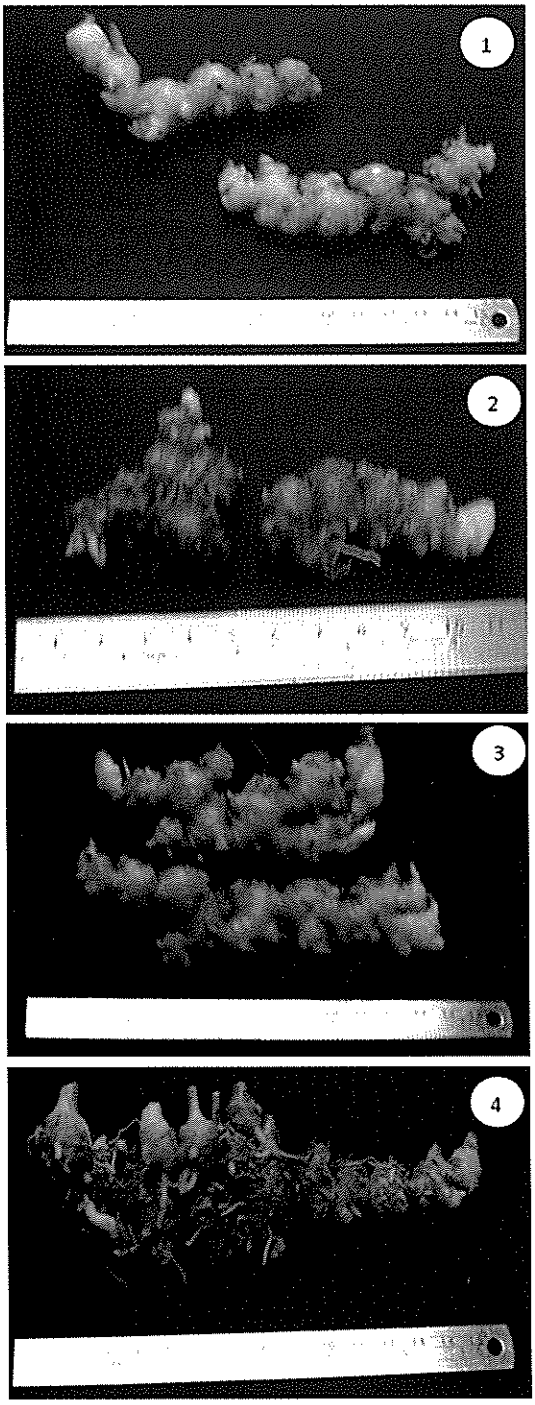

Figure 2. Rhizome of *Zingiber officinale*, V1, C0T0 (1) and *Zingiber officinale* var. *rubrum*, V2, C0T0 (2) obtained from control; and rhizome of *Zingiber officinale*, V1, C3T2 (3) and *Zingiber officinale* var. *rubrum*, V2, C1T1 (4) after treatment. C0T0 = Control; C3T2 = colchicine conc. 2%, incubation time 60 min; C1T1 = Colchicine conc. 0.5%, incubation time 30 min.

Table 3. Fresh weight of rhizome (FWRH, g), PH, plant height (PH, cm) and root length (RLEN, cm) from combination of variety, concentration of colchicine and incubation time after transferring to the nursery. V, Variety (V1, *Zingiber officinale*; V2, *Zingiber officinale.* var. *rubrum*); C, concentration of colchicine; T, incubation time. Different alphabets show significant differences ($p<0.05$), based on Duncan's Multiple Range Test (DMRT).

No.	Combination of variety, concentration of colchicine and incubation time	DMRT grouping		
		FWRH	PH	RLEN
1	V1C0T0	141.47a	45.46b	15.45k
2	V1C0T1	81.73f	42.89cd	22.46f
3	V1C0T2	0.00p	0.00k	0.00n
4	V1C0T3	87.05e	41.26ef	19.22hi
5	V1C1T0	80.96f	42.50cd	14.84lm
6	V1C1T1	49.47m	48.24a	19.56h
7	V1C1T2	0.00p	0.00k	0.00n
8	V1C1T3	61.68j	42.07de	19.25hi
9	V1C2T0	0.00p	0.00k	0.00n
10	V1C2T1	58.97k	36.35i	17.35j
11	V1C2T2	0.00p	0.00k	0.00n
12	V1C2T3	0.00p	0.00k	0.00n
13	V1C3T0	0.00p	0.00k	0.00n
14	V1C3T1	0.00p	0.00k	0.00n
15	V1C3T2	120.13b	37.72h	15.28kl
16	V1C3T3	68.05i	41.21ef	14.74m
17	V2C0T0	30.97o	32.73j	22.54f
18	V2C0T1	89.79d	38.80g	23.14e
19	V2C0T2	51.18l	40.85f	23.59d
20	V2C0T3	37.01n	43.38c	20.67g
21	V2C1T0	76.50g	35.72i	29.32a
22	V2C1T1	70.25h	43.16c	25.81c
23	V2C1T2	0.00p	0.00k	0.00n
24	V2C1T3	0.00p	0.00k	0.00n
25	V2C2T0	76.43g	39.25g	26.47b
26	V2C2T1	91.71c	38.78g	18.98i
27	V2C2T2	0.00p	0.00k	0.00n
28	V2C2T3	0.00p	0.00k	0.00n
29	V2C3T0	0.00p	0.00k	0.00n
30	V2C3T1	0.00p	0.00k	0.00n
31	V2C3T2	0.00p	0.00k	0.00n
32	V2C3T3	0.00p	0.00k	0.00n

weight of rhizome, plant height and root length was observed with increasing colchicine concentration up to 1.0% but decreased at 2.0%. For incubation time, results were not consistent. Based on morphological characteristics (fresh weight of rhizome, plant height and root length) for treated plants, significant results were found in all the data. When colchicines was used, various organs of tetraploid gingers become huge in appearance i.e. plant height, the size of leaves and rhizomes, compared to diploids [14].

Histological analysis of shoot tips

Preliminary results showed that the cell size of the shoot tip treated with colchicine (2.0%, C3) and incubation time (T3, 120 minutes) was 1.5 times larger than the control (C0) for sample V1 (Fig. 3). For sample V2, the treated and control shoot tips had similar cell size (Fig. 4).

From this preliminary histological analysis, the effects of colchicine concentration were observed for sample V1, but the result obtained did not confirm or prove that polyploidisation was induced by the treatments. Future work on quantitative analysis is needed.

CONCLUSION

The effect of colchicine treatment on *Z. officinale* and *Z. officinale* var. *rubrum* could be observed in the morphology and histology of the treated plants. An increase in the fresh weight of the rhizomes of the treated plants was observed as compared to the control. However, the results from qualitative histological studies were inconclusive.

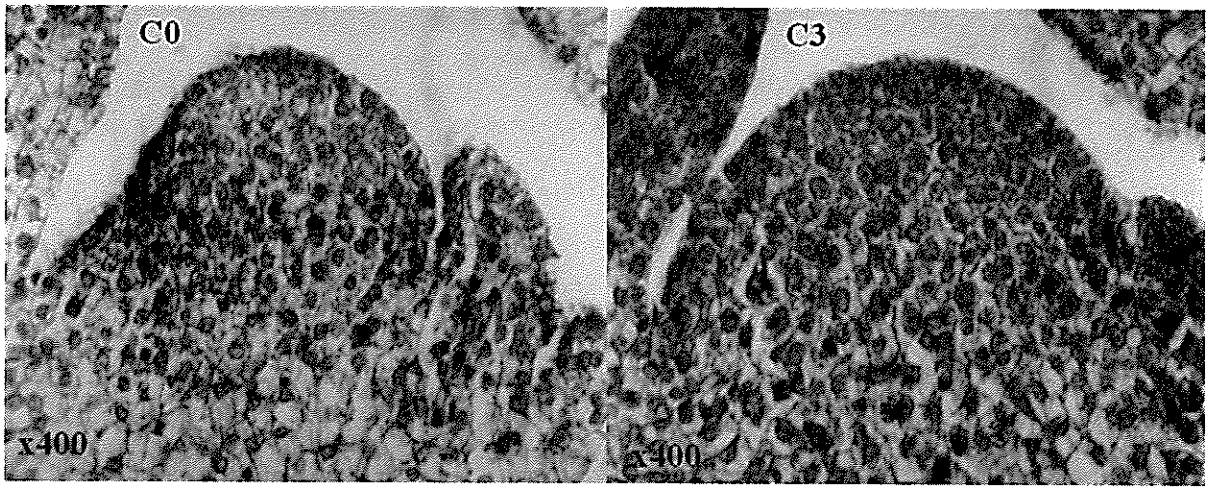

Figure 3. Micrographs of a section of the shoot tips of *Zingiber officinale* (V1). C0 (control) and C3 (treatment with colchicine concentration 2.0% and incubation time 120 minutes).

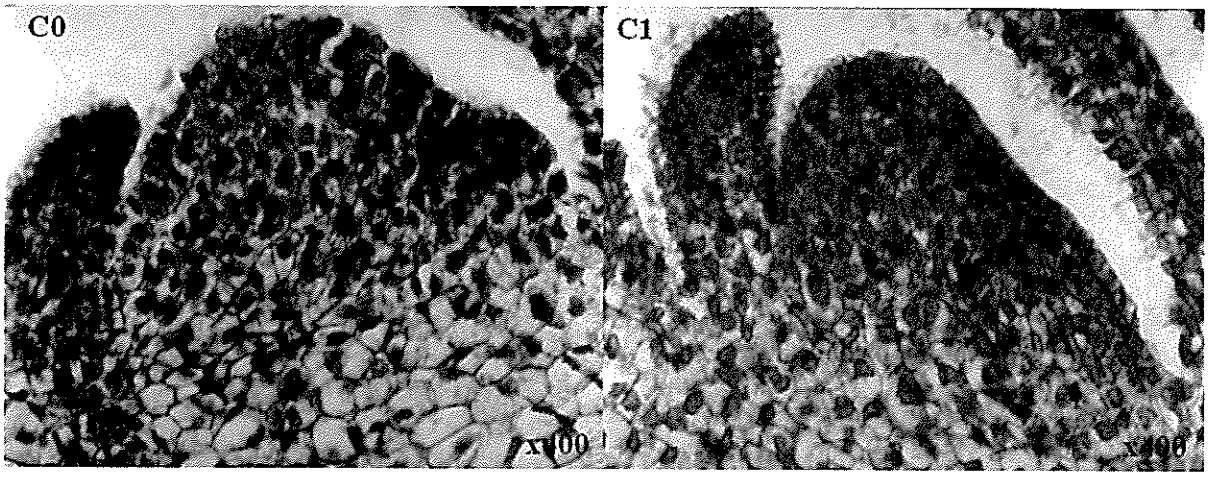

Figure 4. Micrographs of a section of the shoot tips of *Zingiber officinale* var. *rubrum* (V2). C0 (control) and C1 (treatment with colchicine concentration 0.5% and incubation time 30 minutes).

REFERENCES

1. Larsen K., Ibrahim H., Khaw S.H. and Saw L.G. (1999) *Gingers of Peninsular Malaysia and Singapore.* Natural History Publications (Borneo), Kota Kinabalu.
2. Holttum R.E. (1950) The Zingiberaceae of the Malay Peninsular. *The Garden's Bulletin Singapore* **13**: 1-250.
3. Purseglove J.W. (1972) *Zingiberacea.* In Purseglove J.W. (Ed.) *Tropical crops monocotyledons 2* pp. 519-540. Longman Group.
4. Krishnamurthy K. and Sreenivasamurthy V. (1956) Garlic. *Bull. Centr. Food Technol. Res. Inst. Mysore.* **5**, 264-267.
5. Sinha K.P., Sud S.C. and Bahga H.S. (1974) Physiology of digestion in ruminants 3 salivary secretion. Effect of autonomic drugs. *Indian Veterinary Journal* **51**: 15-19.
6. Gujral S., Bhumra H. and Swaroop M. (1978) Effect of ginger (*Zingiber officinale* Roscoe) oleoresin on serum and hepatic cholesterol levels in cholesterol fed rats. *Nutrition Report International* **17**: 183-189.
7. Newall C.A., Anderson L.A. and Phillipson J.D. (1996) *Herbal Medicines A guide for health-care professionals.* The Pharmaceutical Press, London.
8. Van Harten A.M. (1998) *Mutation breeding: theory and practical applications.* Cambridge University Press.
9. Rey H.Y., Sansberro P.A., Collavino M.M., Daviña J.R., Gonzàles A.M. and Mroginski L.A. (2002) Colchicine, trifluralin, and oryzalin promoted development of somatic embryos in *Ilex paraguariensis* (Aquifoliaceae). *Euphytica* **123**: 49-56.
10. Petersen K.K., Hagberg P. and Kristiansen K. (2003) Colchicine and oryzalin mediated chromosome doubling in different genotypes of *Miscanthus sinensis*. *Plant Cell, Tissue and Organ Culture* **173**: 137-146.
11. Gao S.L., Zhu D.N., Cai Z.H. and Xu D.R. (1996) Autotetraploid plants from colchicines-treated bud culture of *Salvia miltiorrhiza* Bge. *Plant Cell, Tissue and Organ Culture* **47**: 73-77.
12. Ma Y., Chen D.H. and Chen J. (1997) Amphidiploid induction from diploid rose interspecific hybrids. *Horticulture Science* **32**: 292-295.
13. Chakraborti S.P., Vijayan K., Roy B.N. and Qadri S.M.H. (1998) In vitro induction of tetraploidy in mulberry (*Morus alba* L.). *Plant Cell Reports* **17**: 799-803.
14. Adaniya S. and Shirai D. (2001) *In vitro* induction of tetraploid ginger (*Zingiber officinale* Roscoe) and its pollen fertility and germinability. *Scientia Horticulturae* **88**: 277-287.
15. Chauvin J.E., SouchetC., Dantec, J.P. and Ellissèche D. (2003) Chromosome doubling of 2x *Solanum* species by oryzalin: method development and comparison with spontaneous chromosome doubling *in vitro*. *Plant Cell, Tissue and Organ Culture* **73**: 65-73.
16. Adaniya S. (2001) Optimal pollination environment of tetraploid ginger (*Zingiber officinale* Roscoe) evaluated by *in vitro* pollen germination and pollen tube growth in styles. *Scientia Horticulturae* **90**: 219-226.
17. Eigsti O.J. and Dustin P. (1957) *Colchicine in agriculture, medicine, biology, and chemistry.* The Iowa State College Press, Ames, Iowa. U.S.A.
18. Johansen D.A. (1940) *Plant microtechnique.* McGraw-Hill, New York.
19. Gomez K.A and Gomez A.A. (1984) *Statistical procedures for agricultural research.* Second Edition. John Wiley & Sons.

Journal of Science and Technology in the Tropics (2010) **6**: 17-21

Diversity and abundance of Dacinae fruit flies (Insecta: Diptera: Tephritidae) in Chini 2, Runchang and Sungai Bebar, Pahang, Peninsular Malaysia

Hoi Sen Yong[1], Y. F. Ng[2] and Phaik Eem Lim[1,3]
[1]Institute of Biological Sciences, University of Malaya, 50603 Kuala Lumpur, Malaysia
(E-mail: yong@um.edu.my)
[2]Centre for Insect Systematics, School of Environmental and Natural Resource Sciences, Faculty of Science and Technology, Universiti Kebangsaan Malaysia, 4300 Bangi, Selangor D.E., Malaysia
[3]Institute of Ocean and Earth Science, University of Malaya, 50603 Kuala Lumpur, Malaysia

ABSTRACT The diversity and abundance of Dacinae fruit flies of the family Tephritidae were studied at seven localities in the Pekan District, Pahang Darul Makmur, in the east coast of Peninsular Malaysia. Male fruit flies were collected in the morning by using the attractants methyl eugenol and cue-lure. Three species (*Bactrocera carambolae*, *Bactrocera papayae* and *Bactrocera umbrosa*) of the methyl eugenol group were recorded. *Bactrocera carambolae* was present in all seven localities, being most abundant in a forest fringe locality near a river but uncommon in the two Sungai Bebar localities. *Bactrocera papayae* was present in four localities with human habitation but absent in the three forest areas. It was most common in the two localities in Chini 2 with village setting. *Bactrocera umbrosa* was found in three localities with typical village setting with fruit trees of *Artocarpus* species. The cue-lure group was present in five of the seven localities studied. Four species were present – *Bactrocera infesta*, *Bactrocera melastomatos*, *Bactrocera nigrotibialis* and *Bactrocera* cf *tau*. *Bactrocera nigrotibialis* was the predominant species while *B. infesta* occurred in quite large number in a river bank locality. The other two species (*B. melastomatos* and *B.* cf *tau*) appeared to be uncommon. *Bactrocera infesta* represented the first documented record for Peninsular Malaysia.

Keywords *Bactrocera* species – *Bactrocera infesta* – methyl eugenol – cue-lure – Pekan District Pahang – new record

INTRODUCTION

Fruit flies of the family Tephritidae are plant feeders. Many members of the subfamily Dacinae are of great economic and agricultural importance because of damage caused to commercial fruits and vegetables. The damage, if uncontrolled, may result in a total loss of the crop. The subfamily is represented by some 800 species worldwide, with some 300 species in Asia/ South-east Asia [1, 2].

Dacinae fruit flies of the genus *Bactrocera* were previously referred to the genus *Dacus* [1]. They may be polyphagous or exhibit great specificity for host fruits [3]. The degree of host specificity appears to be related to the extent of genetic diversity [4]. These fruit flies also show variability in their attraction to male chemical lures [3].

Most of the studies on Dacinae fruit flies concern the species of agricultural importance. The present paper reports the diversity and abundance of Dacinae fruit flies, as determined by application of male chemical lures, in seven localities – urban areas in Chini 2, and settlement and forest areas in Runchang and Sungai Bebar – within the Pekan District of the State of Pahang Darul Makmur, Peninsular Malaysia.

MATERIALS AND METHODS

During a field trip in September 2009, we studied the diversity and abundance of Dacinae fruit flies in seven localities at Chini 2, Runchang and Sungai Bebar. These localities are situated in the Pekan District, Pahang Darul Makmur, in the east coast of

Peninsular Malaysia. Chini 2 is a small town of the Chini Felda scheme while Runchang is an Orang Asli settlement in the Sungai Bebar area. The surrounding of Sungai Bebar is peat swamp forest.

Male fruit flies were collected in the morning by means of the sex attractants methyl eugenol (4-allyl-1, 2-dimethoxybenzene) and cue-lure (4-[4-(acetyloxy) phenyl]-2-butanone). A small amount of each lure was applied separately and away from each other on the upper surface of a green leaf – the lures are very effective and not affected by the leaf. Insects attracted to the lures over a period of about 30 minutes were collected with the aid of specimen tubes and plastic bags. The specimens were preserved in ethanol in the field and subsequently identified using current literature and personal experience [1, 2, 5, 6]. Representative individuals were also photographed in the field.

The diversity of the fruit flies was analysed using BioDiversity Professional Ver 2.0 1997. Shannon-Weiner index and Jaccard cluster analysis were applied for this study.

RESULTS

The diversity and relative abundance of Dacinae fruit flies collected in Chini 2, Runchang and Sungai Bebar are listed in Table 1. Three species of methyl eugenol group were present – *Bactrocera carambolae* Drew and Hancock, *Bactrocera papayae* Drew and Hancock and *Bactrocera umbrosa* (Fabricius). The cue-lure attractant yielded four species – *Bactrocera infesta* (Enderlein), *Bactrocera melastomatos* Drew and Hancock, *Bactrocera nigrotibialis* (Perkins) and *Bactrocera* cf *tau*.

For the methyl eugenol group all three species were present in three localities, C2, R1 and R2. Two species (*B. carambolae* and *B. papayae*) were collected in C1 and only *B. carambolae* was found in R3, SB1 and SB2. Fruit flies of the cue-lure group were found in five of the seven localities studied, not present in C2 and R2 (Table 1). *Bactrocera nigrotibialis* was the predominant species while *B. infesta* occurred in quite large number in a river bank locality. The other two species (*B. melastomatos* and *B.* cf *tau*) appeared to be uncommon.

The Shannon-Weiner diversity index of the Dacinae fruit flies revealed that R1 had the highest H' (0.58) followed by R2 (H'= 0.432) and C2 (H'= 0.401) (Table 1). Locations SB1 and SB2 yielded the lowest H' of 0.126 and 0.110 respectively (Table 1). The Jaccard cluster analysis showed that R2 and C2, and SB2 and R3 had respectively similarity of 100% (Fig. 1).

DISCUSSION

An extensive trapping effort, using Steiner traps baited with methyl eugenol or cue-lure and provided with malathion, was conducted over 12-36 months in the 1990s in Peninsular Malaysia and Thailand [7]. The trapped fruit flies were collected on a 1-2 week

Table 1. Species and number of Dacinae fruit flies collected in September 2009 by methyl eugenol and cue-lure attractants from Chini 2, Runchang and Sg. Bebar (Pekan District, Pahang, Peninsular Malaysia). C1, edge of secondary vegetation and fence of apartments in Chini 2; C2, abandoned village house along main road and near housing estate in Chini 2; R1, near school and Orang Asli house with orchard and secondary vegetation in Runchang; R2, near Orang Asli house in Runchang; R3, secondary forest near river in Runchang; SB1, river bank near abandoned aquaculture area along Sg. Bebar; SB2, forested area upstream from SB1 of Sg. Bebar.

Lure/species	C1	C2	R1	R2	R3	SB1	SB2
Methyl eugenol							
B. carambolae	22	28	12	4			
B. papayae	58	26	16	6	63	1	3
B. umbrosa		5	8	12			
Cue-lure							
B. infesta			1			28	
B. melastomatos			1				
B. nigrotibialis	2		1		49		40
B. cf *tau*						1	
Number of species	3	3	6	3	2	3	2
Shannon H'	0.299	0.401	0.580	0.432	0.298	0.126	0.110

basis. There were 12 stations in the state of Pahang, Peninsular Malaysia – the exact localities were however not stated, but presumably in agricultural areas. In that exercise, only three species (*B. carambolae*, *B. papayae* and *B. umbrosa*) of the methyl eugenol group and a single species (*B. cucurbitae*) of the cue-lure group were recorded in Pahang.

In another study carried out in the Endau-Rompin rain forest in southern Peninsular Malaysia from August to November 1985, tephritid fruit flies were collected by 'Malaise trap', hand collection, and methyl eugenol baited and cue-lure baited traps [8]. The lure-baited traps were set for four days per month, with one trap for methyl eugenol and four for cue-lure. This study yielded four *Bactrocera* species and 28 non-Dacinae species – quantitative data were not provided. The methyl eugenol baited traps yielded fruit flies of the *B. dorsalis* complex – *B. dorsalis* (Hendel) does not occur in Peninsular Malaysia and the complex consists of many species [5]. The cue-lure baited traps produced two species, *B. nigrotibialis* and *B. tau*. *Bactrocera latifrons* (Hendel), which is not attracted to both methyl eugenol and cue-lure, was collected in the Malaise trap, in addition to *B. dorsalis* complex and *B. tau*.

The diversity of *Bactrocera* species in the present study is comparable to studies using lure-baited traps (with male attractants methyl eugenol and cue-lure). It is also similar to studies employing the same method of applying the lures on green leaves [9, 10]. The study in Negeri Sembilan yielded two species (*B. carambolae* and *B. papayae*) of the methyl eugenol group and three species (*B. melastomatos*, *B. nigrotibialis* and *B. tau*) of the cue-lure group [9]. In Kelantan, the two localities studied (Pantai Melawi and Selising) supported different species and different density of the common species – *B. carambolae*, *B. papayae*, *B. melastomatos* in both localities, *B. caudata* only in Pantai Melawi, and *B. umbrosa* only in Selising [10]. The presence or absence of *Bactrocera* species and their abundance are dependent on the availability of their host plants/fruits [11]. For example, in the present study *B. umbrosa* was found only in localities with typical village setting. This species is rather host specific [12], infesting fruits of *Artocarpus* spp. which were not evident in the localities where it was not collected.

In the extensive study carried out in Pahang [7], the *Bactrocera* species showed seasonal abundance in number. *Bactrocera carambolae*, *B. papayae* and *B. umbrosa* had higher number in September than other months, while *B. cucurbitae* showed a peak in November. The present study carried out in September 2009 did not yield *B. cucurbitae*; it may be attributed to the absence of host plants Cucurbitaceae which were not evident in all the seven localities studied.

Of the cue-lure group of fruit flies, *B. nigrotibialis* (Fig. 2) was the predominant species. It occurred in large number in two forest areas but only a single individual was encountered in an inhabited area. It was present in the Endau-Rompin rain forest [8] but not recorded in the extensive trapping carried out in 12 stations in Pahang [7]. This species is not confined to the forest as it is present in the University of Malaya campus (unpublished data).

An unexpected find in the present study was the large number of *B. infesta* (Fig. 3) attracted to cue-lure in locality SB1 (river bank near an abandoned

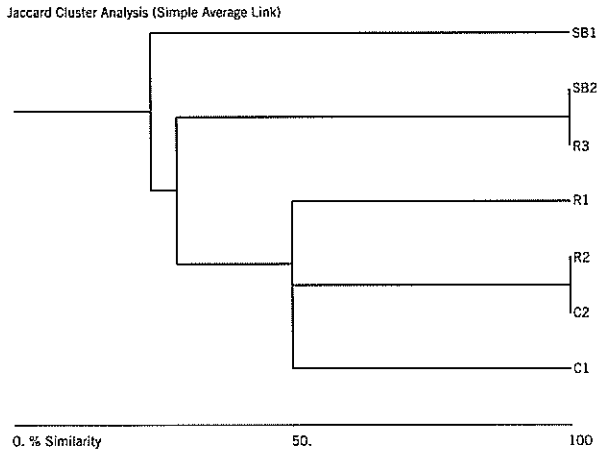

Figure 1. Dendrogram of Dacinae fruit flies species similarity of different localities in Chini District, Pekan, Pahang .

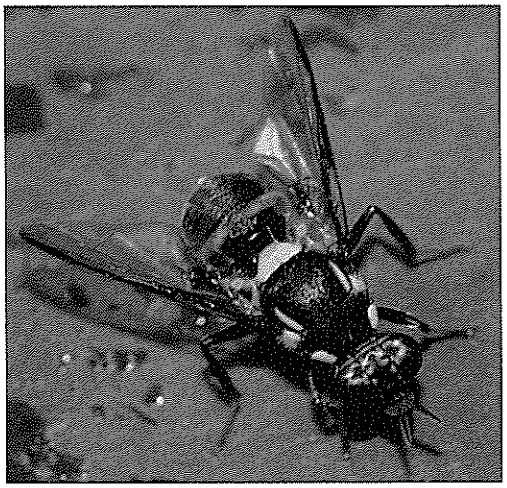

Figure 2. Male *Bactrocera nigrotibialis*.

JOURNAL OF SCIENCE AND TECHNOLOGY IN THE TROPICS

INSTRUCTIONS TO CONTRIBUTORS

JOSTT is a multi-disciplinary journal. It publishes original research articles and reviews on all aspects of science and technology relating to the tropics. All manuscripts are reviewed by at least two referees, and the editorial decision is based on their evaluations.

Manuscripts are considered on the understanding that their contents have not been previously published, and they are not being considered for publication elsewhere. The authors are presumed to have obtained approval from the responsible authorities, and agreement from all parties involved, for the work to be published.

Submission of a manuscript to JOSTT carries with it the assignment of rights to publish the work. Upon publication, the Publishers (COSTAM and ASM) retain the copyright of the paper.

Manuscript preparation

Manuscripts must be in English, normally not exceeding 3500 words. Type double spaced, using MS Word, on one side only of A4 size with at least 2.5 cm margins all round. Number the pages consecutively and arrange the items in the following order: title page, abstract, key words, text, acknowledgements, references, tables, figure legends.

Title page

Include (i) title, (ii) names, affiliations and addresses of all authors, (iii) running title not exceeding five words, and (iv) email of corresponding author.

Abstract and key words

The abstract, not more than 250 words, should be concise and informative of the contents and conclusions of the work. A list of not more than five key words must immediately follow the abstract.

Text

Original research articles should be organized as follows: Introduction, Materials and Methods, Results, Discussion, Acknowledgement, References. The International System of Units (SI) should be used. Scientific names and mathematical parameters should be in italics.

References

References should be cited in the text as numbers enclosed with square [ ] brackets. The use of names in the text is discouraged. In the reference section, the following examples should be followed:

1. Yong H.S., Dhaliwal S.S. and Teh K.L. (1989) A female Norway rat, *Rattus norvegicus*, with XO sex chromosome constitution. *Naturwissenschaften* **76**: 387-388.
2. Beveridge W.I.B. (1961) *The Art of Scientific Investigation*. Mercury Book, London.
3. Berryman A.A. (1987) The theory and classification of outbreaks. In Barbosa P. and Schultz J.C. (eds.) *Insect outbreaks* pp. 3-30. Academic Press, San Diego.

Tables

Tables should be typed on separate sheets with short, informative captions, double spacing, numbered consecutively with Arabic numerals, and do not contain any vertical lines. A table should be set up to fit into the text area of at most the entire page of the Journal.

Illustrations

Black-and-white figures (line drawings, graphs and photographs) must be suitable for high-quality reproduction. They must be no bigger than the printed page, kept to a minimum, and numbered consecutively with Arabic numerals. Legends to figures must be typed on a separate sheet. Colour illustrations can only be included at the author's expense.

Proofs and reprints

Authors will receive proofs of their papers before publication. Order for reprints must be made when returning the proofs.

Submission

Manuscripts (including all figures but not original artwork), together with a CD version of the text, should be submitted to:

The Editorial Office
Journal of Science and Technology
in the Tropics
Academy of Sciences Malaysia
902-4 Jalan Tun Ismail
50480 Kuala Lumpur, Malaysia

E-mail: jostt@akademisains.gov.my

JOSTT is listed in Scopus

aquaculture area along Sg. Bebar). As far as we are aware there is no published record of this species for Peninsular Malaysia – we had however encountered it before but not published. It was originally described as *Polistomimetus infestus* Enderlein 1920 and later treated as *Dacus* (*Pacifodacus*) *infestus* [7]. It looks remarkably like *Callantra sphaeroidalis* (Bezzi) but the first two segments of the antennae are short [6]. The type-locality is Sumatra; it has been recorded in Indonesia, Thailand and Laos. It is a rufous species with only a short median yellow vitta, a petiolate abdomen, a very large apical spot in the wing, and a complete black band along lower surface of face [6]. As far as known, there is no published information on its attraction to lure and host plants.

The present method of using chemical attractants does not uncover the presence of tephritid species that do not respond to such lures [3], e.g. *B. arecae* and *B. latifrons*. In the study using four collection methods in the Endau-Rompin rain forest, Malaise traps accounted for 20 out of 32 species and hand collection 12 species, compared to three species by methyl eugenol and cue-lure [8].

In sum, different localities in the present study yielded different composition and abundance of *Bactrocera* species, due most likely to the presence and availability of host plants/fruits. Of the seven species present, *B. infesta* constitutes a new record for Malaysia. The higher number of *Bactrocera* species and Shannon H' in localities R1, R2 and C2 are attributed to the presence and availability of host/ fruit and orchards in or near the localities. These areas also showed higher similarity percentage as indicated by Jaccard cluster analysis.

Acknowledgement – The field work was supported by the research grant UKM-GUP-ASPL-07-04-048. We thank our institutions (University of Malaya and Universiti Kebangsaan Malaysia) for facilities and financial support; and the Forestry Department of Pahang Darul Makmur for permission to carry out field research.

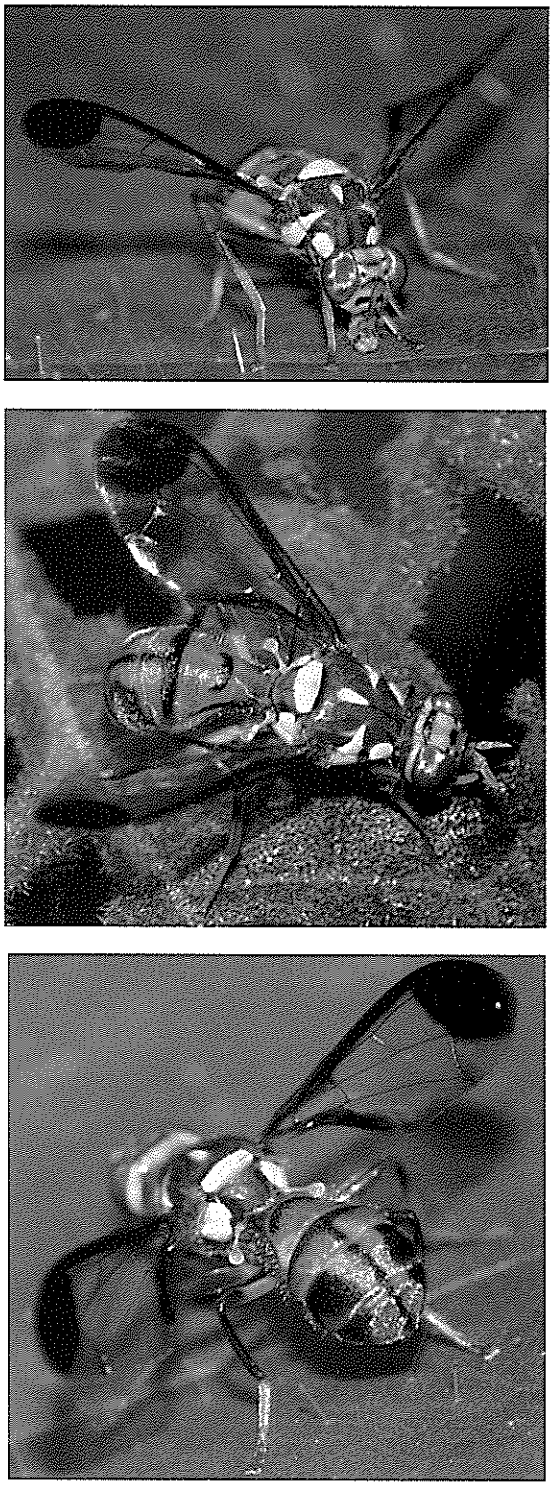

Figure 3. Male *Bactrocera infesta*.

REFERENCES

1. Drew R.A.I. (1989) The taxonomy and distribution of tropical and subtropical Dacinae (Diptera: Tephritidae). In Robinson A.S. and Hooper G. (Eds.) *Fruit Flies,Their Biology, Natural Enemies and Control* Vol. 3A pp. 9-14. Elsevier, Amsterdam.
2. Yong H.S. (1995) Genetic differentiation and relationships in five taxa of the *Bactrocera dorsalis* complex (Insecta: Diptera: Tephritidae). *Bulletin of Entomological Research* **85**: 431-435.
3. Yong H.S. (1996) Host specificity and response to chemicals in Dacinae fruit flies (Insecta: Diptera: Tephritidae). In Turner I.M., Diong C.H., Lim S.S.L. and Ng P.K.L. (Eds.) *Biodiversity and the Dynamics of Ecosystems*. DIWPA Series Volume **1**:191-194.
4. Yong H.S. (1992). Host specificity and genetic variability in Malaysian fruit flies (Insecta: Diptera: Tephritidae). *Proceedings of the National IRPA (Intensification of Research in Priority Areas Seminar (Agriculture Sector), Volume 1: Crops and Plants*, Kuala Lumpur, Malaysia, pp. 233-234.
5. Drew R.A.I. and Hancock D.L. (1994) The *Bactrocera dorsalis* complex of fruit flies (Diptera: Tephritidae: Dacinae) in Asia. *Bulletin of Entomological Research Supplement No. 2*: 1-68.
6. Hardy D.E. (1973) The fruit flies (Tephritidae-Diptera) of Thailand and bordering countries. *Pacific Insects Monograph* **31**: 1-353.
7. Clarke A.R., Allwood A., Chinajariyawong A., Drew R.A.I., Hengsawad C., Jirasurat M., Krong C.K., Kritsaneepaiboon S. and Vijaysegaran S. (2001) Seasonal abundance and host use patterns of seven *Bactrocera* Macquart species (Diptera: Tephritidae) in Thailand and Peninsular Malaysia. *The Raffles Bulletin of Zoology* **49**(2): 207-220.
8. Tan C.L., Md. Hanifah Y. and Chan H.F. (1994) Diversity of fruit flies species (Diptera: Tephritidae) collected in Endau-Rompin, Malaysia. In Yong H.S. and Khoo S.G. (Eds.) *Current research on tropical fruit flies and their management* pp. 27-31. The Working Group of Malaysian Fruit Flies, Kuala Lumpur.
9. Yong H.S., Sofian-Azirun M. and Hashim R. (2009) Dacinae Fruit Flies (Insecta: Diptera: Tephritidae) of Lata Kijang Kenaboi, Negeri Sembilan, Peninsular Malaysia. *Malaysian Journal of Science* 28 (4): 61-64.
10. Yong H.S., Hashim R., Sofian-Azirun M. and Mat Diah S.Z. (2009) Diversity and abundance of Dacinae fruit flies (Insecta: Diptera: Tephritidae) in Pantai Melawi and Selising, Kelantan, Peninsular Malaysia. *Malaysian Journal of Science* **28** (Special Issue): in press.
11. Yong H.S. (1994) Host fruit preferences in two sympatric taxa of the *Bactrocera dorsalis* complex (Insecta: Diptera: Tephritidae). In Yong H.S. and Khoo S.G. (Eds.) *Current research on tropical fruit flies and their management* pp. 1-8. The Working Group on Malaysian Fruit Flies, Kuala Lumpur.
12. Yong H.S. (1988) Allozyme variation in the Artocarpus fruit fly *Dacus umbrosus* (Insecta: Tephritidae) from Peninsular Malaysia. *Comparative Biochemistry and Physiology* **91B**: 85-89.

Journal of Science and Technology in the Tropics (2010) **6**: 23-30

The mammal fauna of Pulau Singa Besar, Langkawi, Kedah, Peninsular Malaysia

Lim Boo Liat[1], Norhayati Ahmad[2,3], O. Noor Alif Wira[4], Shahrul Anuar Md. Sah[5]
[1]Jalan Koop Cuepacs 3 E, Taman Cuepacs, 43200 Cheras, Selangor, Malaysia
[2]School of Environment and Natural Resource Sciences, Faculty of Science and Technology, University Kebangsaan Malaysia, 43600 UKM Bangi, Selangor, Malaysia
[3]Institute for Environment & Development (LESTARI) , Universiti Kebangsaan Malaysia, 43600 UKM Bangi, Selangor, Malaysia
[4]Department of Wildlife and National Parks, Penang, Malaysia
[5]Department of Biological Science, Universiti Sains Malaysia, Penang, Malaysia
(Email: chizlim54@yahoo.com)

Abstract Studies on the mammal fauna of Pulau Singa Besar, Langkawi were carried out during 2001 and 2002. A total of 51 species – 21 non volant and 30 volant species – from past and recent studies were recorded. Two species, the Smooth otter (*Lutrogale perspicillata*) and Indian False vampire (*Megaderma lyra*) are new records for the Langkawi Archipelago. The species diversity between the non volant and volant mammals is discussed.

Keywords mammals – Malaysia – bats – diversity – island

INTRODUCTION

Pulau Singar Besar, Langkawi is one of the 104 islands in the Langkawi Island archipelago. It is a permanent forest reserve, uninhabited, and was established as a bird and animal sanctuary in 1990. The island consists of various pristine forest types, such as dipterocarp lowland tropical forest, mangrove coastal forest, and sandy beach forest. In terms of the mammal fauna, the island has been known for the high density of mousedeer (*Tragulus kanchil*, *T. napu*), wildboar (*Sus scrofa*), and Long-tailed macaque (*Macaca fascicularis*).

Not much was known of its mammal species diversity until the late 1980s. A survey was carried out on the vertebrate fauna and 17 species of mammals were recorded [1]. After a lapse of 10 years, more comprehensive studies on the vertebrate fauna (amphibian and reptile, mammal, bird) were carried out at different periods of 8–10 days each in 2001 and 2002 under the purview of the Department of Wildlife and National Parks (DWNP). We report here the results of the 47 mammal species.

MATERIALS AND METHODS

Pulau Singa Besar is located south of the main Langkawi island, wedged in between the small island of Pulau Beras Basah on the west and the larger island of Pulau Dayang Bunting on the east (Fig. 1). The island is 11.3 km^2 in area, reaches 270 m in elevation and is nearly entirely covered by pristine dipterocarp forest. The island is traversed by steep valleys drained by seasonal streams. Limestone outcrops are prominent on the north-eastern part of the island. Caves of varying depths and widths occur in this limestone area. There are three clear water streams that flow to the east of the island, Sg. Boton and Sg. Pantai, while Sg. Sepai flows to the northern coast.

The island, as in the Kadawi region, experiences dry periods between December-April. During the north-east monsoon, the island is exposed to torrential rain and storms. Day temperature varies from 27°C under shade and 37°C in the open on the beach. Night temperature is around 24–27°C. It is hot and humid most of the time [1].

Journal of Science and Technology in the Tropics (2010) 6: 23-30

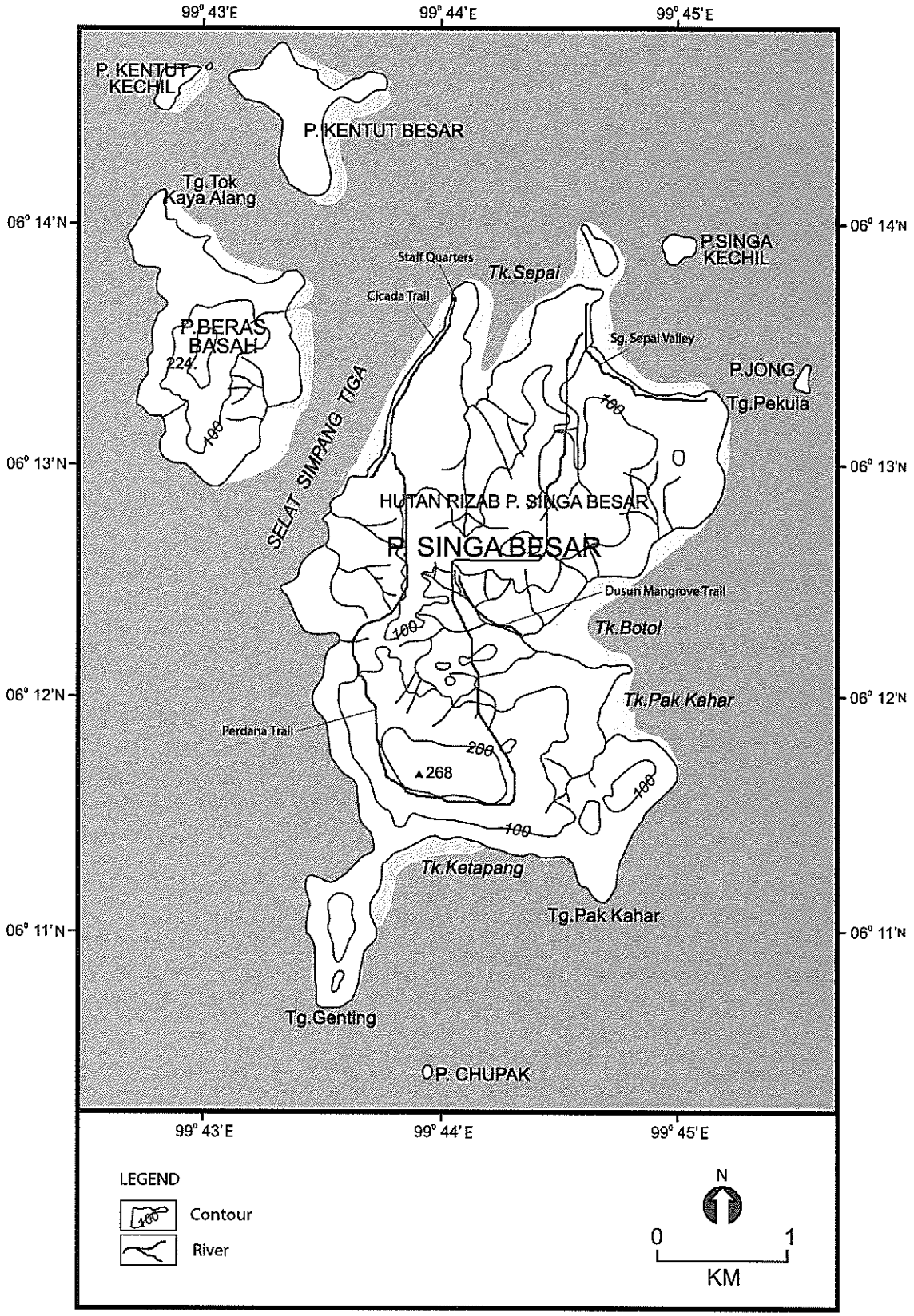

Figure 1. Map of Pulau Singa Besar and the trails where trapping of mammals was carried out.

The field team comprised eight members, six of whom were from the DWNP, Kuala Lumpur. Three field trips were carried out: 2-14 May 2001, 2-8 February 2002, and 2-13 June 2002. Trapping of the mammals was carried out at designated trails: Mangrove boardwalk (MBW), Cicada trail (CT), Perdana trail (PT), Dusun trail (DT), Sungai Sepai trail (SS) and the Staff quarters (SQ). Trappings were carried out by four field workers along two trails for each of the field trip. Fifty collapsible traps and two harp traps were deployed at each sampling site. Thus, the three field trips covered all the six trapping sites. All mammals captured were processed, i.e. measurements were taken and reproductive conditions noted. While visiting the various traps during the day and night, any nocturnal and diurnal animals sighted were noted and identified up to the species level whenever possible. Voucher specimens for some of the volant mammals (1–4 individuals) were collected and preserved using ethanol and some of the non-volant species were skinned for voucher specimens. All the voucher specimens were deposited in the museum collection at the Institute of Biodiversity, Bukit Rengit, Lanchang, Pahang, Peninsular Malaysia.

Mangrove boardwalk (MB)

The mangrove boardwalk meanders through a patch of mangrove forest next to the Staff quarters (SQ) and Interpretation Center (IC) building just before entering the forest. Rat traps were laid throughout the 200-m length of the boardwalk. Harp traps were set at 2 m apart at the mid-point on the boardwalk.

Cicada trail (CT)

This trail starts from a small section of the boardwalk proceeding along the sandy beach. It is about 2 km long. The trail is flanked on the left by disturbed forest and the right by the sea coast. It is a popular trail among tourists during weekends and public holidays. Traps were laid in the forest and at the fringe. Harp traps were set in the forest.

Perdana trail (PT)

The trail starts from the end of CT, heads south-west through various forest types (scrub, secondary and primary forests), meanders to northeast and ends at Sg. Sepai Valley (SS). The terrain is undulating with some parts very steep. The trail is about 6 km from PT to SSV. As the trail is very long, the 50 traps were divided into two areas along the trail at 25 m interval. The first 25 traps were spread out along 1.5 km from the beginning of the CT and ended at the base of the steep point at about 800 m high; the second set of 25 traps were laid just below the steep base and ended at the SSV. The harp traps were set at the midpoint of PT and the other at the midpoint of SSV.

Dusun trail (DT)

The trail starts at 1.5 km of the PT, takes a 45 degree turn to the right and descends another 0.5 km to a small orchard of mostly durian trees. Another way of getting to the DT is via boat during high tide through the mangrove forest. Traps were laid in the plantations, fringe of mangrove and along forest trails and stream banks. Harp traps were set in the plantations and also in the entrance of crevices of rock boulders in the area.

Sungai Sepai valley (SS)

This area is one of the campsites for visitors to the island. The forest here is disturbed primary forest edged by a small stretch of mangrove forest. Deeper into the secondary forest is pristine forest habitat. A large forest stream, about 1-2 m wide undulating to a stretch of limestone rocks, provides the source of clean water for the campsite. Traps and harp traps were set in the primary part of the forest.

Staff quarters (SQ)

There are four buildings making up the staff quarters next to the MW and IC near the jetty. Traps and harp traps were set at a stretch of disturbed forest behind the SQ.

RESULTS AND DISCUSSION

A total of 47 mammals was recorded from the six study sites from the three field trips in 2001 and 2002 on the island. This comprised 18 species of non-volant mammals from 12 families and 29 species of volant mammals from eight families (Appendix 1). The greater number of volant species was probably due to the availability of roosting sites (crevices of rock boulders, caves, hollow trees) in the island. The low species diversity of the non volant mammals in island ecosystem is generally low and Pulau Singa Besar is no exception. This is also shown on studies of other islands, for example, 45 mammal species (including 19 bat species) in Pulau Tioman, Pahang and 23 species (including 15 bat species) in Pulau

Perhentian [2-4]. This is due to the isolation from the mainland where emigration and immigration are marginal and also limited sizes of the landmass. In the case of arboreal species (bats and birds), they are very mobile and if it is within their flight range, the island would serve as part of their transit shelters for resident and migrant animals, as well as for food resources.

Among the six study sites, higher species richness, ranging from 21–38 species were recorded at CT, PT, DT, and SSV. The higher number of species is associated with the diversity of habitats (scrub, secondary and primary forests) found in each of these study sites. The markedly lower species richness recorded at MBW (8 species) and SQ (12 species) was probably due to the less diverse habitat of the coastal mangrove forest as compared to the other sites (Appendix 1).

Non-volant mammals

All the 18 mammal species recorded in the island (Appendix 1: No. 1-18) are common species, except the Smooth otter (*Lutrogale perspicillata*), which is a new record for Langkawi. Most abundant among the 18 species were the tree-shrew, long-tailed macaque, plantain squirrel, three species of field and forest rats, wild boar and mouse-deer (Appendix 1: Nos. 4, 5, 7, 9-11, 17, and 18). The least encountered was the White-toothed ground shrew (*Crocidura fuliginosa*) (Appendix 1: No 1). This species is a tiny, burrowing animal. Pit fall traps have been proven to be the most suitable trapping technique to obtain this species [5].

Previous study [1] recorded 15 species of non-volant mammals on Pulau Singa Besar, of which, four species were additional records for the island: the Slow loris (*Nycticebus coucang*), Black giant tree squirrel (*Ratufa bicolor*), Eurasian otter (*Lutra lutra*) and the Three-striped palm civet (*Arctogalidia trivirgata*). With these, the non-volant mammals increased to 22 species on Pulau Singa Besar. Of these, 20 species were recorded on the main Langkawi island [6], except *Niviventer cremoriventer* and *Lutrogale perspicillata*. However, all the 22 species recorded from Pulau Singa Besar are common in the mainland of Peninsular Malaysia, except the Eurasian otter.

Volant mammals

The 29 species of bats recorded on the island comprised seven species of fruit bats (Pteropodidae) and 22 species of insectivorous bats from seven families: Emballonuridae, Nycteridae, Megadermatidae, Rhinolophidae, Hipposiderosidae, Vespertilionidae and Molossidae (Appendix 1: No. 19–47).

Fruit bats

All the seven species of fruit bats are common on the island; the Lesser Dog-faced fruit bat (*Cynopterus brachyotis*) and the Cave fruit bat (*Cynopterus Eonycteris spelaea*) (Appendix 1; No. 20, 22) were more common than the rest (Appendix 1: No. 19, 21, 23-25). Both these species were netted in all the six study sites with greater frequency of captures (27, 17 individuals respectively) compared to the others which were netted between 2-4 study sites and with less frequency of captures, ranging from 4–12 individuals.

Mustaffa Babjee [1] recorded four species of fruit bats on the island. One of them, the Island Flying fox (*Pteropus hypomelanus*) was a new locality record for Langkawi, which increased the fruit bat fauna to eight species from the island to date, compared to five species in the main Langkawi island [6]. However, all the eight species recorded on the island are also common in lowland and hill forests in mainland Peninsula Malaysia.

Insectivorous bats

The species richness of this group was reflected by the troglodytic habits where the roosting environments are available on the island. At least 12 species (Appendix 1: No. 29-33, 36-40,42, 45) were cave dwellers [7-9]. Among the 22 species, three species, the Intermdiate Horseshose bat (*Rhinolophus affinis*), Bicolored Roundleaf bat (*Hipposideros bicolor*) and Common Roundleaf bat (*Hipposideros galeritus*), were common with high frequency of captures (44, 38, and 27, respectively). Of particular interest was a species with a single specimen netted, the Indian False vampire (*Megaderma lyra*), which is uncommon. This species is carnivorous in habit [6].

Fourteen of the 22 species on the island were also recorded on the main Langkawi island [6]. On the mainland of Peninsular Malaysia, all the 22 species are common in lowland and hill forests.

Reproductive status

The examination of pregnant females was based on visible observation of advance pregnancy of the animals. This method was used to conserve the species from being sacrificed for detail examination

of the reproductive tracts, and also to prevent the animal from being overly stressed by holding it too long before release.

A total of 35 species, comprising eight species of non-volant (63 individuals) and 27 species of volant mammals (138 individuals), was examined in May 2001 and February and June 2002 (Table 1). Of the non-volant mammals, two species (9 individuals) were not gravid. For the females of the other six species (Table 1: No. 1-2, 4-6, 8) with 54 individuals, about 33% (18 individuals) were visibly pregnant. The number of individuals pregnant during the three periods showed no marked difference, being 5, 7, and 6 respectively.

Of the 27 species of volant mammals examined, 13 species (26 individuals) were not gravid. In the other 14 species (Table 1: No. 9-10, 12-14, 19, 21, 24-25, 28, 30, 33-35) with 112 individuals, 36.7% (41 individuals) were visibly pregnant. The number of individuals pregnant during May 2001, February and June 2002 was 15, 4, and 22 which suggests that there was a high birth trend in May and June.

Table 1: Number of visibly pregnant females of non-volnt and volant mammals of Pulau Singa Besar, Langkawi, Kedah, Peninsular Malaysia.

No.	Species	No. Indiv. Examined	2-14 May 2001	2-12 Feb 2002	2-13 Jun 2002	Total
NON-VOLANT MAMMALS						
1	*Tupaia glis*	7		2		2
2	*Callosciurus notatus*	7	1			1
3	*C. caniceps*	5				
4	*Rattus tiomanicus viclana*	21	4	3	5	12
5	*Rattus exulans*	7			1	1
6	*Leopoldamys sabanus*	8		1		1
7	*Niviventer crimoriventer*	4				
8	*Maxomys surifer*	4		1		1
VOLANT MAMMALS						
9	*Rousettus amplexicaudatus*	2	1			1
10	*Cynopterus brachyotis*	12	1		3	4
11	*C. horsfieldii*	2				
12	*Eonycteris speleae*	9	1		2	3
13	*Penthetor lucasi*	8		1		1
14	*Macroglossus minimus*	5	1			1
15	*Emballonura monticola*	4				
16	*Taphozous melanopogon*	1				
17	*Nycteris tragata*	4				
18	*Megaderma spasma*	1				
19	*Rhinolophus affinis*	24	4	2	5	11
20	*R. trifoliatus*	3				
21	*R. coelophyllus*	3			1	1
22	*R. pusilllus*	2				
23	*R. lepidus*	3				
24	*Hipposideros bicolor*	21	4	1	6	11
25	*H. galeritus*	11	1		2	3
26	*H. cinareus*	1				
27	*H. diadema*	2				
28	*H. larvatus*	5	1			1
29	*Myotis muricola*	1				
30	*M. hasseltii*	1			1	1
31	*Murina suillus*	1				
32	*Kerivoula papillosa*	1				
33	*K. intermedia*	4			1	1
34	*Scotophilus kuhli*	4	1			1
35	*Tadarida mops*	3			1	1
	Total	201	20	11	28	59

Conclusion

The high species richness of the chiropteran fauna in Pulau Singa Besar could be due to: (1) the island with its pristine forest and surrounded by limestone outcrops and traversed by valleys with seasonal streams, provides abundant roosting sites, such as caves, crevices of rock boulders, tree holes, etc.; and (2) bats could fly from neighbouring Pulau Basah on the west and the larger Pulau Dayang Bunting on the east. The non volant mammals are mostly terrestrial residential species where emigration-immigration is limited. Thus, the low species richness of this group of animals in the island ecosystem is a natural phenomenon [10].

With the additional four species, *Pteropus hypomelanus, Nycticebus coucang, Lutra lutra* and *Ratufa bicolor* recorded in earlier study [1], the mammal fauna of the island now stands at 51 species.

Acknowledgements – We are grateful to the staff of DWNP, particularly the Director-General, Dato' Musa Nordin (retired) for his support; and the General Manager of the Langkawi Development Authority (LADA), for supporting the logistic in the field.

REFERENCES

1. Mustaffa Babjee A. (1990) *Pulau Singa Langkawi: bird and animal sanctuary*. Department of Veterinary Sciences, Ministry of Agriculture, Malaysia.
2. Lim B.L., Kelvin K.P.L. and Yong H.S. (1999) The terrestrial mammals of Pulau Tioman, Peninsular Malaysia, with a catalogue of specimens at the Raffles Museum, National University of Singapore. *Raffles Bulletin of Zoology* **6**: 101-123.
3. Yong H.S. (1974) Diversity and abundance of small mammals in two Malaysian offshore islands. *Malayan Nature Journal* **27**: 27-29.
4. Tamblyn A., Malley R., Turner C. and Hughes T. (2009) The bat fauna (Mammalia, Chiroptera) of Pulau Perhentian, Peninsular Malaysia. *Malayan Nature Journal* **61**(1): 10-22.
5. Nor Zalipah M., Juliana S. and Lim B.L. (2007) A note on the arboreal monkey-footed rat in a pit-fall trap. *Journal of Wildlife and Parks* **24**: 63-65.
6. Medway Lord (1983) *The wild mammals of Malaya (Peninsular Malaysia) and Singapore*. 3rd Edn. Oxford University Press, Kuala Lumpur.
7. Medway, Lord (1965) Identification of Malaysian cave bats. *Malayan Nature Journal* 19: 88-107.
8. Lim B.L. (1967) Abundance and distribution of Malaysian bats in different ecological habitats. *Federal Museum Journal* (N.S.) II (1966): 61-76.
9. Norhayati A., Shukor M.N., Shahrul Anuar M.S., Nurul Ain E. and Norzalipah M. (2007) Note on the bats of Gua Kelawar, Langkawi Island, Kedah. *Journal of Wildlife and Parks* **24**: 1-6.
10. Alle W.C. and Schmidt X. (1951) *Ecological animal geography*. Chapman and Hall Ltd., London.

Appendix 1: Mammal species recorded on Pulau Singa Besar, Langkawi, Kedah, Peninsular Malaysia. (MB=Mangrove Boardwalk, CT=Cicada Trail, PT=Perdana Trail, DT=Dusun Trail, SS=Sungai Sepai Valley, SQ=Staff Quarters; S=Sighted, S-TR=Sighted and track signs, R=Released).

No.	Order/Family/Species	MB	CT	PT	DT	SS	SQ	Total		Voucher No.
								Male	Female	
	INSECTIVORA									
	Soricidae									
1	*Crocidura fuliginosa*				1			1	0	35
	DERMOPTERA									
	Galeopterida									
2	*Galeopterus variegatus*				S - 1			1		-
	PHOLIDOTA									
	Manidae									
3	*Manis javanicus*			S -1				1		-
	SCANDENTIA									
	Tupaiidae									
4	*Tupaia glis*	2	1	1	4	3	2	6	7	36-37
	PRIMATE									
	Cercopithecidae									
5	*Macaca fascicularis*	S	S	S	S	S	S	-	-	-
6	*Trachypithecus obscurus*				S	S		-	-	-
	RODENTIA									
	Sciuridae									
7	*Callosciurus notatus*	S - 1	1	2	1	1	4	3	7	38-40
8	*C. caniceps*		1	2	1	4	1	4	5	41
	Muridae									
9	*Rattus tiomanicus viclana*		12	12	5	2	6	6	21	42-43
10	*Rattus exulans*		2	6	2	3	2	8	7	44-45
11	*Leopoldamys sabanus*		4	6	2	3		7	8	46-47
12	*Niviventer cremoriventer*				3	2		1	4	48-49
13	*Maxomys surifer*		1	1	2	4		4	4	51-
	Hystricidae									
14	*Hystrix brachyura*				S - 1	S - 1		2		-
	CARNIVORA									
	Viveridae									
15	*Paradoxurus hermaphroditus*	S - 1	S - 2	S - 1	1	S - 1	1	2	5	R
	Mustelidae									
16	*Lutragale perspicillata*	S - 2			S - 2			4		-
	ARCTIODACTYLA									
	Suidae									
17	*Sus scrofa*		S	S	S + Tr	S + Tr	S - 3	4		-
	Tragulidae									
18	*Tragulus kancil/napu*		S - 2	S - 1	S - 1	S - 2		6		-

Journal of Science and Technology in the Tropics (2010) **6**: 3

Editorial

PUBLISH OR PERISH

When one chooses a scientific career, it becomes a norm to publish. One has to disseminate one's findings and one's work. It is part of the challenge of being a scientist and it is expected of a scientist. Some institutions set target for scientists to publish at least two scientific papers in a refereed journal a year. Such targets are good as there is a propensity for scientists in general not to publish.

There are many forms of publications. The usual is a scientific journal and most professions or institutions have their own dedicated journals to provide a conduit for their scientific staff to publish. However, the growing concerns on the environment and the destruction of forests have been used as an argument to choose electronic publications and the widespread use of the internet allows this. However, among the more senior scientists, the preference is still the written media. Publishing in peer-reviewed journals should be encouraged as this will provide a more international audience. The impact factor of the journal should also be taken into consideration. The number of times that an article is cited or the citation index is also an indicator of the readership of the article.

The other issue often debated is proceedings of seminars and conferences. Conferences, workshops and seminars provide excellent channels for the dissemination of research findings and ideas, and proceedings of such meetings are critically important to record the presentations that would be lost otherwise.

There is an increasing propensity for joint authorship of papers. While this is inevitable considering that research is seldom undertaken by an individual but rather by a team, the tendency for the head of the organization to be the main author should not be encouraged unless he or she was really the main researcher involved in the project. The main scientist that undertook the major part of the research and who wrote the article must be the main author.

Some disciplines are more amenable to publications. For example, in taxonomic research it is much easier to publish when the scientist has completed the study of a certain species of plant or animal or microorganism. However, in some other disciplines, it is much more difficult and time consuming. Nonetheless, the key to good research is innovation and such innovative discoveries or ideas should be published.

Finally there is the fundamental issue of scientific writing. Many scientists have never been taught the art or science of scientific writing. It is proposed that every young scientist undergo a course on scientific writing early in their career as this will give them confidence and provide them a good foundation to publish their findings later.

Dr. Salleh Mohd. Nor and Dr. Mohinder Singh
Co-Chairman, Editorial Board

	CHIROPTERA									
	Pteropodidae									
19	*Rousettus amplexicaudatus*		1		4			3	2	52
20	*Cynopterus brachyotis*	2	5	3	8	5	3	14	12	53-54
21	*C. horsfieldii*			1	3	2		4	2	55
22	*Eonycteris spelaea*	1	1	3	6	4	2	8	9	56-57
23	Penthetor lucasi			2	4	4	2	4	8	58
24	Macroglossus minimus	2		2	4	2		5	5	59
25	Balionycteris maculata			2	2			3	1	60
	Emballonuridae									
26	*Emballonura monticola*		1		3	3		3	4	61
27	*Taphozous melanopogon*				1	2		2	1	62
	Nycteridae									
28	*Nycteris tragata*			2	2	2		2	4	63
	Megadermatidae									
29	*Megaderma spasma*					3		2	1	64
30	*M. lyra*				1			1		65
	Rhinolophoridae									
31	*Rhinolophus affinis*		12	8	13	11		20	24	66-67
32	*R. trifoliatus*			3		2		2	3	68-69
33	*R. coelophyllus*			3	2	3		5	3	70-71
34	*R. pusillus*			3		1		2	2	72-73
35	*R. lepidus*		1	3		2		3	3	74-75
	Hipposideridae									
36	*Hipposideros bicolor*		11	12	9	6		17	21	76-78
37	*H. galeritus*			3	10	14		16	11	79-80
38	*H. cineraceus*					2		1	1	81
39	*H. diadema*				3			1	2	82
40	*H. larvatus*		2		5	2		4	5	83-84
	Vespertilionidae									
41	*Myotis muricolor*		3					2	1	85
42	*M. hasseltii*	1				3		3	1	86-87
43	*Murina suillus*		1		2	1		3	1	88-89
44	*Kerivoula papillosa*					3		2	1	90
45	*K. intermedia*			2			4	2	4	93
46	*Scotophilus kuhli*			2			4	2	4	94
	Molossidae									
47	*Tadarida mops*				2	3		2	3	95-96
	Total no. species	8	21	28	36	38	12			
	Total No. Individuals	12	64	86	101	112	30			

Journal of Science and Technology in the Tropics (2010) **6**: 31-38

Antiproliferative and antioxidant properties of leaf extracts of *Pereskia bleo* (Cactaceae) and their ability to limit natural and oxidant-induced apoptotic cell death

Hui Meng Er*, Hong Lim Lee, Ammu Kutty Radhakrishnan

Faculty of Medicine and Health, International Medical University, No.126 Jalan 19/155B, Bukit Jalil, 57000 Kuala Lumpur, Malaysia

(*Corresponding author E-mail: huimeng_er@imu.edu.my)

Abstract The anti-proliferative activities of methanol extract of leaves of *Pereskia bleo* and its ethyl acetate, *t*-butanol and aqueous fractions were studied in normal mouse fibroblast cells (NIH/3T3) and mouse mammary cancer cells (4T1). Although the extracts did not show significant anti-proliferative effect, they exhibited selectivity in inhibiting the proliferation of the cancer cells (4T1) compared to the normal cells (3T3). The antioxidant properties of the leaf extracts and their ability to limit natural and oxidant-induced cell death were also studied. Among the extracts, the *t*-butanol extract possessed the highest antioxidant property. The extracts were also able to limit natural and oxidant-induced cell death in normal mouse fibroblast cells.

Keywords *Pereskia bleo* leaf extracts – anti-proliferative – antioxidant – apoptotic cell death

INTRODUCTION

Pereskia bleo (Kunth) DC (Cactaceae) is commonly consumed by some ethnic groups in Malaysia for its medicinal properties. It is claimed to have antidiabetic and antihypertensive properties [1]. Besides, it is widely believed by the local community that the drink prepared by boiling the plant leaves in water is effective in preventing and treating cancers. Hence, the plant is commonly cultivated in the gardens. However, there are very little *in vitro* and *in vivo* studies to support most of these claims.

It has been shown previously that the methanol extract of *P. bleo* can kill T47-D human mammary cancer cells [2], suggesting that this plant has the potential to be developed as a candidate for treatment of cancers. However, in another study, it was reported that the methanol and aqueous extracts of the leaves did not possess any significant anti-proliferative activity on mouse mammary cancer cells (4T1) and normal mouse fibroblast cells (3T3) [3]. Moreover, it was also reported that the aqueous extracts of the leaves could form mutagenic compounds when these are metabolized by liver enzymes [3].

Although the methanol extract and its ethyl-acetate fraction has been reported to have high cytotoxic effect on human nasopharyngeal epidermoid carcinoma (KB) cells [4], their cytotoxic activity in other cell lines such as human cervical carcinoma cell line (CasKi), human colon carcinoma cell line (HCT116), hormone-dependent breast carcionoma cell line (MCF-7), and non-cancer human fibroblast cell line (MRC-5) was less significant [4]. In another study it was reported that the hexane, dichroloromethane, ethyl acetate and methanol extracts of the leaves were also non-effective in inducing cell death towards MCF-7 (human breast cancer), HT-29 (human colon carcinoma) and CEM-SS (human T4-lymphoblastoid) cell lines [5].

Anti-proliferative studies carried out on the methanol extract of the stem and its ethyl acetate, *t*-butanol and aqueous fractions on mouse mammary cancer cells (4T1) and normal mouse fibroblast cells (NIH/3T3) did not indicate significant antiproliferative

activity [6]. A detailed analysis on the methodologies employed in the previous studies suggested that the inconsistent findings on the anti-proliferative activity could be attributed to differences in the parts of the plant studied (e.g. leaf, stem, whole plant), plant extraction procedure, cell lines used and anti-proliferation assay conditions [3].

The diversity of secondary metabolites in plants is well known. They play a major role in contributing to the plants' natural defense mechanism against predators or diseases caused by microorganisms. As the stems of *P. bleo* are heavily covered with sharp spines that can protect the plant against preys, they may also be associated with high level of secondary metabolites of important medicinal properties, such as anticancer activity. However, previous study has shown that the stem extracts do not possess significant anti-proliferative activity against NIH/3T3 and 4T1 cells [6]. In the current study, the same procedure was employed for the extraction and fractionation of the leaves of the plant using the same solvents, and the anti-proliferative activities of the extracts were assessed using the same cell lines.

The mechanism of cell death caused by oxidative stress has been studied widely [7]. The generation of endogenous reactive oxygen or nitrogen species as a result of oxidative stress can lead to tissue injury implicated in many diseases. Many antioxidant compounds are found in higher plants and they have been shown to possess the ability to quench free radicals and reactive oxygen species *in vitro* [8]. In this study, the *in vitro* antioxidant property of the leaf extracts, as well as their ability to limit natural and oxidant-induced cell death were evaluated.

MATERIALS AND METHODS

Plant Material

The plant cuttings of *P. bleo* were collected from Taman Pertanian (Agricultural Garden) of the Universiti Putra Malaysia (UPM), Selangor, Malaysia. The voucher specimen (No. ACP 0116) was deposited in the herbarium of Institut Biosains of UPM.

Preparation of leaf extracts

The leaves of *P. bleo* were separated, cleaned with water and dried in a convection oven at 40°C until consistent weights were obtained. The dried leaves were blended into powder form using an electric blender. A weighed amount (20 g) of the leaf powder was extracted with methanol (250 mL) using a soxhlet extractor for four hours. The process was repeated five times in order to obtain sufficient amount of the extracts for further testing and the extracts were combined. The methanol solvent in the combined extract was removed under reduced pressure at 40°C using a rotary evaporator and the extract was further dried using a vacuum concentrator at 40°C until a consistent weight was obtained. A portion of the methanol extract was fractionated by partitioning into ethyl acetate, *t*-butanol and water. The solvents in these fractionated extracts were removed under reduced pressure at 40°C using a rotary evaporator. The ethyl acetate and *t*-butanol extracts were further dried to consistent weight using a vacuum concentrator at 40°C. The aqueous extract was freeze-dried to a consistent weight. The yields of the methanol, ethyl acetate, *t*-butanol and aqueous extracts were 7.7%, 0.2%, 3.8% and 7.1%, respectively, based on the dry weight of the leaves.

ABTS radical cation scavenging activity of *P. bleo* leaf extracts

The assay is based on the ability of substances with antioxidant properties to scavenge 2,2'-azinobis-(3-ethylbenzothiazoline-6-sulfonic acid) (ABTS) radical cations, which are blue-green in colour and absorb at 734 nm [9]. Any positive reaction will lead to the decolourisation of the ABTS radical cations. The methanol extracts of the leaves were dissolved in 0.01 M phosphate buffered saline (PBS) while the ethyl acetate and *t*-butanol extracts were dissolved in 0.8% (v/v) DMSO. Trolox and vitamin C were used as positive controls. To perform this assay, the ABTS solution (715 µL, 5 mM) was mixed with potassium persulphate solution (285 µL, 2.5 mM) and the reaction mixture was kept in the dark at room temperature for 12-16 hours for the generation of ABTS radical cations.

The ABTS radical cation solution was appropriately diluted with 0.01 M PBS to give an absorbance of 0.7 ± 0.2 at 734 nm. To 990 µL of this diluted ABTS radical cation solution, 10 µL of each of the concentrations of the leaf extracts, Trolox or vitamin C was added. The absorbance of the mixture at 734 nm was recorded at every minute for a period of 12 minutes. The experiment was repeated five times for each concentration of the extracts (2.5 to 50 µg/mL for *t*-butanol extract; 5 to 100 µg/mL for the other extracts), Trolox (0.25 to 2.5 mM) or

vitamin C (0.25 to 2.5 mM). Lower concentrations of the *t*-butanol extract were used compared to the other extracts due to the difficulty in dissolving this extract. The percentage inhibition of ABTS radical cation at each time point was calculated using the formula: Percentage inhibition = [(Initial absorbance - Absorbance at time of interest) / Initial absorbance] x 100%.

Cell lines

The NIH/3T3 (normal mouse fibroblast cell line) and 4T1 (mouse mammary cancer cell line) cells were purchased from the American Type Culture Collection (ATCC, Rockville). They were cultured in RPMI 1640 medium containing L-glutamine and supplemented with 10% FBS, 1% HEPES buffer solution, 1% sodium pyruvate (100 mM) and 0.5% penicillin-streptomycin in a humidified 5% CO_2 incubator at 37°C.

Anti-proliferation assay

Cell proliferation was analysed using the MTT assay [10]. This assay is based on the ability of the mitochondria of living cells to reduce a chemical, 3-(4,5-dimethylthiazol-2-yl)-2,5-diphenyltetrazolium bromide (MTT), which is a yellow tetrazolium salt, to purple formazan product that is insoluble in the aqueous phase. The NIH/3T3 or 4T1 cells (100 µL of $5x10^4$ cells) were cultured in a sterile 96-well flat-bottom tissue culture plate. The plate was incubated at 37°C in a humidified 5% CO_2 incubator for two hours. The methanol, ethyl acetate, *t*-butanol and aqueous extracts of the leaves were appropriately diluted (50 to 800 µg/mL) in medium containing 0.8% (v/v) dimethyl sulphoxide (DMSO). Various concentrations (25 to 100 µg/mL) of cisplatin, which was used as a positive control was also prepared in culture medium containing 0.8% (v/v) DMSO. The diluted solutions were filtered using sterile 0.22 µm filter units. Following the two hour incubation, 100 µL of the diluted leaf extracts or cisplatin were added to the 96-well culture plates containing the NIH/3T3 or 4T1 cells (in triplicates). The final concentrations of the leaf extracts in this assay ranged from 12.5 to 400 µg/mL while cisplatin ranged from 1.6 to 50 µg/mL. Cells cultured in medium containing 0.4 % (v/v) DMSO were used as negative control. The plates were incubated at 37°C in a humidified CO_2 incubator for 72 hours. Then MTT solution (20 µL, 5 mg/mL in PBS) was added to each of the wells and the plate was returned to the incubator for 4 hours. Following this, the supernatant in each well was removed carefully (the purple formazan product was attached to the bottom of the well). Dimethylsulphoxide (50 µL) was then added to each well to dissolve the purple formazan product. The absorbance of the solution in each well was determined using an ELISA plate reader at 570 nm. The percentage cell viability in each well was calculated by the formula: Percentage cell viability = (Absorbance at 570 nm of treated well / Absorbance at 570 nm of negative control) × 100%.

Cell death detection by enzyme-linked immunosorbent assay (ELISA)

The NIH/3T3 cells were diluted in culture medium to a concentration of 1 x 10^5 cells/mL. This diluted cell suspension (50 µL) was added to the wells of a sterile 96-well flat-bottom tissue culture plate. The plate was left in a humidified 5% CO_2 incubator at 37°C for two hours. The extracts from the leaves (methanol, ethyl acetate, *t*-butanol and aqueous extracts) were dissolved in DMSO and diluted with the culture medium to a concentration of 100 and 200 µg/mL. The concentration of DMSO in the diluted solutions was 0.8% (v/v). These solutions were filtered using a sterile 0.22 µm filter unit. A 50 µL aliquot of the diluted solution (200 or 100 µg/mL) of the leaf extracts, Trolox or vitamin C was then added (in triplicates) to the respective wells in the plate containing NIH/3T3 cells at the concentration of 5 x 10^3 cells per well. To test for the ability of these extracts to protect NIH/3T3 cells against DPPH (2,2-diphenyl-1-Picrylhydrazyl) induced cell death, 50 µL of 30 µM DPPH solution was added to the relevant wells one hour after the NIH/3T3 cells were incubated in the presence of the appropriately diluted extracts, Trolox, Vitamin C or cultured medium. The plate was incubated at 37°C for 24 hours. Trolox and vitamin C were used as the positive controls while medium containing 0.4% (v/v) DMSO served as the negative control.

Cell death due to apoptosis was performed using the Cell Death Detection ELISA^{PLUS} kit according to the manufacturer's instruction as described previously [3]. This assay is based on a quantitative sandwich-enzyme-immunoassay principle that utilises mouse monoclonal antibodies directed against DNA and histones associated DNA fragments. Briefly, the plate was centrifuged at 200 × g for 10 minutes at room temperature after 24 hours. The supernatant was

completely removed. Then, the pellet in each well was resuspended in 200 µL of lysis buffer (provided by manufacturer) and the plate was incubated at room temperature for 30 minutes. Following this, the plate was centrifuged at 200 × g for 5 minutes. An aliquot of 20 µL of the supernatant containing the cytoplasmic fraction in each well was carefully transferred into appropriate wells of a streptavidin-coated plate (provided by manufacturer) for further analysis. Then, 80 µL of an immunoreagent (provided by manufacturer) was added into each well. The plate was covered with an adhesive foil and gently shaken at 200 rpm for two hours. The solution in each well was then removed and the wells were thoroughly rinsed thrice with 300 µL of incubation buffer (provided by manufacturer). Following this, 100 µL of ABTS solution (provided by manufacturer) was added into each well and the plate was gently shaken at 200 rpm until suitable colour development was obtained (20-30 minutes). The absorbance of each well was determined using an ELISA plate reader at 405 nm with a reference wavelength of 490 nm. The enrichment factor was calculated using the following formula provided by the manufacturer: Enrichment factor = (Absorbance at 405 nm of treated cells) / (Absorbance at 405 nm of untreated cells).

RESULTS

ABTS radical cation scavenging activity of *P. bleo* leaf extracts

The percentage inhibition of the ABTS radical cations over 12 minutes by the leaf extracts at the highest concentrations is shown in Figure 1. Figure 2 shows the percentage inhibition of ABTS radical cations at the sixth minute versus concentrations of the leaf extracts, as well as the linear regression equations for the graphs of the leaf extracts. The Trolox Equivalent (TE) per gram dry extract for the leaf extracts are presented in Table 1. Among the leaf extracts, the *t*-butanol leaf extract exhibited the highest ABTS radical cation scavenging activity and this was followed by the ethyl acetate leaf extract. The methanol leaf extract and aqueous leaf extract showed comparable ABTS radical cation scavenging activity and were the lowest among the leaf extracts.

Table 1. Trolox Equivalent (TE) µmole per gram dry extract of *Pereskia bleo* leaf extract and vitamin C.

Extract	TE ± S.D.
Methanol leaf extract	176 ± 2
Ethyl acetate leaf extract	208 ± 3
t-Butanol leaf extract	416 ± 15
Aqueous leaf extract	181 ± 2
Vitamin C	5158 ± 3

Anti-proliferation assay

There was a gradual decrease in cell viability with increasing concentrations of all the leaf extracts of

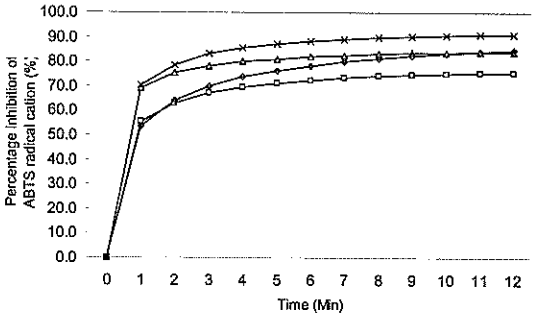

Figure 1. Percentage inhibition of ABTS radical cations in the presence of the extracts from the leaves of *Pereskia bleo* (100 µg/mL of methanol, ethyl acetate or aqueous extracts, 50 µg/mL of *t*-butanol extract) over 12 minutes. The data are expressed as the mean percentages inhibition of ABTS radical cations ± standard deviation (S.D.). □ denotes methanol extract at 100 µg/mL; Δ denotes ethyl acetate extract at 100 µg/mL; × denotes *t*-butanol extract at 50 µg/mL; ◊ denotes aqueous extract at 100 µg/mL.

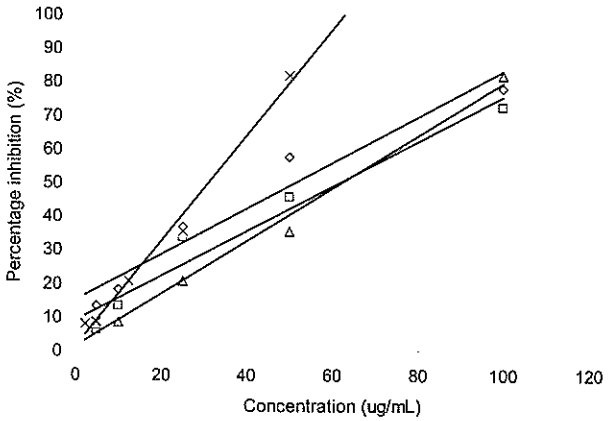

Figure 2. Percentage inhibition of ABTS radical cations by various concentrations of the extracts from the leaves of *Pereskia bleo* at the sixth minute. □ denotes methanol extract; Δ denotes ethyl acetate extract; × denotes *t*-butanol extract; ◊ denotes aqueous extract. The linear regression equations for methanol extract: y = 0.6668x + 8.9156; ethyl acetate extract: y = 0.7867x + 0.9745; *t*-butanol extract: y = 1.5734x + 0.9745; aqueous extract: y = 0.683x + 14.789.

P. bleo against both the 4T1 and 3T3 cells (Fig. 3). However, the IC_{50} values for all the extracts were greater than the highest tested concentration (400 µg/mL). We could not use concentrations higher than 400 µg/mL due to insolubility of these extracts at high concentrations. The percentage cell viability values of the 4T1 and 3T3 cells treated with 400 µg/mL of the various leaf extracts for 72 hours are presented in Table 2. All the extracts resulted in a greater reduction of the percentage viability of the 4T1 cells compared to the 3T3 cells.

Table 2. The percentage of viable 4T1 and 3T3 cultured cells treated with 400 µg/mL of extract from the leaves of *Pereskia bleo* for 72 hours.

Extract	% ± S.D. of viable cells	
	4T1 cells	3T3 cells
Methanol leaf extract	80.81 ± 0.97	107.55 ± 2.00
Ethyl acetate stem extract	72.63 ± 1.65	73.36 ± 7.76
t-Butanol leaf extract	78.55 ± 4.92	100.37 ± 3.57
Aqueous leaf extract	77.44 ± 2.10	105.89 ± 5.41

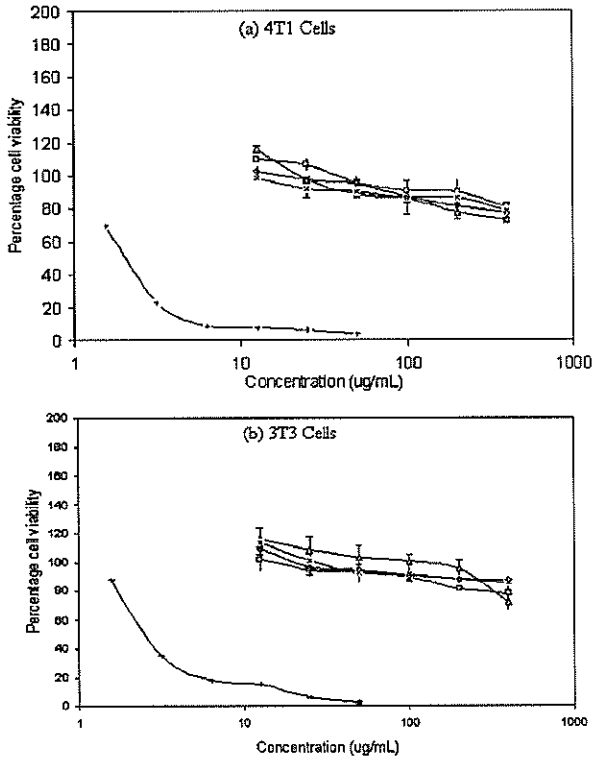

Figure 3. Percentage of viable (a) 4T1 cells and (b) 3T3 cells cultured in the presence of the methanol, ethyl acetate, *t*-butanol and aqueous extracts of the leaves of *Pereskia bleo* for 72 hours. The data are expressed as the mean percentages of cell viability ± standard deviation (S.D.). □ denotes methanol extract; Δ denotes ethyl acetate extract; × denotes *t*-butanol extract; ◊ denotes aqueous extract; + denotes cisplatin.

Ability of leaf extracts of *P. bleo* to limit natural apoptotic cell death in 3T3 cells

Figure 4 shows the enrichment factors calculated when 3T3 cells were cultured in the presence and absence of 50 µg/mL or 100 µg/mL extracts from the leaves of *P. bleo*. The enrichment factor for untreated cells (i.e. negative control) was 1.0. Enrichment factor value less than 1.0 indicated a reduction in cell death by apoptosis. All the leaf extracts were able to reduce natural apoptotic cell death in 3T3 cells. The ability to limit natural apoptotic cell death in 3T3 cells was greater at 50 µg/mL than at 100 µg/mL for all extracts.

Ability of leaf extracts of *P. bleo* to limit oxidant-induced apoptotic cell death in 3T3 cells

An increase in apoptotic cell death was observed in the 3T3 cells cultured for 24 hours in the presence of 10 µM DPPH (Fig. 5). However, the extent of the DPPH-induced apoptotic cell death was reduced when the cells were pre-incubated with extracts from the leaves for one hour before DPPH were added to the culture wells. There was no significant difference in the level of oxidant-induced apoptotic cell death when the 3T3 cells were cultured in the presence of 50 µg/mL of the leaf extract, compared to the higher concentration used i.e.100 µg/mL. The protective effects of all the extracts against oxidant-induced cell death were greater than Trolox or vitamin C.

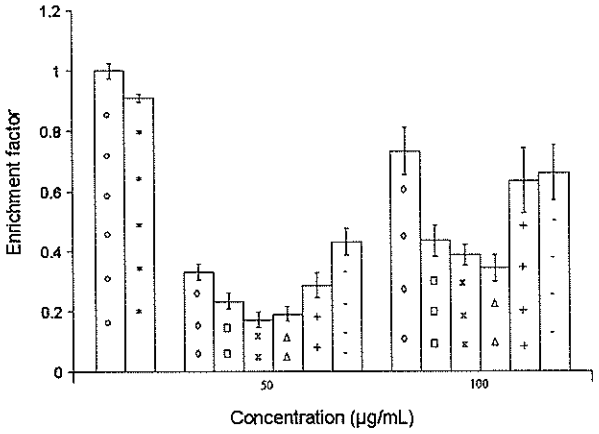

Figure 4. The ability of extracts from the leaves of *Pereskia bleo* to limit natural apoptotic death in 3T3 cells. The data are expressed as the mean enrichment factors ± standard deviation (S.D.). ○ denotes cells in media only; * denotes cells in media containing 0.4% DMSO; ◊ denotes aqueous extract; □ denotes methanol extract; × denotes *t*-butanol extract; Δ denotes ethyl acetate extract; + denotes vitamin C; - denotes trolox.

Among the extracts, the ethyl acetate extract showed the highest protective effect against oxidant-induced apoptotic cell death.

DISCUSSION

The sequential fractionation of the crude methanol extracts of the leaves of *P. bleo* used in this study showed that the bioactive compounds with antioxidant activity were concentrated in the *t*-butanol extract (416 µmole Trolox Equivalent per gram dry weight), followed by the ethyl acetate extract. The methanol and aqueous extracts had similar antioxidant properties. These antioxidant properties are moderate compared to those of commercial black teas and green teas which have antioxidant capacity ranging between 235 µmole Trolox Equivalent per gram dry weight and 1526 µmole Trolox Equivalent per gram dry weight [9]. The antioxidant effects of the extracts are also much less than that of Vitamin C, a known antioxidant compound, which has an antioxidant capacity of 5158 Trolox Equivalent per gram dry weight [9]. As such, the leaf of *P. bleo* cannot be considered to be a rich source of antioxidants.

The IC_{50} values for all the crude and fractionated extracts of the leaves of *P. bleo* were greater than 400 µg/mL. The extracts could not be tested at higher concentrations due to the lack of solubility. According to the National Cancer Institute guideline, the crude extract of a plant should have an IC_{50} value of less than 20 µg/mL in order to be considered as cytotoxic against the treated cells [11]. The results suggested that these extracts did not contain significant amount of compounds with anti-proliferative properties. Since the anti-proliferative activity of the fractionated extracts (ethyl acetate, *t*-butanol and aqueous extracts) are not greater than that of the crude methanol extract, the methanol extract is unlikely to contain any significant amount of anti-proliferative compounds. A comparison with the reported anti-proliferative activity of the stem extracts of *P. bleo* [6] shows that the leaf extracts have higher anti-proliferative activity. Moreover, the leaf extracts have a higher anti-proliferative effect on the 4T1 mouse mammary cancer cells compared to the normal 3T3 mouse fibroblast cells. However, the reverse trend has been reported for the stem extracts [6]. This indicates that the leaf extracts of *P. bleo* might be a better target to be developed as anti-cancer agent compared to the stem extracts.

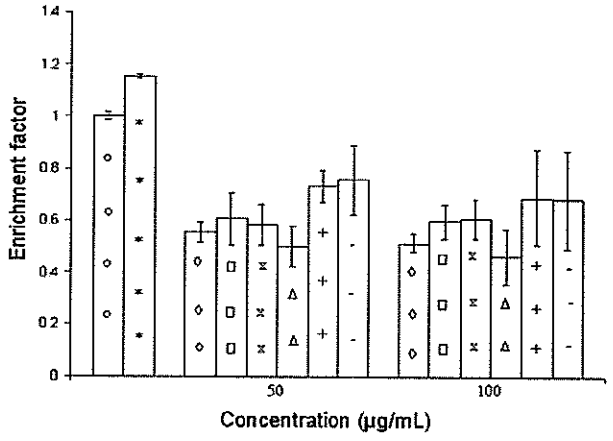

Figure 5. The ability of extracts from the leaves of Pereskia bleo to limit DPPH-induced apoptotic death in 3T3 cells. The data are expressed as the mean enrichment factors ± standard deviation (S.D.). o denotes cells in media only; * denotes cells treated with DPPH; ◊ denotes aqueous extract; □ denotes methanol extract; × denotes t-butanol extract; Δ denotes ethyl acetate extract; + denotes vitamin C; - denotes trolox.

Treatment of the normal mouse fibroblast cells (3T3) with the leaf extracts of *P. bleo* for 24 hours resulted in a lower level of apoptosis in the cells compared to that occurring in the non extract-treated cells grown under the same conditions. The results indicated that all the methanol, ethyl acetate, *t*-butanol and aqueous extracts had the ability to protect the 3T3 cells against natural programmed cell death by apoptosis. The protective effects were more obvious at 50 µg/mL compared to 100 µg/mL of the extracts. The higher level of apoptosis at the higher extract concentration was consistent with the results of the anti-proliferation assay which showed a gradual decrease in cell viability with increasing extract concentration. All the fractionated extracts of the leaves of *P. bleo* showed higher apoptosis-limiting activities than the crude methanol extract, except the aqueous extract. This suggested that the crude methanol extracts contained bioactive component(s) that could protect the normal mouse fibroblast cells against natural apoptotic cell death, and these components could be concentrated by fractionating the crude methanol extracts.

The protective effects of the leaf extracts of *P. bleo* against oxidant-induced cell death were also evaluated by pre-treating the 3T3 cells with the extracts before the oxidant, 2,2-Diphenyl-1-Picrylhydrazyl (DPPH), was added. All the extracts were able to limit oxidant-induced cell death, with the ethyl acetate extract being

the most effective. The ability to limit oxidant-induced cell death was not significantly different between 50 µg/mL and 100 µg/mL of the extracts, indicating that the maximum effective concentration was reached.

The findings on the protective effects of the extracts against oxidant-induced cell death were consistent with the moderate antioxidant activities of the extracts determined by the ABTS radical cation scavenging assay. Nevertheless, the *t*-butanol extract possessed the highest *in vitro* antioxidant activity, whereas the ethyl acetate extract was more effective in limiting oxidant-induced cell death. The ability of the extracts to scavenge ABTS radical cation implied that these extracts could act as reactive oxygen species scavenger in diseases caused by oxidant-induced cell death. An example of plants which possess such property is *Pogostemon cablin*, a well-known Korean traditional medicine that has been proven to be beneficial for patients with cerebral stroke [12]. The water extract of *P. cablin* has been shown to be able to protect the human neuroglioma cells against necrotic and apoptotic cell death induced by hydrogen peroxide. The protective effects of the *P. bleo* extracts against oxidant-induced cell death should be investigated further for their potential to be developed for treatment of neurodegenerative diseases which can be caused by reactive oxygen species.

From this study, we can conclude that all of the crude methanol and fractionated ethyl acetate, *t*-butanol and aqueous extracts of the leaves of *P. bleo* do not have significant anti-proliferative effect on both the mouse mammary cancer cells (4T1) and the normal mouse fibroblast cells (3T3). They are not cytotoxic, based on the criterion that a crude extract should have an IC_{50} of less than 20 µg/mL for it to be considered cytotoxic against the treated cells [11]. Nevertheless, the leaf extracts exhibited selectivity in inhibiting the proliferation of the mouse mammary cancer cells as opposed to the normal mouse fibroblast cells. One possible mechanism for the selective killing of the cancer cells may be related to the ability of the extracts to activate the p53 function in tumour cells, causing their growth arrest or apoptosis, as reported in Ashwagandha (*Withania somnifera*), a herb commonly used in Ayurvedic medicine [13]. Among the extracts tested, the *t*-butanol extract of the leaves of *P. bleo* possesses the highest antioxidant property. Yet, the antioxidant capacity is only moderate when compared to other known antioxidant substances such as green tea leaves and vitamin C. The ability of the extracts of the leaves of *P. bleo* in limiting natural and oxidant-induced cell death in normal mouse fibroblast cells suggests that the plant may be useful as a remedy for diseases related to oxidative stress.

Acknowledgement – We would like to thank Taman Pertanian Malaysia, Universiti Putra Malaysia, for kind donation of the *Pereskia bleo* plant. This work was supported by a grant from the International Medical University.

REFERENCES

1. Goh K.L. (2000) *Malaysian Herbaceous Plants*. Millennium Edition. Advanco Press, Malaysia.
2. Tan M.L., Sulaiman S.F., Najimuddin N., Samian M.R. and Tengku Muhammad T.S. (2005) Methanolic extract of *Pereskia bleo* (Kunth) DC. (Cactaceae) induces apoptosis in breast carcinoma, T47-D cell line. *Journal of Ethnopharmacology* **96**: 287-294.
3. Er H.M., Cheng E. and Radhakrishnan A.K. (2007) Anti-proliferative and mutagenic activities of aqueous and methanol extracts of leaves from *Pereskia bleo* (Kunth) DC (Cactaceae). *Journal of Ethnopharmacology* **113**: 448-456.
4. Abd Malek S.N., Abdul Wahab N., Yaacob H., Sim K.S., Hong S.L., Lee G.S. and Rahman S.N.S.A. (2008) Cytotoxic activity of *Pereskia bleo* (Cactaceae) against selected human cell lines. *International Journal of Cancer Research* **4**: 20-27.
5. Wahab S.I.A., Abdul A.B., Mohan S.M., Al-Zubairi A.S., Elhassan M.M. and Ibrahim M.Y. (2009) Biological activities of *Pereskia bleo* extracts. *International Journal of Pharmacology* **5**: 71-75.
6. Lee H.L., Er H.M. and Radhakrishnan A.K. (2009) In vitro anti-proliferative and antioxidant activities of stem extracts of *Pereskia bleo* (Kunth) DC (Cactaceae). *Malaysian Journal of Science* **28**: 225-239.
7. Ryter S.W., Kim H.P., Hoetzel A., Park J.W., Nakahira k., Wang X. and Choi A.M.K. (2007) Mechanisms of cell death in oxidative stress. *Antioxidants and Redox Signaling* **9**: 49-89.
8. Larson R.A. (1988) The antioxidants of higher plants. *Phytochemistry* **27**: 969-978.
9. Re R., Pellegrini N., Proteggente A., Pannala A., Yang M. and Rice-Evans C. (1999) Antioxidant activity applying an improved ABTS radical cation decolorization assay. *Free Radical Biology and Medicine* **26**: 1231-1237.
10. Carmichael J., DeGraff W.G., Gazdar A.F., Minna J.D. and Mitchell J.B. (1987) Evaluation of a tetrazolium-

based semiautomated colorimetric assay: assessment of radiosensitivity. *Cancer Research* **47**: 943-946.

11. Geran R.I., Greenberg N.H., Macdonald M.M., Schumacher A.M. and Abbott B.J. (1972) Protocols for screening chemical agents and natural products against animal tumours and other biological system. *Cancer Chemotherapy Reports* **3**: 59-61.
12. Kim H.W., Cho S.J., Kim B., Cho S.I. and Kim Y.K. (2010) *Pogostemon cablin* as ROS scavenger in oxidant-induced cell death of human neuroglioma cells. *Evidence-based Complementary and Alternative Medicine* **7**: 239-247.
13. Widodo N., Kaur K., Shrestha B.G., Takagi Y., Ishii T., Whadhwa R. and Kaul S.C. (2007) Selective killing of cancer cells by leaf extract of Asgwagandga: Identification of a tumor-inhibitory factor and the first molecular insights to its effect. *Clinical Cancer Research* **13**: 2298-2306.

Journal of Science and Technology in the Tropics (2010) **6**: 39-42

Abdominal colour polymorphism in female Asian Golden Web Spider *Nephila antipodiana* (Araneae: Nephilidae)

Yong Hoi Sen[1], Rosli Hashim[1], Daicus Belabut[1] and Lim Phaik Eem[1,2]
[1]Institute of Biological Sciences, University of Malaya, 50603 Kuala Lumpur, Malaysia
[2]Institute of Ocean and Earth Science, University of Malaya, 50603 Kuala Lumpur, Malaysia
(E-mail: yong@um.edu.my)

Abstract *Nephila antipodiana* (Batik Golden Web Spider) occurred in large numbers in several localities in Kelantan and Terengganu, east coast of Peninsular Malaysia. Three abdominal (opisthosomal) colour morphs – yellow, greenish-yellow and reddish-brown – were present in adult female spiders. Only two colour morphs appear to be present in a particular locality. The yellow morph occurred in all the localities investigated. Of the two non-yellow morphs, the reddish-brown morph was found only in one locality while the greenish-yellow morph was more widespread. The present study does not show unequivocally the association of colouration with habitat usage. Whether yellow colour in *N. antipodiana* confers a selective advantage remains to be verified. In addition to opisthosomal colour polymorphism, the colour and number of spots (or sigillae) on the dorsal surface of the abdomen of female *N. antipodiana* are also variable. The juvenile spiders have different colour pattern from the adults.

Keywords polymorphism – golden web spider – Arachnida – Malaysia – opisthosoma colour

INTRODUCTION

The Batik (or Asian) Golden Web Spider *Nephila antipodiana* (Walckenaer 1842) was first reported in Peninsular Malaysia (and Malaysia) in 2009 [1]. It was originally described as *Epeira antipodiana* Walckenaer 1842. It is distributed in China, Philippines to New Guinea, Solomon Is., and Queensland [2]. In Southeast Asia it has been recorded in Singapore, Indonesia, Thailand and the Philippines [3, 4]. It has also been found in Borneo (Joseph K.H. Koh, pers. comm.).

It is evident from the literature that *N. antipodiana* is a variable species [1, 3-5]. In the Philippines the dorsal colour of the abdomen (opisthosoma) in the female is yellow, with six pairs of subovate yellow spots dorsally arranged longitudinally in rows, each spot with a thin black margin [4]. The abdomen of the female spider in Australasia is pale yellow, with darker markings on anterior and posterior margins, and without large yellow spots [5]. In Singapore the dorsal colour of the abdomen may be yellowish green [3] or reddish brown [1] with yellow spots.

Although abdominal (opisthosomal) colour variation occurs in the species, as evidenced in the different colour morphs, there is no report on polymorphism. We report here the occurrence of polymorphism in the dorsal abdominal colour of adult female *N. antipodiana* in Peninsular Malaysia.

MATERIALS AND METHODS

A field survey of *N. antipodiana* was carried out from 12-15 February 2010 in Kelantan and Terengganu, Peninsular Malaysia. The dorsal colour (yellow, greenish-yellow, and reddish-brown) of the abdomen of every adult female spider in a chosen locality was recorded. The number of juvenile and associated male individuals was also recorded. Five localities were studied – four in Kelantan (Pantai Melawi and Sungai Dua in Bachok, Tok Bok in Machang, and Gua Musang highway) and one in Terengganu (Lata Belatan). Pantai Melawi consisted of eight patches which were separated although not far from each other.

Bachok is situated near the coast, with typical Malay village setting. Both Machang and Gua Musang are in the interior. Lata Belatan is a forest

recreation park – the study was carried out along the road bordered by plantation.

Representative specimens were collected and preserved in ethanol. Photographs were also taken of the various colour morphs and life stages.

RESULTS

Three principal abdominal colour morphs – yellow (Figs. 1, 2), greenish yellow (Fig. 3) and reddish brown (Fig. 4) – were observed in the adult female *N. antipodiana*. Their occurrence and abundance in four localities in Kelantan and one in Terengganu are summarized in Table 1. The juveniles (Fig. 5) and males were not included as the former had different colour pattern and the male did not show colour variation.

The yellow morph was present in all the five localities. Of the other two morphs, the greenish-yellow morph was found only in Kelantan while the reddish-brown morph was observed in Lata Belatan, Terengganu. The frequency of the yellow morph ranged from 7.69% in Sungai Dua, Bachok to 25.71% in Lata Belatan, Terengganu (Table 1).

DISCUSSION

Colour and pattern variation in spiders has been widely investigated [6]. To-date three major classes of pigments – ommochromes (yellow, red, brown), bilins (blue, green) and guanine (white, silver) – have been identified. The earlier work before 1998 on the evolution and ecology of spider colouration has been well reviewed [6]. Although polymorphisms have been reported for a number of species, the genetic bases have generally not been elucidated. In general, sex linkage appears to be absent but sex limitation is quite common. It is acknowledged that the manifestation of spider colouration is very complex, involving a host of possible factors. Various functions have been suggested – cryptic/disruptic, mimetic and aposematic as well as thermoregulatory.

The Hawaiian happy-face spider, *Theridion grallator* Simon (Theridiidae) provided the most spectacular example of colour polymorphism in spiders. In this spider, the opisthosomal colour may be controlled by simple Mendelian alleles at a single autosomal locus or multiple closely linked loci. The plain yellow morph is recessive to the other colour morphs [7, 8]. More recently, another species *Theridion californicum* Banks has been found to exhibit an equally extraordinary visible colour and pattern polymorphism [9]. The polymorphism comprises one common morph (Yellow) and at least ten relatively rare patterned morphs, with Yellow probably recessive to all other morphs.

In the present study, the yellow morph of female *N. antipodiana* occurred in all the localities investigated (Table 1). Lata Belatan had the highest percentage (25.71%). This locality had denser vegetation, being in a plantation area. In Gua Musang highway, an open area, the percentage was 16.98%. Although it has been suggested that yellow colour is most cryptic in the below-leaf environment and hence selected for

Table 1. Abundance of abdominal colour morphs in adult female *Nephila antipodiana* from four localities in Kelantan and Terengganu, east coast of Peninsular Malaysia, recorded in February 2010.

Locality	Greenish Yellow	Yellow	Reddish Brown	% Yellow
Bachok: Pantai Melawi				
1 outside chalet	2	2		50.00
2 coconut palms	28	3		9.68
3 house compound	39			0
4 waste land	18			0
5 coconut palms	26	1		3.70
6 *Hibiscus tiliaceus*	33	5		13.16
7 coconut palms	8	6		42.86
8 open space	7	2		22.22
Total (1 – 8)	161	19		10.56
Bachok: Sungai Dua	24	2		7.69
Machang: Tok Bok	82	10		10.87
Gua Musang: highway	44	9		16.98
Terengganu: Lata Belatan		27	78	25.71

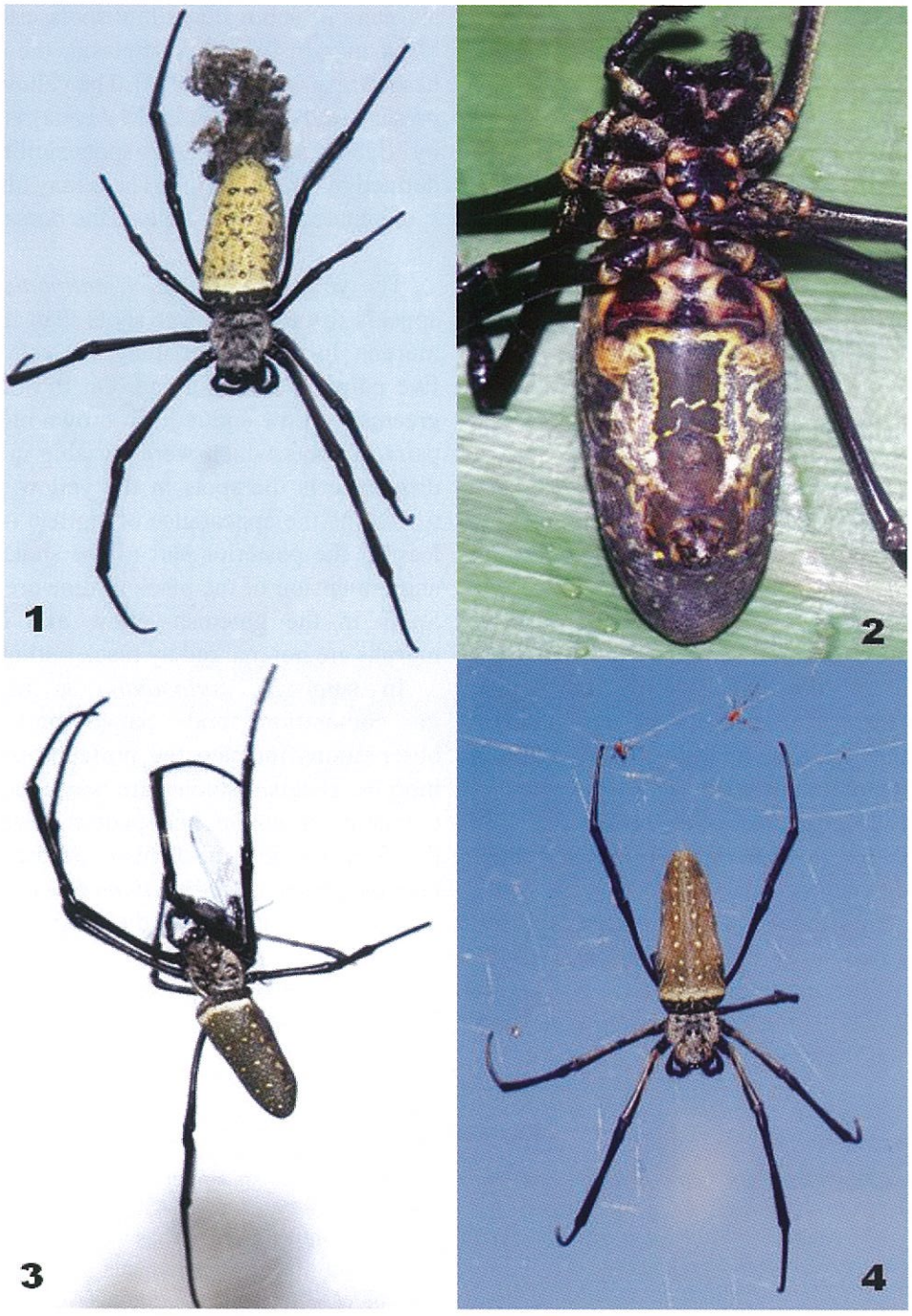

Figures 1-4. Abdominal colour morphs of adult female *Nephila antipodiana* (photos: H.S. Yong). **1**. Yellow morph; **2**. Venter of a Yellow morph; **3**. Greenish-yellow morph; **4**. Reddish-brown morph.

[9], the present study does not show unequivocally the association of colouration with habitat usage. Whether yellow colour in *N. antipodiana* confers a selective advantage remains to be verified. In Pantai Melawi with a mixture of micro-habitats, the percentage of yellow morph ranged from 9.68% to 42.86% in patches with coconut palms while in an open space it was 22.22% in contrat to 13.16% in an area with *Hibiscus tiliaceus* (Table 1).

It is noteworthy that in the present study only two colour morphs appear to be present in a particular locality (Table 1). Of the two non-yellow morphs, the reddish-brown morph was found only in one locality (Lata Belatan) whereas the greenish-yellow morph

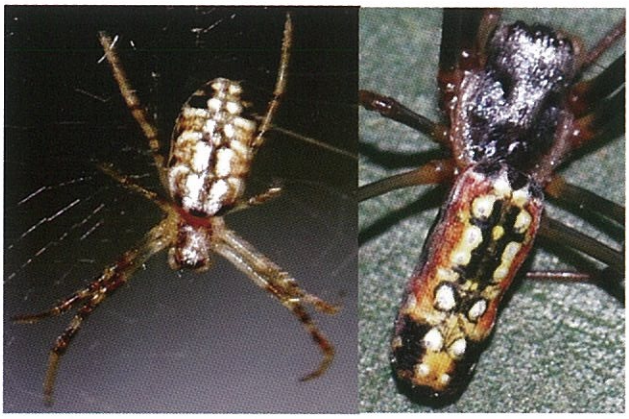

Figure 5. Juvenile female *Nephila antipodiana* with different colour pattern from adult female spider. (photo: H.S. Yong)

was more widespread. The reddish-brown morph was found in Teluk Chempedak, Pahang where *N. antipodiana* was first reported for Peninsular Malaysia [1]. In this locality, a yellow individual had been observed in the hill forest (H. S. Yong, unpublished information). At the University of Malaya, a single individual of the greenish morph had been found among ornamental palms (H. S. Yong, personal observation). The significance of the presence of only a single non-yellow morph in a particular locality remains to be elucidated.

In addition to opisthosomal colour polymorphism, the colour and number of spots (or sigillae) on the dorsal surface of the abdomen of *N. antipodiana* are also variable. The dorsum may be marked with spots or sigillae. In the Philippines, the yellow morph has six pairs of subovate yellow spots, each with a thin black margin [4]. In Australasia, the dorsal surface has four pairs of sigillae [5]. The yellow morph in the present study (Peninsular Malaysia) is characterized by five pairs of yellow spots/sigillae, each well defined by black margin. There may also be a sigilla/spot situated at the middle of the dorsal surface (Fig. 1).

The yellow morph of *N. antipodiana* in general appears to possess fewer spots than the non-yellow morphs. In the present study, the yellow morph had five pairs of spots/sigillae. On the other hand, the greenish-yellow and reddish-brown morphs had nine pairs of spots which were variable in size. Another difference is the spots in the yellow morph tended to assume the appearance of sigillae – depression at least at the posterior part of the spot. The intensity and dimension of the black outline are also variable. Spots in the greenish-yellow and reddish-brown morphs are not marked by black outline.

In sum, *N. antipodiana* is highly variable in colouration and pattern/marking. Cursory observations indicate the presence of other colour morphs. Detailed studies are needed to elucidate the ontogeny of colour and pattern development, and the function and mechanism of the variation and polymorphism. *N. antipodiana* could be an excellent model for evolutionary and ecological studies.

Acknowledgements – We thank the University of Malaya for financial and other supports to carry out this study.

REFERENCES

1. Yong H.S. (2009) *Nephila antipodiana* (Araneae: Nephilidae) from Pahang: a new record for Peninsular Malaysia. *Journal of Science and Technology in the Tropics* **5**: 19-21.
2. Platnick N.I. (2010) *The world spider catalog, version 10.5*. American Museum of Natural History, online at http://research.amnh.org/entomology/spiders/catalog/index.html.
3. Koh J.K.H. (1989) *A guide to common Singapore spiders*. Singapore Science Centre, Singapore.
4. Barrion A.T. and Litsinger J.A. (1995) *Riceland spiders of South and Southeast Asia*. CAB International, Wallingford, UK.
5. Harvey M.S., Austin A.D. and Adams M. (2007) The systematic and biology of the spider genus *Nephila* (Araneae: Nephilidae) in the Australasian region. *Invertebrate Systematics* **21**: 407-451.
6. Oxford G.S. and Gillespie R.G. (1998) Evolution and ecology of spider coloration. *Annual Review of Entomology* ***43***: 619-643.
7. Gillespie R.G. and Tabashnik B. (1989) What makes a happy face? Determinants of colour pattern in the spider *Theridion grallator* (Araneae, Theridiidae). *Heredity* **62**: 335-363.
8. Oxford G.S. and Gillespie R.G. (1996) Genetics of a colour polymorphism in *Theridion grallator* (Araneae: Theridiidae), the Hawaiian happy-face spider, from Greater Maui. *Heredity* **76**: 238-248.
9. Oxford G.S. (2009) An exuberant, undescribed colour polymorphism in *Theridion californicum* (Araneae, Theridiidae): implications for a theridiid pattern ground plan and the convergent evolution of visible morphs. *Biological Journal of the Linnean Society* **96:** 23-34. With 2 figures.

Journal of Science and Technology in the Tropics (2010) **6**: 43-47

Scaled down operation of the United Nations University/International Centre for Theoretical Physics Plasma Focus Facility (UNU/ICTP PFF) as an extreme ultraviolet source

Rattachat Mongkolnavin[1*], Prajya Tangitsomboon[1] and Chiow San Wong[2]
[1]Department of Physics, Faculty of Science, Chulalongkorn University, Bangkok 10330, Thailand
[2]Plasma Research Laboratory, Physics Department, Faculty of Science, University of Malaya, 50603 Kuala Lumpur, Malaysia
(*E-mail: rattachat.m@chula.ac.th)

Abstract The possibility of operating the 3.3 kJ United Nations University/International Centre for Theoretical Physics Plasma Focus Facility (UNU/ICTP PFF) with a scaled down electron temperature so as to tune the emission spectrum to the EUV region is being considered. In particular, we investigated the scaled down operation of this plasma focus device from its original 3.3 kJ electrical input energy to as low as 960 J. Experiments show that for discharges performed at 8 kV and with a shortened electrode length of 9 cm from the original 16 cm, the emission was predominantly in the wavelength range of 12 to 18 nm.

Keywords plasma focus – EUV source

INTRODUCTION

The development of Extreme Ultraviolet (EUV) radiation sources is recently gaining much interest in semiconductor manufacturing industry due to the expectation that the Next Generation Lithography (NGL) will be using the wavelength of 13.5 nm [1]. Many types of EUV radiation sources, including the laser produced plasma and pulsed discharge sources such as the capillary discharge [2, 3], vacuum spark [4, 5] and plasma focus [6, 7] are being considered by researchers worldwide. These radiation sources, especially the pulsed discharge sources are favourable as EUV radiation source because of their lower cost and simplicity in operation when compared to other radiation sources.

The United Nations University/International Centre for Theoretical Physics Plasma Focus Facility (UNU/ICTP PFF) is a 3.3 kJ Mather type plasma focus [8] which is optimized to produce fusion neutrons with deuterium as the operating gas [9]. With argon or xenon as the working gas, it is known to be capable of producing intense radiation in the X-ray region [10-12]. The typical plasma produced by the optimized UNU/ICTP PFF has electron temperature of several keV and expected electron density of greater than 10^{19} cm^{-3} [8].

In this work, we consider the possibility of scaling down the temperature of the UNU/ICTP PFF argon plasma focus so as to operate it as an EUV radiation source. The scaling can be done in two approaches. The first approach is by reducing the electrical input energy or by increasing the operating pressure while the original geometry of the UNU/ICTP PFF is maintained. In this case, the dynamics of the current sheet is slowed down so that the focusing occurs at a time after the peak of the discharge current for electrodes with original length of 16 cm. This will effectively make the focus less efficient although the required electron temperature of around 110 eV can be obtained. In the second approach, the reduced efficiency caused by the mismatch of the dynamic characteristic time and the electrical characteristic time can be compensated by reducing the length of the electrodes. A discharge voltage of as low as 6.5 kV corresponding to an electrical input energy of 634 J is shown to be sufficient.

According to the Coronal Equilibrium Model (CEM), there are two possible ranges of temperature at which argon plasma is expected to consist of

ionic species that can be considered as emitters of line radiations at wavelength around 13.5 nm. At a temperature of around 10 to 20 eV, the Ar^{6+} and Ar^{7+} are prominent, whereas at a temperature of around 100 to 130 eV, the argon plasma is expected to consist of predominantly the Ar^{10+} and Ar^{11+} ionic species. The population distribution of these two groups of ionic species as predicted by the CEM is illustrated in Figure 1. These ionic species are known to be able to emit intense line radiations at or near 13.5 nm as listed in Table 1 [13].

In order to test the possibility of tuning the UNU/ICTP PFF to produce condition which is sufficient to produce intense EUV radiation but not X-ray, we scaled down the operating parameters, particularly the input electrical energy. In order to match the slower dynamics of the current sheet due to the lowering of the input energy, the electrode lengths of the device were reduced to 9 cm and 7.5 cm and the discharge voltage was reduced to 8 kV and 6.5 kV respectively, corresponding to input energy of 960 J and 634 J respectively. The operating pressure was adjusted within the range of 0.5 to 2.5 mbar for fine tuning. Focusing action was obtained over this range of pressure and the radiation emission in the EUV region was observed consistently.

Table 1. Expected lines near 13.5 nm from argon ions Ar^{6+}, Ar^{7+}, Ar^{10+} and Ar^{11+}.

Ion	Wavelength (nm)	Transition	Upper level	Lower level
Ar^{6+}	13.4797	5p-3s	$(3s5p)^1P_1$	$(3s^2)^1S_0$
Ar^{7+}	13.5591	9f-4d	$(9f)^2F_{7/2}$	$(4d)^2D_{5/2}$
Ar^{10+}	13.57	2p-2s	$(2s2p^5)^1P_1$	$(2p^4)^3P_1$
Ar^{10+}	13.563	2p-2s	$(2s2p^5)^1P_1$	$(2p^4)^3P_1$
Ar^{11+}	13.6	2p-2s	$(1s^22p^5)^2P_{3/2}$	$(2s2p^4)^4P_{3/2}$

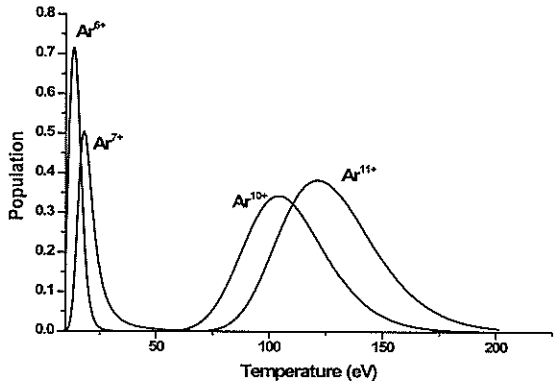

Figure 1. The temperature range at which argon ions Ar^{6+}, Ar^{7+}, Ar^{10+} and Ar^{11+} are prominent predicted by Coronal Equivalent Model.

EXPERIMENTAL SETUP

The experimental setup is shown schematically in Figure 2. The electrode system consisted of a central hollow copper anode of 1.9 cm diameter, and a cathode of six copper rods arranged in a circle of 6.4 cm diameter concentric with the anode. The anode was insulated from the cathode at the back-wall by a Pyrex glass tube. Three anode lengths were used, including the original length of 16 cm, and two other shorter lengths of 9 cm and 7.5 cm. The plasma focus was operated with argon at pressures in the range of 0.5 to 2.5 mbar. The discharge voltage was varied from 6 kV to 12.5 kV. The diagnostics used included the Rogowski coil for discharge current measurement, resistive voltage divider for transient voltage measurement, PIN Si-diodes for X-ray measurement, and silicon p-n junction photodiode with integrated multilayer thin film filter for EUV measurement.

The BPX65 PIN Si-diode operated with its glass window removed is now commonly used for the measurement of soft X-ray from pulsed plasma due to its fast rise-time of 2 ns [10, 12]. BPX65 diode purchased off the shelf has a typical spectral response of above 0.1 A/W in the wavelength range of 450 nm to 1050 nm, with a peak spectral response of 0.55 A/W at 900 nm [11]. However, with the front glass window of its TO-18 casing removed, its spectral response can be extended to the X-ray region. In order to exclude photons in the visible region, the diode was covered by 24 μm aluminized Mylar.

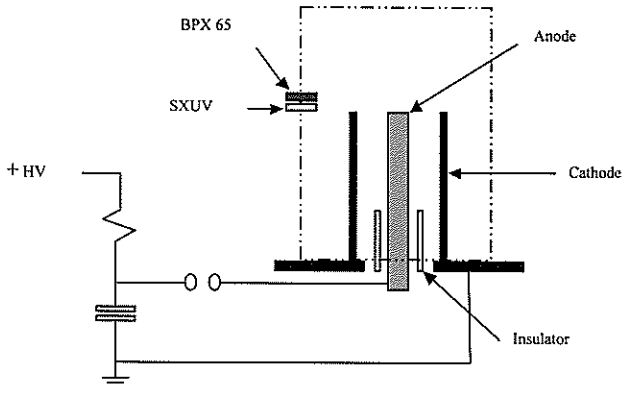

Figure 2. Schematics showing the experimental setup.

A silicon p-n junction photodiode with 100 nm silicon and 200 nm zirconium directly deposited filter [15] was used to measure EUV radiation in the wavelength range of 12 nm to 18 nm. The responsivity curves of the modified BPX65 covered with 24 μm aluminized Mylar and SXUV diode with 100 nm Si and 200 nm Zr multilayer filter, plotted on the same graph, are shown in Figure 3. It can be seen that the filtered BPX65 was responsive to photons with wavelength below 1 nm, with peak response of 0.147 A/W at wavelength of 0.35 nm. On the other hand, the silicon p-n junction diode had a clear pass band in the range of 12 to 18 nm, with peak response of 0.095 A/W at wavelength of 12.8 nm. While the visible range was clearly rejected by the filter, the response of this diode to photons in X-ray region was not certain. In the experiments described here, the filtered BPX65 and the filtered SXUV were used to measure the radiation emitted from the plasma simultaneously. They were mounted to view the plasma in the side-on location at a distance of 30 cm from the axis of the electrode system. This allowed us to identify without ambiguity the spectral range of the radiation detected.

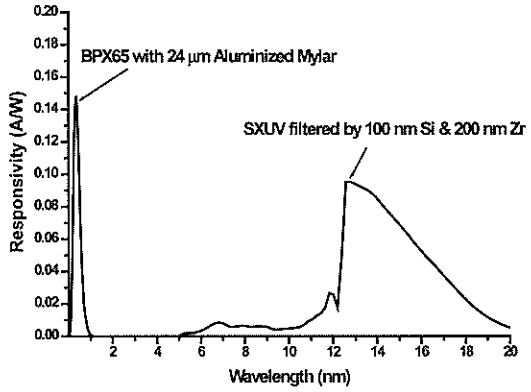

Figure 3. The responsivity curves of BPX65 PIN diode (with 24 μm aluminized Mylar) plotted together with that of SXUV p-n junction diode with 100 nm Si and 200 nm Zr.

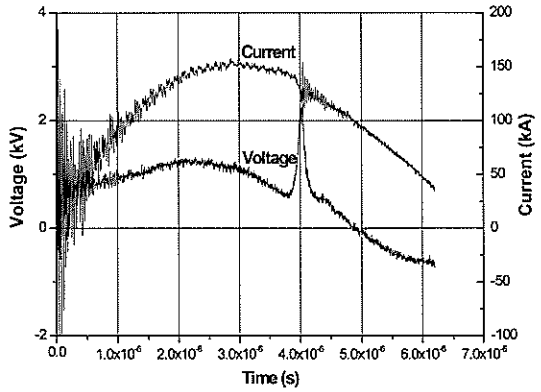

Figure 4. The typical current and voltage signals of a plasma focus discharge.

RESULTS AND DISCUSSION

In its original design, the UNU/ICTP PFF had an electrode length L = 16 cm. For a typical focusing discharge at discharge voltage V = 12.5 kV and at an operating pressure P = 0.5 mbar argon, the signature voltage spike and current dip (Fig. 4) are consistently obtained. Under this operating condition, the current sheet in the axial acceleration phase of the plasma focus dynamics achieves an average speed of about 4 cm μs^{-1}. The X-ray emission characteristics of the plasma produced under similar condition had been studied and reported before [7, 9]. In this study, the measurement of the emission was extended to the EUV region by using a SXUV silicon p-n junction photodiode together with a BPX65 PIN diode. The signals obtained, together with the voltage spike of a typical 12.5 kV discharge, operated at 0.5 mbar argon of the UNU/ICTP PFF with an electrode length of 16 cm are shown in Figure 5

The X-ray emission for a typical focusing discharge of the UNU/ICTP PFF at V = 12.5 kV, P = 1.5 mbar argon and with L = 16 cm is as shown in Figure 5. This X-ray pulse is similar to those observed in many plasma focus devices as reported in the literature [10-12]. It indicates the hottest phase of the plasma produced. The occurrence of the hottest phase of the plasma coincided with the peak of the voltage spike. Correspondingly, the SXUV diode registered a large EUV pulse. From the area under

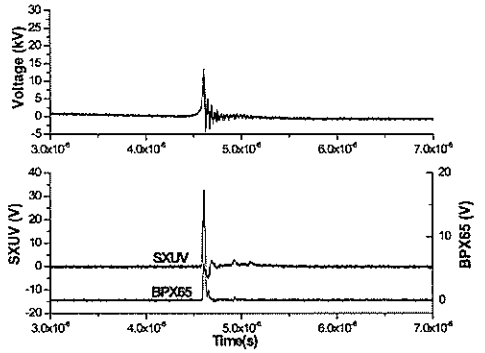

Figure 5. The voltage, EUV and X-ray signals obtained simultaneously for a 12.5 kV discharge of a plasma focus with electrode length L = 16 cm and operated with 1.5 mbar argon.

this EUV pulse, the total photon energy emitted from the plasma (assuming isotropic source) in the range of 12 to 18 nm could be estimated to be about 50 mJ.

While the detection of the X-ray pulse for the 12.5 kV discharge is known to indicate the formation of a focused plasma with temperature of probably greater than 1 keV, the absence of X-ray radiation in a 8 kV discharge is believed to indicate a lower temperature plasma. The set of similar signals (Fig. 5) obtained for an 8 kV discharge at 0.5 mbar argon is shown in Figure 6. In this discharge, the length of the electrodes of the UNU/ICTP PFF was shortened to 9 cm. This discharge displays several features of its radiation emission which are distinctly different from that of the 12.5 kV discharge. Firstly, no X-ray was detected for this discharge indicating lower temperature plasma. The voltage signal showed multiple spikes with low amplitudes. The corresponding EUV signal also consisted of multiple pulses which occurred over duration of more than 2 μs. The peak amplitude of the pulse, however, was much lower than those observed for discharges at 12.5 kV. However, due to long pulse width, the area under this pulse corresponded to total photon energy of about 100 mJ. The input energy of the UNU/ICTP PFF was further tuned down to 540 J by operating at condition of V = 6.5 kV and L = 7.5 cm. The output EUV pulse was insignificantly low as compared to those operated at 8 kV discharge voltage.

In order to fine tune the EUV output from the plasma focus at the three discharge voltages tested, namely V = 12.5 kV, 8 kV and 6 kV, the operating pressure was varied from 0.5 mbar to 2.5 mbar for a series of discharges. From the area under the EUV pulse, the total photon energy emitted in the range of 12 to 18 nm was estimated and plotted (Fig. 7). It can be seen that discharges with higher input energy of 2.3 kJ was able to produce EUV pulses with higher amplitudes and shorter duration, but the total energy corresponding to the photons emitted within the spectral range of 12 to 18 nm was lower than those emitted from discharges at 960 J input energy. EUV energy of up to 100 mJ can be obtained from a 8 kV discharge operated with 0.5 mbar argon.

CONCLUSION

By adjusting the operating parameters of the UNU/ICTP PFF operated with argon from its originally designed values of discharge voltage V = 15 kV, electrode length L = 16 cm and P = 0.5 to 2.5 mbar argon, we have obtained the possible experimental conditions to operate it to produce plasmas with conditions sufficient for emission up to the EUV spectral range of 12 to 18 nm. The radiation energy corresponding to this spectral range emitted from a discharge with V = 12.5 kV, L = 16 cm and P = 0.5 to 2.5 mbar may be up to 95 mJ. This emission, however, is accompanied by emission of X-ray photons in the wavelength range of 0.3 to 3 nm. The plasma produced under this condition is expected to have achieved an electron temperature of up to several keV. However, when the same plasma focus device is operated at a scaled down condition of V

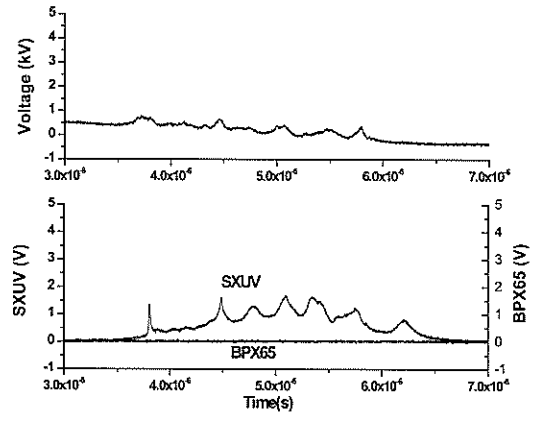

Figure 6. The voltage, EUV and X-ray signals obtained simultaneously for a 8 kV discharge of a plasma focus with electrode length L = 9 cm and operated with 0.5 mbar argon.

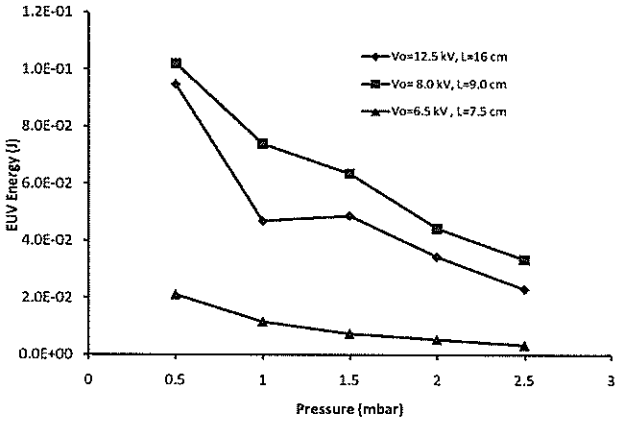

Figure 7. The variation of output EUV energy for three sets of operation condition of discharge voltage V and electrode length L at various pressure P. (i) V = 12.5 kV, L = 16 cm; (ii) V = 8 kV, L = 9 cm; and (iii) V = 6.5 kV, L = 7.5 cm.

= 8 kV, L = 9 cm and with operating pressure in the range of P =0.5 to 2.5 mbar argon, up to 102 mJ of EUV photon energy can be produced and in this case, no X-ray photon is produced. We expect the electron temperature achieved in this case to be in the range of several tens electron-volts. If one is currently having the UNU/ICTP PFF and intend to use it as an EUV source to test for the effect of EUV on a substract which has good absorption in both the X-ray and EUV regions, it may be necessary to eliminate the X-ray component of the emission. In this case the scaled down operation of the existing UNU/ICTP PFF may be a possible solution. With this possibility demonstrated, it is still necessary to point out that the device can be further tuned to obtain the condition for optimum EUV output.

Acknowledgements – The authors would like to extend their great appreciation to Asian African Association for Plasma Training (AAAPT) for its support to initiate plasma focus research in this laboratory and to the Graduate School, Chulalongkorn University for financial support.

REFERENCES

1. Banine V. and R. Moors (2004) *J. Phys. D: Appl. Phys.* **37**: 3207.
2. Mohanty S.R., Robert E., Dussart R., Viladrosa R., Pouvesle J.M., Fleurrier C. and Cachoncinlle C. (2003) *Microelectron. Eng.* **65**: 47.
3. Hong D., Dussart R., Cachoncinlle C., Ressenfeld W.E.S., Gotze S., J. Pons J., Viladrosa R., Fleurier C. and Pouvesle J.M. (2000) *Rev. Sci. Instrum.* **71**: 15.
4. Xiaoming G., Meisheng X., Rubin Y., Chaofeng H., Wirpszo K.W. and Emilio P. (2001) *Proc. SPIE* **4343**: 491.
5. Chew S.H. and Wong C.S. (2006) *J. Sci. & Technol. in the Tropics* **2:** 125.
6. Fomenkov I.V., Ness R.M., Oliver I.R., Melnychuk S.T., Khodykin O.V., Bowering N.R., Rettig C.L. and Hoffman J.R. (2003) *Proc. SPIE* **5037**: 807.
7. Rawat R.S., Zhang T., Phua C.B.L., Then J.X.Y., Chandra K.A., Lin X., Patran A. and Lee P. (2004) *Plasma Sources Sci. Technol.* **13**: 569.
8. Lee S., Tou T.Y., Moo S.P., Eissa M.A., Gholap A.V., Kwek K.H., Mulyodrono S., Smith A.J., Suryadi S., Usada W. and Zakaullah M. (1988) *Am. J. Phys.* **56**: 62.
9. Yap S.L., Wong C.S., Choi P., Dumitrescu C. and Moo S.P. (2005) *Jpn. J. Appl. Phys.* **44**: 8125.
10. Favre M., Lee S., Moo S.P. and Wong C.S. (1992) *Plasma Sources Sci. Technol.* **1**: 122.
11. Mohammadi M.A., Verma R., Sobhanian S., Wong C.S., Lee S., Springham S.V., Tan T.L., Lee P. and Rawat R.S. (2007) *Plasma Sources Sci Technol.* **16**: 785.
12. Ng C.M., Moo S.P. and Wong C.S. (1998) *IEEE Trans. Plasma. Sci.* **26**: 1146.
13. http://Spectr-w3.snz.ru
14. http://129.105.69.13/datasheets/Optoelectronics/Photodiode_UDT_catalog.pdf
15. http://www.ird-inc.com

Journal of Science and Technology in the Tropics (2010) **6**: 49-52

An atmospheric pressure non-thermal plasma jet in nitrogen for surface modification of polyethylene

D. P. Subedi[1], R. B. Tyata[1], A. Shrestha[1], D. Baral[1], D. K. Madhup[1] and C. S. Wong[2]
[1]Department of natural Sciences, School of Science, Kathmandu University, Nepal
[2]Plasma Research Laboratory, Department of Physics, University of Malaya, 50603 Kuala Lumpur, Malaysia

Abstract In this paper, an atmospheric pressure plasma jet (APPJ) in nitrogen has been set up for possible application in polymer surface modification. The effect on the hydrophilicity of a polyethylene (PE) surface exposed to the plasma jet was investigated for different exposition times and distances from the nozzle. It has been confirmed that the jet can modify polymer film with a work distance of more than 60 mm.

Keywords non-thermal plasma jet – surface modification – polyethylene – polymer film – hydrophilicity

INTRODUCTION

In the last one decade, research on non-thermal plasma at atmospheric pressure has become a subject of great interest because of its applications in various fields. The characteristic of these types of plasma is the existence of thermal non-equilibrium between the electrons and the ions. The treatment of materials by non-thermal atmospheric pressure plasma is a promising technology that is simple to set-up, easy and economical to operate and does not require vacuum equipments.

Among the various applications of the non-thermal atmospheric pressure cold plasmas are sterilizations of living tissue without damage and blood coagulation [1], modulation of cell attachment [2], biological and chemical decontamination [3-5], water decontamination and pollution control [6,7], nanotechnology [8], surface cleaning, etching, thin film deposition, surface modification and material processing [9-13]. Atmospheric pressure plasma can be generated by various methods: corona, glow, arc, dielectric barrier discharge (DBD), RF discharge and microwave discharges. The main problem with these systems is that the working space is often limited because of the electrode configuration. In an atmospheric pressure plasma jet, the plasma constituents are expelled through an orifice by a gas flow which makes it possible for the treatment of large objects. Forster *et al.* [14] reported an atmospheric pressure plasma jet in a DBD configuration. This type of plasma can be operated under high gas flow rate. In 2003, Toshifuji *et al.* [15] reported a relatively cold arc plasma jet produced under atmospheric pressure having potential application for surface modification. Quite recently, Takemura *et al.* [16] developed an atmospheric pressure plasma jet with long flame which can modify polymer film with a work distance of over 200 mm. Recently, a double layered atmospheric pressure plasma jet had also been reported [17].

In the present study, a non-thermal nitrogen plasma jet was generated using a high voltage power supply with output frequency of 10 to 30 kHz under atmospheric pressure. The application of this plasma jet to treat surface of polymer material is also demonstrated.

EXPERIMENTAL SETUP

The schematic diagram of the plasma jet system is depicted in Figure 1. A brass rod of diameter 3 mm was placed inside a glass tube of inner diameter 4 mm and outer diameter 6 mm. At one end of the glass tube a steel cap electrode (9 mm diameter, 0.5 mm thickness and 20 mm long) with an orifice of 2 mm diameter, was mounted. The inner electrode was connected to high voltage (0-20 kV) and high frequency (10-30 kHz) power supply and the outer electrode was grounded.

In this study, nitrogen is used as the working gas.

Journal of Science and Technology in the Tropics (2010) 6: 5-9

Comparison of water and gastrografin as an oral contrast medium for abdominopelvis computed tomography

K. C. Kanaga[1], S. E. Laila1, P. Y. Teh[1] and J. Shukriah[2]
[1]Diagnostic Imaging and Radiotherapy Programme, Faculty of Allied Health Sciences,
Universiti Kebangsaan Malaysia, Jalan Raja Muda Abd Aziz, 50300 Kuala Lumpur, Malaysia
(Email: kanagakkc@yahoo.com)
[2]Diagnostic Imaging Department, Kuala Lumpur Hospital, Jalan Pahang, 50300 Kuala Lumpur, Malaysia

Received 25-01-2010; accepted 06-04-2010

Abstract The aim of this study was to determine if water was comparable to gastrografin as an oral contrast medium in defining anatomic details of abdominopelvis computerized tomography. A total of 98 patients referred to the Diagnostic Imaging Department, Hospitak Kuala Lumpur from January to April 2009 for abdominopelvis CT with intravenous contrast enhancement were studied using Siemens Somatom Sensation 16 scanner. The results showed that water, with superior distension and delineation capabilities of the gaster and bowel, was comparable to gastrografin as an oral contrast medium.

Keywords gastrografin – water – contrast medium – quantitative – qualitative

INTRODUCTION

Multidetector computed tomography (CT), with high speed multiplanar imaging has led to a paradigm shift in abdominopelvis imaging. CT is also capable of producing thinner slices within short scan time and fast intravenous infusion of contrast material [1]. With this new technique, the use of high-attenuation positive contrast medium to outline the stomach and small bowel may degrade image quality especially in procedures requiring maximum intensity reconstruction [2]. Besides, adequate mural enhancement for diagnosis of abnormalities may be absent due to the almost non-existent difference between enhanced bowel wall and high attenuation intraluminal content [3]. An oral contrast medium should have a high distension capability that delivers optimal differentiation between lumen and bowel wall. Excellent mixing of contrast medium and the contents of gastro-intestinal tract may lead to consistent pacification and accurate interpretation of the images [4].

Neutral contrast agent produces improved image quality and facilitates the diagnosis of bowel wall abnormalities. It has been proven to be effective in the diagnosis of Crohn's disease [5], neoplasms [6] and bowel-ischemia [7]. Distension and delineation of the stomach and duodenum in imaging of pancreatic and biliary disease has been demonstrated using neutral contrast [8]. The most widely used neutral contrast agent is water as it has shown excellent result in the upper gastrointestinal tract; however its clinical use for the distal parts of the small bowel is limited due to its rapid absorption [9].

Studies have been done to investigate a negative contrast agent that can be used routinely for all types of CT abdominopelvis as an alternative for the positive oral contrast agent but the results obtained have been inconclusive [10, 11].

This study was designed to determine if water was comparable to gastrografin as an oral contrast medium in defining anatomic details. The hypothesis of our study was water would be as effective or even better then gastrografin for abdominopelvis CT.

MATERIALS AND METHODS

A total of 98 patients referred to the Diagnostic Imaging Department, Hospital Kuala Lumpur from January to April 2009 for abdominopelvis CT with

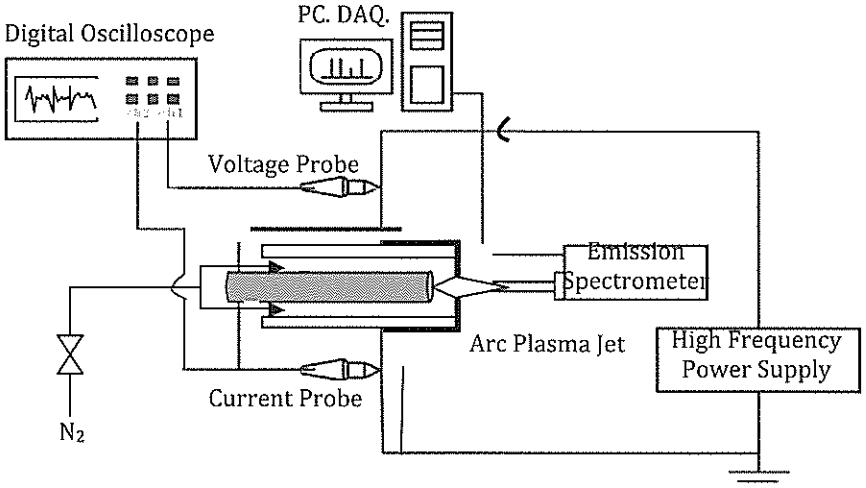

Figure 1. Experimental setup of the plasma jet.

In order to evaluate the effectiveness of the plasma jet in modifying the PE surface, hydrophilicity test was performed. The contact angle of water droplets at the surface of the PE film was measured using a *rame'-hart Contact Angle Goniometer*. This unit was equipped with standard software to analyze the drop image for the calculation of surface energy. The system offered a high level of computer aided precision in measuring contact angle and therewith facilitating the calculation of surface energy using different model equation.

The water droplet contact angles on the surface of PE films treated at different distances from the nozzle of the jet and for different exposure times were measured. Each contact angle presented in this paper was an average of at least four measurements made on different positions on the surface of PE.

RESULTS AND DISCUSSION

An example of the plasma jet obtained is shown in Figure 2. A discharge between the centre electrode and the steel cap containing the orifice is expected to be produced and the jet is formed due to the flowing nitrogen stream. The electron temperature of the plasma near to the orifice is expected to be several electron-volts. However, the temperature of the ions and the neutral atoms/molecules is relatively cold and was measured by using an IR thermometer to be in the range of 28°C to 30°C. The length of the jet was found to be dependent on the gas flow rate (Fig. 3).

The flow rate of nitrogen was varied from 1 to 5 litres per minute. To measure the length of the jet, a scale was placed behind the jet while taking the image of the jet by a digital camera. The lengths were then determined from the photograph. It is clear that the length of the jet increases proportionally with the gas flow rate at the beginning and then levels off after 4 litres per minute (Fig. 3).

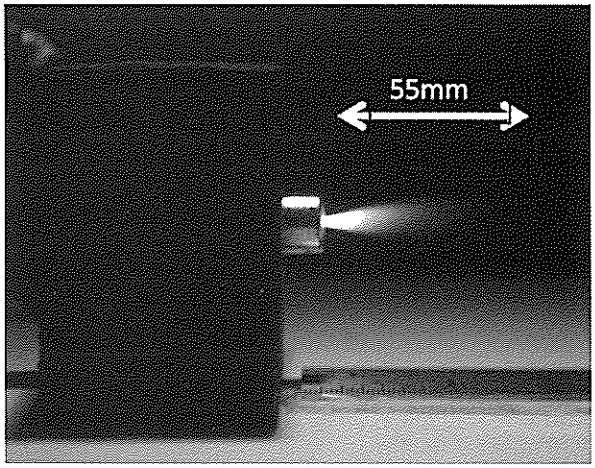

Figure 2. A picture of the non-thermal plasma jet.

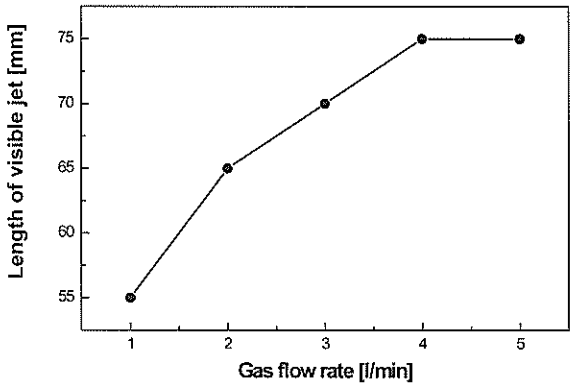

Figure 3. Dependence of the jet length of APPJ on the flow rate of nitrogen.

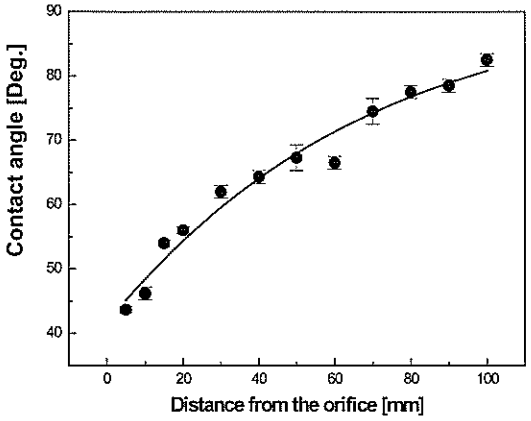

Figure 4. Water contact angle of the PE film as a function of distance from the orifice of APPJ. The gas flow rate was 3.0 l min^{-1} and the exposure time was 10 s.

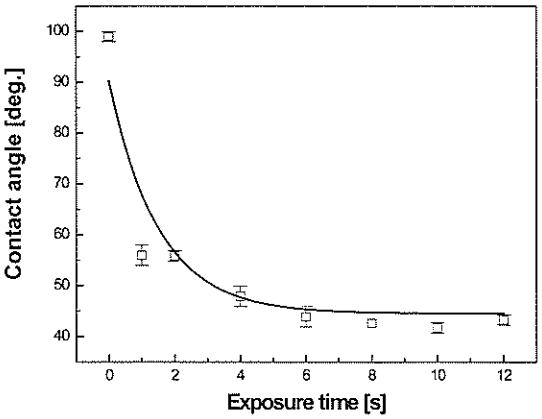

Figure 5. Water contact angle of PE sample as a function of the exposure time in APPJ. The distance of the sample from the orifice was 5 mm and the gas flow rate was 3.0 l/min.

Figure 4 shows the water contact angle of the PE film as a function of distance from the orifice of APPJ. In order to investigate the effectiveness of PE surface modification by the APPJ, hydrophilicity tests were carried out on the PE films before and after the treatment. At least three drops of the test liquids were placed on the sample and the contact angles were measured from the profile of the drops. The untreated sample had contact angle of 98° with water. Whereas after the exposure to the jet, a minimum contact angle of 39° was measured for sample placed at a distance of 5 mm from the orifice for a time of 10 s. For the same exposure time, a contact angle of 82° was measured when the sample was placed at a distance of 100 mm from the orifice.

Figure 5 shows the contact angle of PE sample as a function of the exposure time in APPJ. The treatment time ranged from 1 s to 12 s. As shown in the figure, the contact angle of the film changed from 98° for the untreated to the lowest value of 43° after the treatment.

CONCLUSION

An atmospheric pressure plasma jet has been developed and tested. The irradiation of the jet onto the polymer surface can improve the hydrophilicity of the sample without any damage to the material. The advantages of the present jet system are that the power consumption is low and there is no need of matching network. This plasma source can be used for the treatment of non-planar surface and heat sensitive materials.

REFERENCES

1. Fridman G. (2006) *Plasma Chemistry and Plasma processes* **26**: 425.
2. Stoffels, E., Kieft I. and Sladek R. (2003) *J. Phys. D: Appl. Phys.* **36**: 2908.
3. Laroussi M. (2005) *Plasma Process Polym.* **2**: 391.
4. Walsh J.L. and Kong M.G. (2008) *Appl. Phys. Lett.* **93**: 111.
5. Lu X., Ye T., Cao Y., Sun S., Xiong Q., Tang Z., Xiong Z., Hu J., Jiang Z. and Pan Y. (2008) *J. Appl. Phys.* **104**: 053.
6. Bruggeman P. and Leys C. (2009) *J. Phys. D: Appl. Phys.* **42**: 053.
7. Kolb J.F., Joshi R.P., Xiao S. and Schoenbach K.H. (2008) *J. Phys. D: Appl. Phys.* **41**: 234.
8. Gonzales-Aguilar J., Moreno M. and Fulcheri L. (2007) *J. Phys. D: Appl. Phys.* **40**: 2361.
9. Schutze A., Jeong J.Y, Banayan S.E, Park J., Selwyn G.S. and Hicks R.F. (1998) *IEEE Trans. Plasma Sci.* **26**: 1685.
10. Kunhardt E.E. (2000) *IEEE Trans. Plasma Sci.* **28**: 189.
11. Daun Y., Hung C. and Yu Q.S. (2005) *IEEE Trans. Plasma Sci.* **33**: 328.
12. Borcia G., Chiper A. and Rusu I. (2006) *Plasma Sources Sci. Technol.* **15**: 849.
13. Benedict J., Forcke K., Yanguas-Gil A. and Keudell von A. (2006) *J. Appl. Phys.* **99**: 112.
14. Foster S., Mohr C. and Viol W. (2005) *Surface and Coatings Technology* **200**: 827.
15. Tioshifuji J., Katsumata T., Takikawa H., Sakakibara

T. and Shimizu I. (2003) *Surface and Coating Tech.* **171**: 302.
16. Takemura Y., Kubota Y., Yamaguchi N. and Hara T. (2009) *IEEE Trans. Plasma Sci.* **26**: 1604.
17. Choi J., Matsuo K., Yoshida H., Namihira T., Katsuki S. and Akiyama H. (2009) *Japanese J. Appl. Phys.* **48**: 086.
18. Subedi D.P., Madhup D.K., Adhikari K. and Joshi U.M. (2008) *Indian Journal of Pure and Applied Physics* **6**: 540.

Journal of Science and Technology in the Tropics (2010) **6**: 53-57

Compressed natural gas (CNG) cylinder testing and data evaluation using acoustic emission technique

Tonphong Kaewkongka[1,*], Jirapong Lim[2] and Suparerk Sirivedin[3]

[1]Department of Physics, Faculty of Science, Chulalongkorn University, Patumwan, Bangkok 10330, Thailand
[2]Department of Production Engineering, Faculty of Engineering, King Mongkut University of Technology, North Bangkok, Bangsue, Bangkok 10800, Thailand
[3]King Mongkut University of Technology, North Bangkok, Bangsue, Bangkok 10800, Thailand
(*E-mail: tonphong.k@chula.ac.th)

Abstract This paper describes a method of compressed natural gas (CNG) storage cylinder testing using acoustic emission technique. The CNG storage cylinder, which is type I-steel cylinder, was tested as normal and predefined surface crack operating condition. Acoustic emission (AE) signals propagation and transmissions were captured by piezoelectric transducers mounted on surface across the cylinder with and without predefined surface crack. In the experiment, an increased step-wise condition in hydrostatic pressure up to 400 bars was applied to the cylinder. The feature extraction and classification of AE signals from each testing condition was applied. The results are very promising in terms of identifying the defects due to crack propagation.

Keywords acoustic emission – CNG cylinder

INTRODUCTION

The number of vehicles using compressed natural gas (CNG) has grown rapidly for the past decades due to the alternate use of energy and become an important issue in Thailand. In most cases, the nature of the contents renders these cylinders critical to operations and safety. There have been several severe accidents from the explosion of CNG cylinders. Therefore, it may lead to significant loss or catastrophic failures. For health and safety issue, monitoring the condition of the cylinders has received considerable attention over the past few years due to its particular importance of safety, environment and the economical reason [1-3]. A reliable condition monitoring system will reduce the failure and possible loss.

According to inspection standard, it requires that cylinders be visually inspected externally after it has been used for 36 months. This is to ensure that the cylinders that have damage or deterioration will be removed from service or repaired. The visual inspection test needs removal of the cylinder from the vehicle. However, there are possible risks if the internal flaws or defects cannot be examined.

Nowadays there are many kinds of conventional methods available for the CNG storage cylinder detection [4-6]: visual inspection using dye penetration, hydro-static testing, flow or pressure measurement, ultrasonic testing. However, these methods are time consuming due to the requirement of removing the cylinder from the vehicle and revealing the defects of the cylinder after it had already occurred. Recently, acoustic emission (AE) has been extensively applied to vessels testing during pressurization and has proven to be a timely and economical method for structural integrity assessment as described in the standard and code, ISO/DIS 16148.2 [7]. A major advantage of AE inspection is that it allows the whole structural integrity to be tested non-intrusively with minor disruption (no need to remove the cylinder from service, empty and clean for inspection) in a pressurized condition. AE can provide complete coverage of the cylinder with pressurized test and is sensitive to active defects or flaws presence and propagation.

The objective of this research is to demonstrate that a condition-based monitoring using acoustic emission (AE) can provide not only timely detection of defects in the cylinder but also the crack propagation so that maintenance or replacement can be performed prior to the loss of safety function. Therefore the use of acoustic emission method has been proposed for CNG type-I steel cylinder monitoring instead of the conventional methods.

EXPERIMENTAL SETUP AND APPARATUS

Acoustic emission is a natural phenomenon of stress wave generation and propagation spontaneously when a material is subjected under stress [8]. Plastic deformation and growth cracks are the primary sources of acoustic emission in metals. The acoustic signal can be detected by a piezoelectric transducer, which converts the mechanical energy carried by the elastic wave into an electrical signal.

When the defective cylinders are pressurized, stress waves (AE) can be produced by several different sources (e.g. secondary sources or actual propagation of cracks). These sources can result in AE activities generated at pressure less than, equal to or greater than the operating pressure. The stress waves are then propagated throughout the structure.

A systematic approach to classify the dynamic responses of AE signatures associated with the CNG type I steel cylinder operating condition was performed in this study (Fig. 1). The AE testing is usually carried out during a controlled pressurization of a cylinder. Conventional AE parameter, AE_{rms} is used to identify the presence of acoustic emission activities produced when microscopic cracks occur. The AE_{rms} can be calculated using the formula below [9]:

$$AE_{rms} = \sqrt{\frac{1}{T}\int_{t_0}^{t_0+T} v^2(t)dt}$$

where $v(t)$ is the electrical voltage signal obtained from piezoelectric transducer, t_o is the initial time, T is the period of the AE activity.

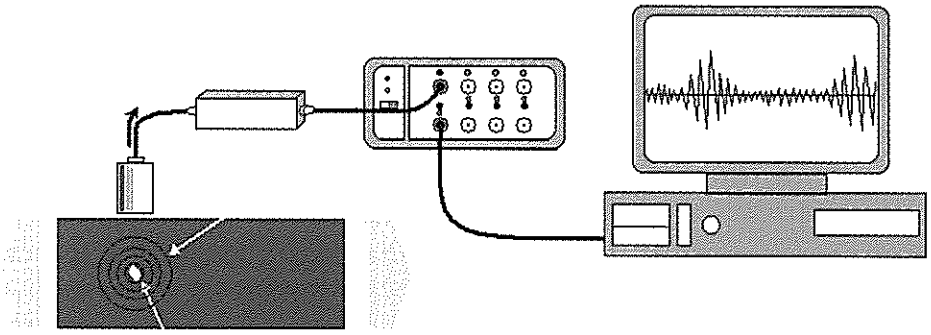

Figure 1. A system of acoustic emission testing.

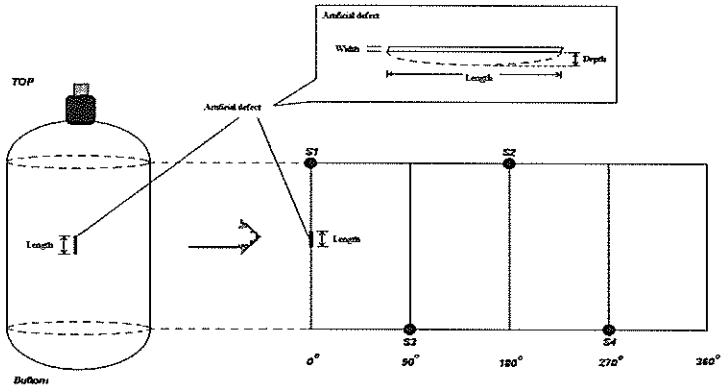

Figure 2. Set up of CNG cylinder testing with four installed AE sensors.

The acoustic emission sensors, model AE-SS1 (Holroyd Instruments, UK) which were made of piezoceramic elements, were mounted on the circumference along the surface of the cylinder (Fig. 2). The acoustic emission sensors of 100 kHz resonance frequency responded well with the material degradation and microscopic crack initiation and growth. The captured acoustic emission signals were then conditioned and amplified with 60 dB-gain signal conditioning unit. The PCI-1714UL was used for A/D conversion and data logger. In the experiments, a normal operating cylinder was tested with four AE sensors by means of mechanical coupling (Fig. 2). The cylinder used in this experiment had a 60 litre capacity. It was made of a steel sheet with a diameter of 300 mm, length of 990 mm and thickness of 8 mm.

To perform hydrostatic test, the cylinder was placed in a chamber which could facilitate a high pressure testing (Fig. 3). For an abnormal operating condition cylinder, a simulated surface crack was performed on a good cylinder. The simulated (artificial) crack (Fig. 4) was made using a grinder to generate a surface defect with length of 30 mm (along the length of cylinder), width of 3 mm and depth of 2 mm.

To eliminate background noise, the threshold of AE signal was set to 39 dB_{AE}. Evidently, the threshold level affects the value of the AE parameters. A typical example is the event duration. By definition, it is the time that the AE event is above the threshold. A step wise increase in hydrostatic pressure was performed up to 400 bars with the testing cylinder. During the test, a pressure sensor was attached with the hydro-testing machine as for load reference for data acquisition.

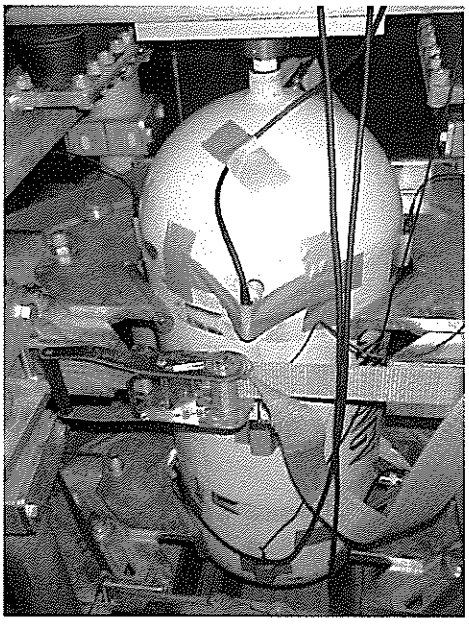

Figure 3. Installation of CNG cylinder in a high-pressure hydrostatic test chamber.

EXPERIMENTAL RESULTS AND DISCUSSION

To verify the proposed approach, the experiment on the normal operating cylinder was performed using hydrostatic test. A hydrostatic test was applied on the testing cylinder with increased pressure up to 300 bars. The AE signals captured from all four sensors

Figure 4. Artificial surface crack generated at the side wall of the cylinder.

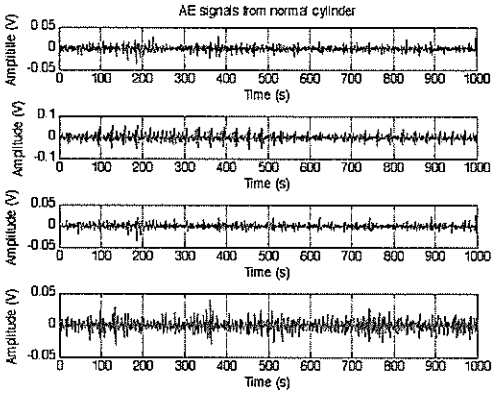

Figure 5. AE signals versus time (data point) from a normal CNG cylinder.

attached on the good or normal operating condition cylinder yielded a calm condition in a random background noise fashion (Fig. 5).

In the experiment, an artificial surface crack (300mm length, 2 mm width) cylinder was tested with the applied pressure up to 300 bars. The experimental results are shown in Figure 6. It illustrates that the time domain signals of the artificial defective wall cylinder gave rise to the abrupt change in higher amplitude to all four AE sensors.

Ultimately, the pressure was increased up to 400 bars which resulted in the crack of the artificial defect of the wall. At this state, the water was leaking out due to the open surface of the previous artificial crack because it could not sustain the increased the internally applied load any further. This resulted in the AE signals as shown in Figure 7.

The AE_{rms} values calculated from the time domain signal are shown in Figure 8. For the normal cylinder, it gave the lowest signal energy around 15.8 mV. This is because there was only background level of the hydrostatic test that was present. It illustrates that the defective cylinder condition yielded the highest value about 211 mV. Its value was about 13.3 times greater than the one from normal operating condition. This is due to the microscopic crack growth as the primary source and the turbulent flow at the surface of the crack as secondary source. Whereas the leakage cylinder shows that the AE_{rms} values were relatively greater than the normal condition at about 20.8 mV (greater by 5 mV).

The methodology described in this paper has been shown to work well for monitoring CNG cylinder operating conditions. The method involves calculation of AE_{rms} values as a mean to identify the abnormal operating conditions of the CNG cylinder together with hydrostatic test. Overall the proposed method can provide timely detection of the presence of crack and leakage of the CNG cylinder and is efficient to implement.

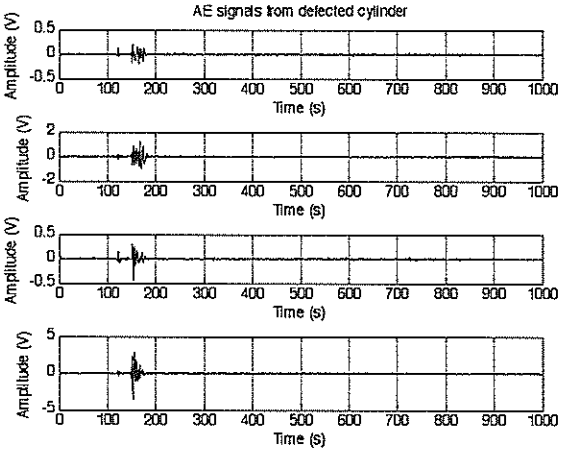

Figure 6. AE signals versus time (data point) from a defective CNG cylinder.

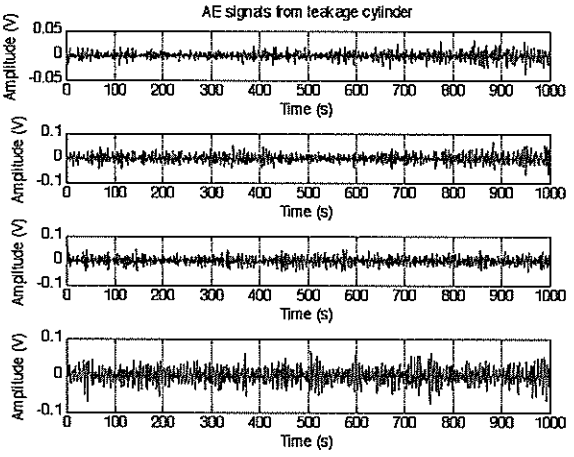

Figure 7. AE signals versus time (data point) from a leaked CNG cylinder.

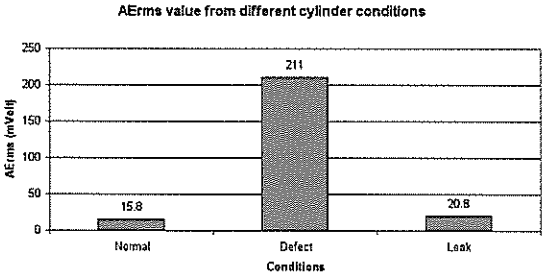

Figure 8. Results of AE_{rms} from different operating conditions.

REFERENCES

1. ASME (2000) Boiler and Pressure Vessel Section XI, Appendix A, Article A-3000.
2. ASTM E2191-08 (2006) *Standard Practice for Examination of Gas-Filled Filament – Wound Composite [3] Pressure Vessels Using Acoustic Emission.*
3. ASTM E1419-02b (2002) *Standard Test Method for Examination of Seamless, Gas-Filled, Pressure Vessels Using Acoustic Emission.*
4. Connolly M.P. and Han Dinh (1996) Fleet Inspection of Compressed Natural Gas Cylinders for Natural Gas Vehicles Using Source Location Acoustic Monitoring.

SAE Technical Paper Series No. 961174.

5. Webster C. (2007) Development of Non-Destructive Evaluation (NDE) Techniques for CNG Fuel Tanks. *Report for Transportation Development Centre of Transport Canada.*
6. Hudak S.J., Jr. (1991) Assuring the Safety of Natural Gas Vehicles. Technology Today Magazine, Sept. 1991.
7. ISO/DIS 16148.2 (2006) Gas cylinders – Refillable seamless steel gas cylinder – Acoustic emission examination for periodic inspection.
8. Pollock A.A. (1973) Acoustic Emission 2 – Acoustic emission amplitudes. *Journal of Non-Destructive Testing***10**: 264-269.
9. Scruby C.B. (1987) An introduction to acoustic emission. *Journal of Physics Instrument Science and Technology* **20**: 946-953.

Journal of Science and Technology in the Tropics (2010) **6**: 59-65

Prompt gamma neutron activation analysis (PGNAA) of hydrocarbons: A Monte Carlo study with GEANT4

Lam YiHua[1], Wong Chiow San[1]* and Kurunathan Ratnavelu[2]
[1]Plasma Research Laboratory, Department of Physics, Faculty of Science, University of Malaya, 50603 Kuala Lumpur, Malaysia
[2]Institute of Mathematical Sciences, University of Malaya, 50603 Kuala Lumpur, Malaysia

*Corresponding author

Abstract In the present work, the results of prompt gamma (γ) neutron activation analysis (PGNAA) calculated by the open source GEANT4 Monte Carlo toolkit were compared with the commercial simulation package MCNP. Both the Monte Carlo simulation packages utilize the phenomenological nuclear reactions to yield γ rays which are coupled with incident neutrons after these reactions. A virtual experimental setup with a 4π solid-angle γ detection was instantiated in the simulations to collect all prompt γ rays from the tested hydrocarbon phantoms. The comparative results present good agreement in getting the characteristic γ energy spectra of hydrocarbon materials.

Keywords GEANT4 – MCNP – Monte Carlo simulations – prompt gamma neutron activation

INTRODUCTION

A material with its specific chemical composition and density can be detected or differentiated from among other types of materials, which have nearly the same chemical composition but have not complied with the same densities, by using prompt gamma (γ) neutron activation analysis (PGNAA) method. It has been used in detecting explosive hydrocarbon material [1]. In addition, certain element in a bulk material or in a biological tissue can be determined via PGNAA, e.g. biomedical protein detection [2].

PGNAA method relies on neutron-nuclear interactions, that is, inelastic scattering (n, n′γ), (n, pγ) and radiative capture (n,γ), to yield γ rays. Although $1/v$ law [3] (v is the incident neutron velocity) is not applicable to every element, isotope and energy range [4], it is still acceptable to be applied in low Z element and in thermal energy range [5]. This law infers that the probability of neutron radiative capture depends on how long the period of time a neutron spends in the region surrounding the nucleus. The longer period of time it spends, the higher probability of neutron radiative capture will occur. Hence, when a low kinetic energy incident neutron, e.g. thermal neutron (~0.025eV) or epithermal neutron (0.1-1eV), enters the narrow separation virtual energy levels in compound nucleus or interacts with compound nucleus [6], the neutron radiative capture cross sections will increase. These low energy interactions raise the possibility of producing stable isotopes and the coupled γ ray, e.g. $^1H(n, \gamma)^2H$ in which ^2H is a stable isotope and γ ray will be radiated. Besides, different materials composed by different chemical compositions (including different isotopes) and densities will have different radiative capture cross sections. By radiating low energy neutrons with certain range of energy distribution on different materials, the produced γ ray energy spectra will be different. Hence, the prompt γ ray energy spectra become an identifying characteristic of the material.

Other than experimental measurements, PGNAA can be simulated by using various types of Monte Carlo computational simulation packages, such as GEANT4 [7,8], MCNP [9] and FLUKA [10,11]. Most of these packages are written in structural programming language (C and FORTRAN). GEANT 4 has been written in object-oriented programming (OOP) architecture (C++), developed and maintained by many laboratories [7,8]. Conceptually, OOP has its distinctive feature in treating particle as a single object which may have encapsulated its own data

intravenous contrast enhancement were studied using Siemens Somatom Sensation 16 scanner. The study was approved by the Ethics Committee of the Ministry of Health Malaysia.

Patients were divided into two groups of 49 patients each. The patients were randomly selected by predefined inclusion and exclusion criteria to participate in either of the two groups. The clinical indications related to liver (30%), pancreas (30%), renal (20%) and GIT (20%) for both groups did not differ statistically with regard to their distribution (χ^2 test).

All patients were required to fast for at least 6 hours. Water or gastrografin (500 mL) was given at 60, 30 minutes and immediately before scanning. For gastrografin 10 mL was diluted into 500 mL solution. A scout image from xiphoid to the symphysis was performed using a 16-detector row CT scanner (Siemens, Somaton Sensation 16), followed by a intravenous contrast bolus administration of Iopamiro 300 with a rate of 3 ml/s. Acquisition of scans was obtained using the same protocol of 5-mm transverse sections.

Two experienced radiologists independently reviewed the images from each examination in transverse and coronal planes on the 3 megapixel workstation. The radiologists were blinded to the clinical history of the patients. An incremental three-point scale (0=worst, 0.5 = moderate, 1=best) was used to rate images from each examination for bowel distension, homogeneity of the lumen, delineation of the bowel wall, presence of artifacts and overall image quality.

Overall bowel distension was graded from totally collapsed (0) to maximal distension (1); homogeneity of the lumen from massively inhomogeneous (0) to completely homogeneous (1). The delineation of the bowel wall was rated twice from indiscernible (0) to clearly visible (1), initially against the intraluminal contrast and then against the surrounding extraintestinal tissue. The presence of artifacts was rated as no artifacts (0) to serious image degradation due to artifacts (1). Finally, overall image quality was assessed from unreadable (0) to perfect (1).

To support the qualitative evaluation, additional quantitative measurements were performed. The maximum cross-sectional diameter of the antrum of the stomach, horizontal part of the duodenum, proximal jejunum, and terminal ileum were measured perpendicular to the axis of the lumen using the outer margins of the intestinal wall for each patient. Attenuation in Hounsfield units (HU) of the lumen and gastrointestinal wall was measured at the same levels of the stomach, duodenum, jejunum, and terminal ileum. Attenuation of the lumen was measured by placing a region of interest (ROI) within a well-distended segment of the small bowel section. Attenuation of the wall was measured by first zooming into the image section until the wall was clearly visible, and then placing an ROI (minimum diameter of 2 mm) over the bowel wall.

Mann-Whitney U-test was used to perform statistical analysis of the differences in median scores between water and gastrografin groups regarding bowel distension, homogeneity of the lumen, differentiation of the bowel wall against luminal content and surrounding fat, the presence of artifacts and overall image quality. Differences were considered significant if $p < 0.05$; inter-observer agreement was evaluated using weighted kappa statistics where a kappa statistics > 0.75 was considered as excellent agreement, 0.4-0.75 as fair to good agreement, and < 0.4 as poor agreement. Values near zero or less than zero reflected only chance agreement.

For the quantitative analysis, the differences in maximum diameters, HU values for the bowel lumen, and contrast values between the neutral oral contrast groups were compared using *t*-test; differences were considered significant if $p < 0.05$

RESULTS

All patients tolerated the administration of oral contrast medium. There was no vomiting, diarrhoea, abdominal pain or allergic reactions to both the oral contrast media. All patients drank the designated amount of fluid within the given time. The images were of diagnostic quality to be evaluated by two independent radiologists with five years of experience. Kappa analysis showed the inter-observer agreement in the excellent category ($k = 0.762$).

The qualitative results were summarized in Figure 1. Delineation of the bowel wall from inside to outside was significantly better using water compared to gastrografin ($p < 0.05$). As for all the other criteria there was no significant difference between water and gastrogafin. The quantitative measurements are summarized in Table 1. Diameters of the gaster and

structure (characteristic data and methods) and respective particle transport physics model. The OOP methodology (the way in composing program) can resemble the physical occurrence, e.g. a neutron, which is treated as an object in the simulation, may collide and be captured by a thermal nucleus (the second object) to yield γ ray (the third object); alternatively, the neutron may undergo a beta decay process to produce a proton (the second object), an electron (the third object) and an anti-neutrino (the fourth object). The created electron may produce γ ray (the fifth object) during Bremsstrahlung process. During radiative decay, annihilation and radiative capture, the interacting particles will be deleted from the computer memory after yielding respective secondary particle(s). In this way, the OOP computational method resembles the physics process as the active interacting particle, e.g. electron, positron and neutron, will disappear after its respective physics process, e.g. annihilation or radiative capture.

In this work, the incident neutrons are assumed to be thermalized and their energies are in accord with Maxwell-Boltzmann (MB) distribution, and the incident energy of highest probability is 0.025 eV. The prompt γ energy spectra of rubber, which are calculated by GEANT4 by means of either inducing thermalized incident neutrons or inducing monoenergetic incident neutrons on target, is compared with the results of prompt γ energy spectra induced by monoenergetic incident neutrons, which was generated by the MCNP [12].

SIMULATION OF PGNAA

Physics list and incident random energy generator

The calculations of the current PGNAA Monte Carlo simulation were processed by GEANT4.8.2.p01, whereas the evaluated neutron cross section input data was by *G4NDL3.10*, a recompiled data of a few evaluated nuclear data (including ENDF-B VI, JENDL, FENDL, CENDL, Brond, EFF, JEF, MENDL) [7]. Besides, data sets such as *G4EMLOW2.3* were used as part of the input data to facilitate the calculation of the γ propagation handled by electromagnetic processes (*Low Energy Electromagnetic*). These data files were input via respective physics process classes. Figure 1 shows the schematic flow of the application program of GEANT4.

Neutron *Elastic*, *Inelastic*, *Capture* and *Fission* handled by the neutron high precision (HP) model [7], [13] are considered in this PGNAA simulation. These four low energy neutron physics models are able to describe high precision final state production which is based on the *G4NDL3.10*. It covers the neutron scattering energy range from thermal energy up to 20 MeV. In addition, Doppler broadening and thermal motions of target nucleus are covered in the final state generator. Both processes are done on-the-fly by the neutron HP models and their associated cross sections, *G4NDL*. Although fission is quite rare to happen, it is included in the simulation as a precaution in the PGNAA simulation. These four processes are considered as post-step reactions and one of them is selected via random number selection by means of comparing the mean free path. Before the selection of physics processes, an element will be selected among elements composing a material and an isotope will be selected from among isotopes which are defined for that element. These two levels of selection (of element and isotope) are calculated via random number selection and comparison of the respective cross sections in GEANT4 kernel (class G4HadronicProcess). However, inside the class G4HadronicProcess, the original method G4HadronicProcess::ChooseAandZ assumes isotope

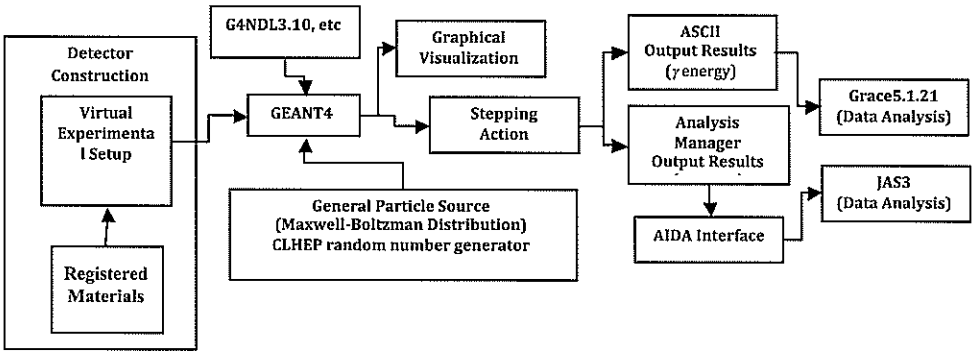

Figure 1. Schematic organization of PGNAA simulation program.

abundance values by retrieving the default values in an instantiated object of G4StableIsotope. These isotope abundance values may not suit the user need. Hence, the method G4HadronicProcess:ChooseAandZ had been altered to suit the user defined isotope abundance values [14].

Besides, the simulations have been separately run with two sets of electromagnetic physics models: (1) *Standard Electromagnetic* physics model; and (2) *Low Energy Electromagnetic* physics models. Both electromagnetic physics models consist of e^-e^+ pair production, photoelectric, γ conversion and Compton scattering. Extra physics models have been attached to e^- and e^+: (1) *Multiple Scattering*; (2) *Low Energy Ionization* and *Low Energy Bremsstrahlung*; or *Standard Ionization* and *Standard Bremsstrahlung*; whereas *Low Energy Rayleigh* has been attached to γ. However, we find that both sets of physics model – *Standard Electromagnetic* and *Low Energy Electromagnetic* produce the same outcomes. Therefore, only one set of results is shown in this paper. Furthermore, the registered processes for proton and ions (deuteron, triton, ^{3}He, alpha, generic ion) are *Multiple Scattering*, *Low Energy Ionization* and respective hadronic routines e.g. low energy proton/deuteron/triton/alpha inelastic and elastic processes.

We assume the process of neutron thermalization will eventually produce neutrons with energy distribution described by Maxwell-Boltzman (MB) distribution,

$$f(E) = \frac{2N}{\sqrt{\pi}} \frac{\sqrt{E}}{(kT)^{\frac{3}{2}}} \exp\left(-\frac{E}{kT}\right). \quad (1)$$

Instead of integrating the distribution function to yield the randomized incident neutron energies, the function can be treated in the form of a histogram with 10000 or more bins. Then the histogram can be normalized to its maximum value. The output of this function *f(E)* can be cumulated as a discrete cumulative distribution [15]. Even random numbers between 0 and 1, which are generated via a Class Library for High Energy Physics (CLHEP-2.0.3.1), are distributed on the $\sum f(E)$-axis. The corresponding x-axis values are the MB randomized incident neutron energies. The MB distribution code has been embedded into a new class inherited from the class G4GeneralParticleSource. The highest probability energy of the random distribution is 0.025eV within the energy range of 0.001eV < *E* < 0.050eV.

Virtual experimental setup

The listed isotopes in Table 1 and materials in Table 2 were constructed in a user defined detector construction class and registered into the GEANT4 kernel. Figure 2 shows the experimental setup, which consisted of two spherical volumes (phantoms), i.e. the internally occluded sphere (black, with radius 0.62 cm) and the exterior occluding hollow sphere (grey, with radius 1.05 cm). The setup was similar to Nunes *et al.* [12] and Sohrabpour *et al.* [16]. The hollow sphere and the inner spheres could be either set as the same material or set as different materials. The total physical volume of both spheres was 1 cm^3. Therrmalized neutrons would be directed in

Table 1. List of registered isotopes.

Registered isotopes	Natural abundance (%)
^{1}H	99.985
^{2}H	0.015
^{12}C	98.80
^{14}C	1.20
^{16}O	99.757
^{17}O	0.038
^{18}O	0.205
^{14}N	99.640
^{15}N	0.360

Table 2. List of registered materials.

Registered materials	Chemical composition	Density (g/cm^3)	Temperature (K)
C4	$C_4H_6O_6N_6$	1.83	273.15
Rubber	C_5H_8	0.94	273.15

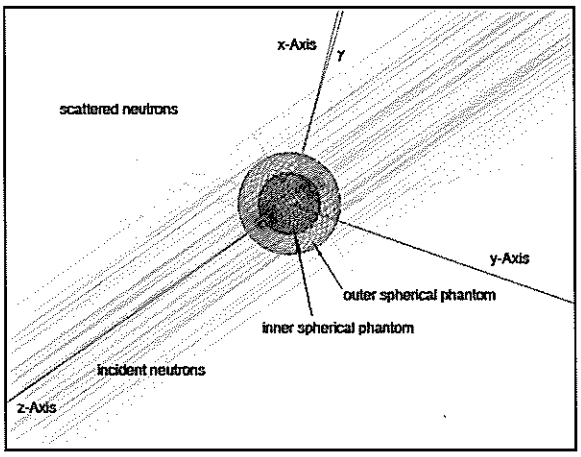

Figure 2. A typical run sample (snapshot) with prompt γ rays.

parallel to the both spheres. The source of neutrons was confined in a plane square (2.5 × 2.5) cm^2, and located 5 cm (arbitrary) from the spheres. As long as the yield γ ray of inelastic (n, n'γ) or capture (n,γ) reaction propagated from spherical volumes to atmosphere in 4π directions, energy of the prompt γ ray would be cumulated for further analysis. There was no variance reduction applied on the analysis. During the simulation, random neutron incident energy and energy of prompt γ ray results were kept in ASCII and Abstract Interfaces for Data Analysis (AIDA) 9170 format files for further analysis which was respectively based on Grace and Java Analysis Studio (JAS3).

Figure 2 shows a typical run of the simulation. Both spherical volumes (inner and outer) were set as explosive C4, and they were placed in the ambience of atmospheric gas (70% N_2, 30 % O_2), alternatively, the ambience could be set as vacuum too. The spherical volumes were exposed to 100 incident neutrons with MB energy distribution. Light grey lines represent the neutron tracks (incident neutrons or scattered neutrons). This typical run produced two γ tracks (grey lines) as labeled in Figure 2. The chemical composition of C4 is given in Table 2.

RESULTS AND DISCUSSION

In this PGNAA simulation, γ energy spectra of a typical plastic explosive (C4), rubber, and C4 occluded by rubber were calculated and compared. Figures 3-5 show the comparison of γ energy spectra produced by GEANT4.8.2.p01 and MCNP (analyzed by Nunes *et al.*) [12]. The γ energy spectra represent the interactions between the thermal neutrons and the nucleus of the constituent elements of C4 and rubber, and represent also γ interactions in the sample material itself. The ratio of non-neutron-capture (i.e. ionization, Bremsstrahlung, transportation, annihilation, radioactive decay and multiple-scattering) processes, which are related to γ yield, to neutron capture process is ~ 0.08. It may be infered that thermal neutron capture process plays a significant role in γ production. The identity of the constituents of the particular material can then be adduced. There are three configurations of virtual experimental setup: (1) both inner and outer spherical phantoms are placed in atmospheric environment and are irradiated by MB distributed energy neutrons (the upper most histogram); (2) both spherical phantoms are located in vacuum and are irradiated by MB distributed

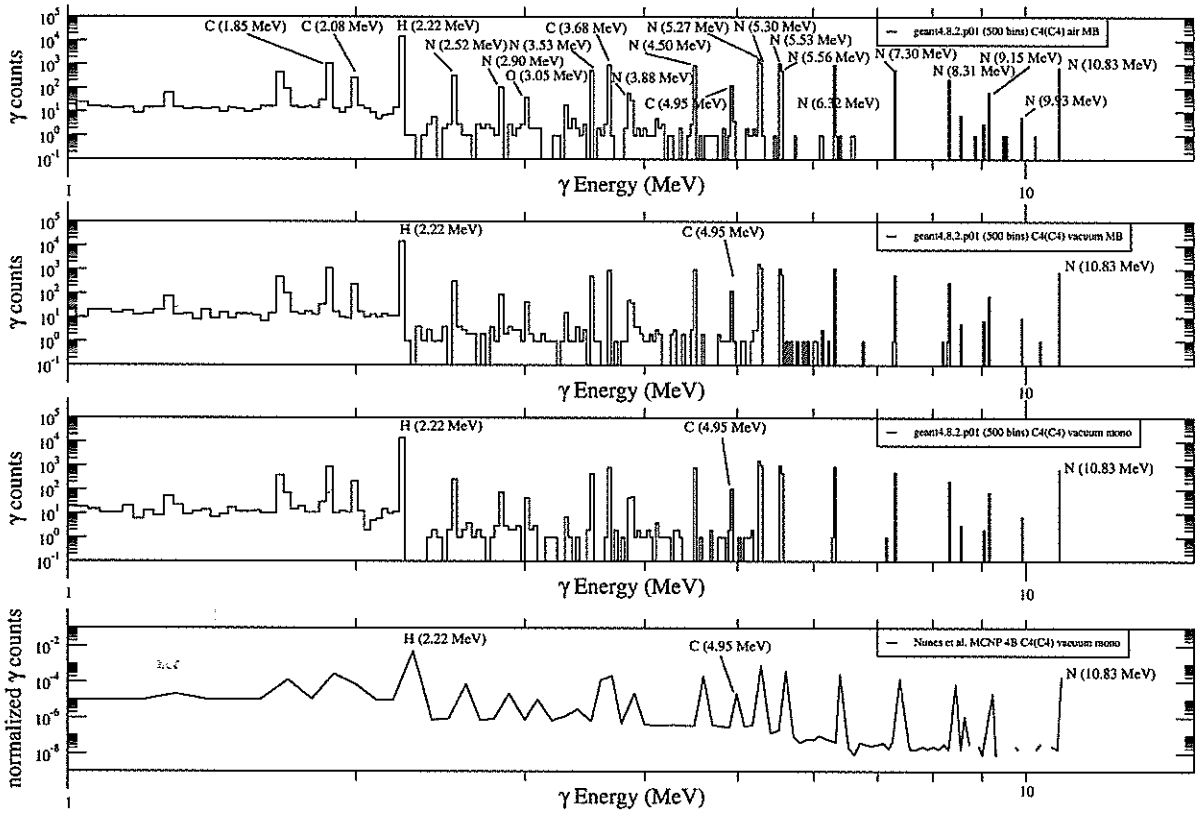

Figure 3. Prompt γ energy spectra of C4 generated by GEANT4.8.2.p01 compared with MCNP.

energy neutrons (the second upper histogram); and (3) both spherical phantoms are situated in vacuum and are irradiated by monoenegetic neutrons (the second lower histogram); with (4) γ energy spectra calculated by MCNP.

In Figure 3, Nunes *et al.*'s results show that hydrogen contributed to the peak of prompt γ ray (2.2 MeV), carbon (4.9 MeV) and nitrogen (10.8 MeV). Their results illustrate that the explosive spectra have significant γ energy peaks which are the signatures for C4 from 1 to 12 MeV (with 100 histogram bins ranges from 1 – 12 MeV).

Obviously, a few major peaks are consistently observed on the corresponding γ energy spectra produced by GEANT4.8.2.p01 (Figure 3). Three of the major peaks (~14600 counts of 2.2 MeV, ~130 counts of 4.9 MeV, ~720 counts of 10.8 MeV) match with γ energy spectra produced by MCNP as stated above. Other than the three major peaks, γ energy spectra produced by carbon from inelastic interactions (marked with *) and from s-wave captures include 1.85 MeV, 3.68 MeV, and *2.08 MeV. In addition, nitrogen contributes *2.52 MeV, *2.90 MeV, *3.88 MeV, *4.50 MeV, 5.27 MeV, 5.30 MeV, *5.53 MeV, *5.56 MeV, 6.32 MeV, 7.30 MeV, 8.31 MeV, 9.15 MeV, 9.93 MeV; whereas oxygen generates γ energy spectrum with 3.05 MeV. All the γ energy spectra above are in agreement with those published in Ref. [19]. It is clear that γ energy spectra calculated by GEANT4.8.2.p01 are discrete at 2.2 MeV and above, whereas γ energy spectra below 2.2 MeV are continuous. This is due to the various electromagnetic processes, for instance, Bremsstrahlung, occur in this energy range.

In Figure 4, a few extra γ energy spectra peaks are recorded at 4.50 MeV, 5.27 MeV, 5.30 MeV, 5.53 MeV, 5.56 MeV, 6.32 MeV, 7.30 MeV, 9.15 MeV, 10.8 MeV in the top histogram compared to the other two histograms below. These extra energy spectra are similar with nitrogen peaks in Figure 3. These background energy spectra may be contributed by the atmospheric gas as the chemical composition setting of rubber (C_5H_8) does not contain nitrogen, besides, nitrogen peaks do not appear in vacuum configuration of these two experimental setups.

When C4 is occluded by rubber, the original rubber's prompt γ energy spectra will mix with characteristic γ energy spectra from C4. This mixture is clearly shown in Figure 5. High peak of the nitrogen (10.8 MeV) and many extra γ energy spectra produced

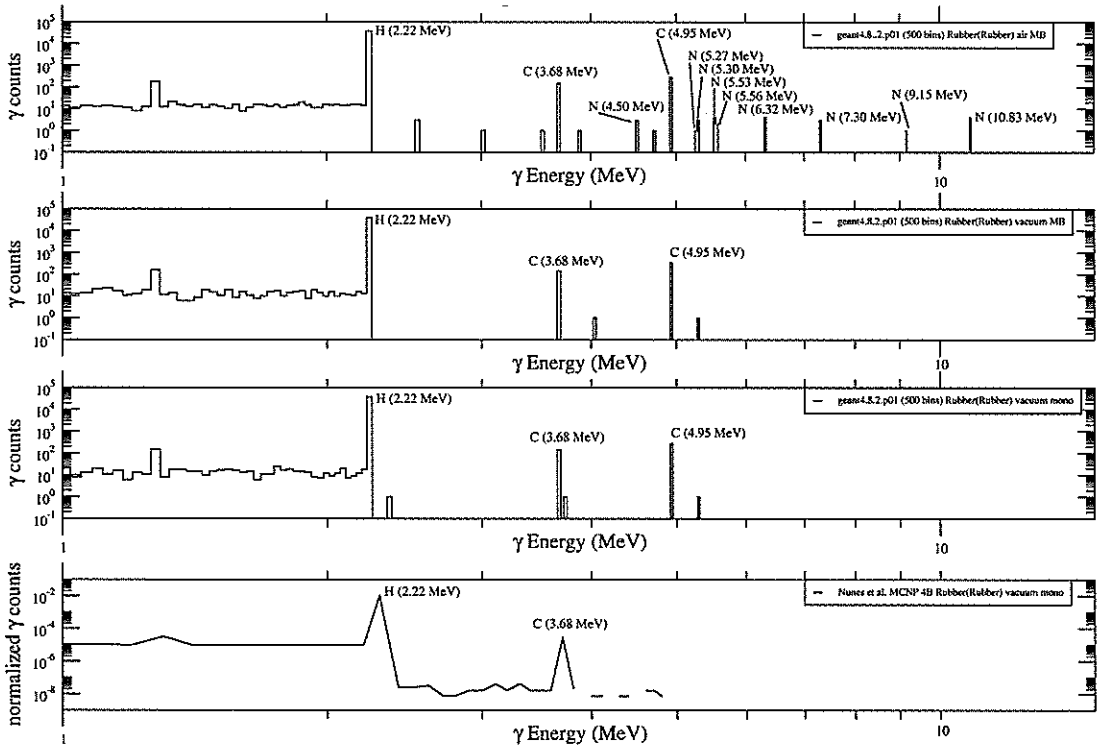

Figure 4. Prompt γ energy spectra of Rubber (C5H8) generated by GEANT4.8.2.p01 compared with MCNP.

by nitrogen indicates that the occluded material has a high concentration of nitrogen. This indication not only differentiates rubber with C4 from rubber without C4, but also depicts the ratio of nitrogen in each phantom in order to determine the presence of plastic explosives [20].

Furthermore, Figure 3 and Figure 5 show that incident neutrons with MB distribution energy will only trigger slightly more extra γ energy spectra compared to mono energetic neutrons. This outcome is plausible as: (1) more types of elements in the chemical composition and MB neutron energy (more random energy) will give rise to more possibilities of inelastic scattering; (2) although the more random of the incident energy, the more transitions incurred by inelastic scattering and capture processes are expected, the difference of randomized neutron energies is small. Hence, small range of randomized neutron energy does not impact much to the prompt γ energy spectra. Figure 4 does not show an obvious difference of γ energy spectra between MB and mono energetic. Obviously, there are not many types of element in the case of neutron-rubber scattering. The targets of these simulations are in static form, Doppler broadening does not affect the outcome of γ energy spectra. Overall, the γ energy spectra calculated by GEANT4.8.2.p01 shows good agreement with MCNP in terms of the ratio of γ energy spectra counts in histograms.

CONCLUSION

The present study on PGNAA computational simulation which focuses on the comparison of the corresponding characteristic γ rays is able to show the differences among explosive and non-explosive occluded materials. Besides, we demonstrate that γ rays generated from s-wave neutron captured are not the only energy spectrum to show the differences, non s-wave neutron capture can also yield γ rays, which are able to provide some significant energy peaks for identifying hydrocarbon materials, e.g. N (5.53 MeV) and N (5.56 MeV) which have almost the same count as N (10.83 MeV) and higher than C (4.95 MeV). Although the incident neutron energies are randomly generated according to Maxwell-Boltzmann distribution in mode 0.025 eV, the prompt γ spectra can still be able to show

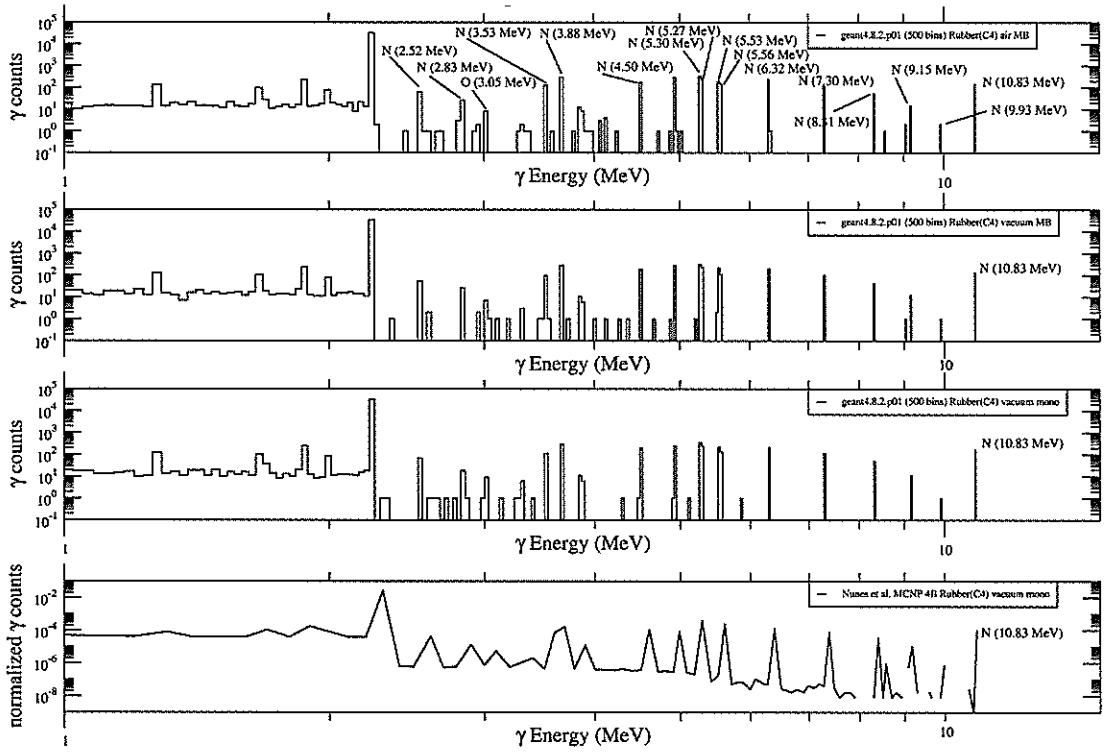

Figure 5. Prompt γ energy spectrum of C4 hidden by Rubber generated by GEANT4.8.2.p01 compared with MCNP.

the differences of γ energy spectrum for identifying some hydrocarbon materials. The attempt of making use of random incident neutron energy instead of mono energetic neutron energy has paved the way to imitate the physical condition in computational simulation. For the time being, we consider GEANT4 should be a good alternative and candidate for PGNAA simulation.

Acknowledements – This work was supported in part by the University of Malaya Fundamental Research Grant (FP010/2004A). The author would like to thank Hans-Peter Wellisch (hadronic process), Mark Donszelmann and Andreas Pfeiffer (data analysis), Vladimir Ivantchenko and Gabriele Cosmo (system installation), John Allison and Fan Lei (particle track visualization) for their suggestions and support.

REFERENCES

1. Shea P. M., Gozani T. and Bozorgmanesh M. (1990) *Nucl. Instrum. Methods Phys. Res. A*, **299:** 444.
2. Nagai T., Fujii I., Muto H. and Inouye T. (1969) *J. Nucl. Med.* **10:** 192.
3. Bethe H. A. (1935) *Phys. Rev.* **47:** 747.
4. Rasetti F., Segrè E., Fink G., Dunning J. R., and Pegram G. B. (1936) *Phys. Rev.* **49:** 104.
5. Bethe H. A. (1936) *Rev. Mod. Phys.* **9:** 69.
6. Soete D. De, Gijbels R. and Hoste J. (1972) *Neutron Activation Analysis*. Wiley-Interscience, England.
7. Agostinelli S. *et al* (2003) *Nucl. Instrum. Methods Phys. Res. A* **506:** 250.
8. Allison J. *et al* (2006) *IEEE Trans. Nucl. Sci.* **53:** 270.
9. Breismeister J.F. (1997) *MCNP: a General Monte Carlo N-Particle Transport Code*, Version 4B, LA-12625-M. Los Alamos National Lab., New Mexico.
10. Fasso' A., Ferrari A., Ranft J. and Sala P. R. (2005) *FLUKA: a Multi-Particle Transport Code*, CERN 2005-10, INFN/TC_05/11, SLAC-R-773.
11. Fasso' A., Ferrari A., Roesler S., Sala P. R., Battistoni G., Cerutti F., Gadioli E., Garzelli M. V., Ballarini F., Ottolenghi A., Empl A. and Ranft J, (2003) *The Physics Models of FLUKA: Status and Recent Developments*, Computing in High Energy and Nuclear Physics 2003 Conference (CHEP2003), La Jolla, California, USA (paper MOMT005) eConf C0303241 (2003), arXiv:hep-ph/0306267.
12. Nunes W. V., Silva A. X., Crispim V. R. and Schirru R. (2002) *Appl. Radiat. Isot.* **56:** 937.
13. Wellisch J. P. (2005) April 17-21 2005 *The Neutron_HP Neutron Transport Code*, Monte Carlo 2005 Topical Meeting ISBN: 0-89448-695-0, Chattanooga, Tennessee, USA.
14. [Online] Available: http://geant4-hn.slac.stanford.edu:5090/HyperNews/public/get/hadronprocess/672/1/3.html.
15. Garcia A. L. (2000) *Numerical Methods for Physics*, 2nd ed. Prentice Hall, New Jersey.
16. Sohrabpour M., Shahriari M., Zarifian V. and Moghadam K. K. (1999) *Appl. Radiat. Isot.* **50:** 805.
17. [Online] Available: http://aida.freehep.org/index.thtml.
18. Zhou ChunMei July 2000 *Thermal Neutron Capture Data for A=1-25*, IAEA, INDC(CPR)-051 [Online] Available: http://www-nds.iaea.org/reports-new/indc-reports/indc-cpr.
19. Vourvopoulos G and Womble P C 2001 *Pulsed Fast/Thermal Neutron Analysis: a Technique for Explosives Detection*, TALANTA **54:** 459.

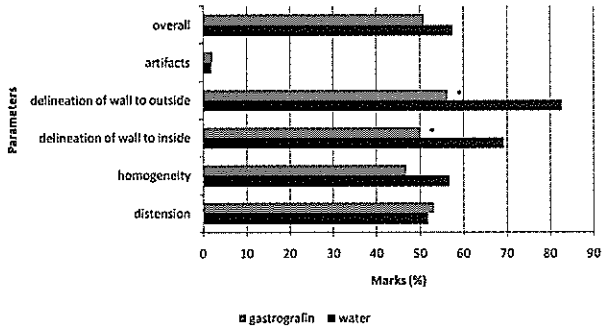

Figure 1. Qualitative evaluation of abdominopelvis CT images, water vs gastrografin

Table 1. Quantitative evaluation of gastrointestinal tract, gastrografin vs water.

Location	Oral contrast	Diameter (cm)	Attenuation of bowel wall (HU)	Attenuation of bowel lumen (HU)	Difference wall to lumen
Gastric	Gastrografin	9.81	128.67	100.24	-28.43
	Water	10.62	-7.46	52.56	60.02
		p>0.05	p<0.001	p<0.001	p<0.001
Duodenum	Gastrografin	1.87	114.63	88.72	-25.91
	Water	2.01	2.52	56.04	53.52
		p>0.05	p<0.001	p<0.001	p<0.001
Jejunum	Gastrografin	1.96	149.24	118.09	-31.15
	Water	1.99	13.86	50.33	36.47
		p>0.05	p<0.001	p<0.001	p<0.001
Iliem	Gastrografin	1.83	145.22	115.74	-29.48
	Water	1.88	12.69	46.62	33.92
		p>0.05	p<0.001	p<0.001	p<0.001

bowel were significantly better using water compared to gastrografin ($p < 0.05$) while the other criteria showed no significant difference using *t*-test and Mann-Whitney U-test .

DISCUSSION

The images demonstrated excellent distension of the gaster with water (Fig. 2) compared to gastrografin (Fig. 3). The quantitative measurements of the diameter of the stomach were supported by the qualitative evaluation by both radiologists which showed excellent agreement. The results were consistent with the study conducted by Matsuoka *et al.* [12] using water which showed better distension at gastric region and consequently better gastric wall visualization. Hence, it is possible to detect abnormalities that caused only slight irregularity on the inner surface of stomach even when the wall thickness was normal.

Small bowel distension would be best shown with calculation of the volume of the bowel but no

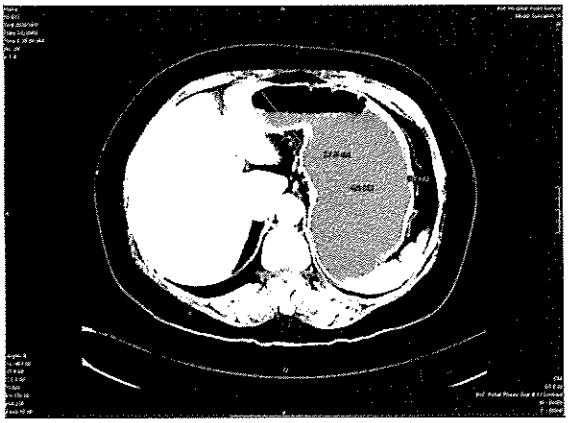

Figure 2. CT images of gaster with water as the oral contrast medium.

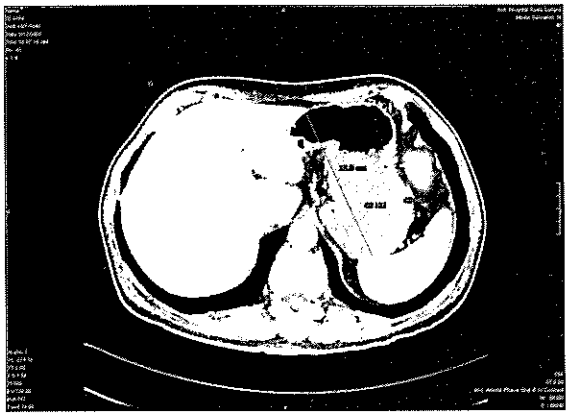

Figure 3. CT images of gaster with gastrografin as the contrast medium.

such technique is yet available [3]. Quantitative measurements of the bowel diameter at different segments were done considering the length of the small bowel, which may give an approximation of the overall distension. The duodenum showed better distension using water, and the diameter of the proximal jejunum and terminal ileum were almost similar in both groups. Bowel distension is important for clear visualization of bowel wall and to assess the exact bowel wall thickness, which may be an indication for gastric tumour [13, 14] or significant inflammatory process at the bowel wall [15]. Horton & Fishman [16] stated that under-distension can simulate wall thickening or mask an abnormality, in the context of attenuation pattern, degree of thickening and whether it is a symmetrical thickening as it enables detection of perienteric abnormalities [15, 17].

The technical advances in CT technology, with high resolution image acquisition, multiplanar

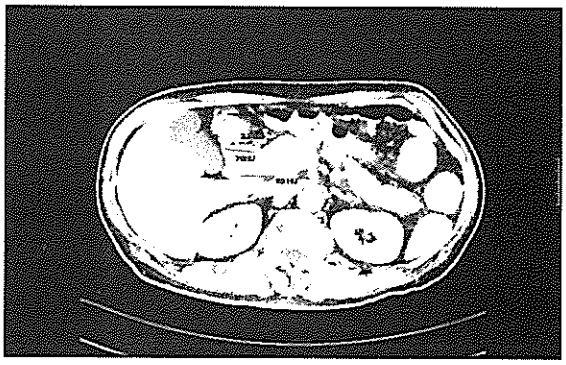

Figure 4. CT images of abdominopelvis with water as the contrast medium.

reconstruction and computer workstations for anatomical reconstruction have made it possible to interpret every structure in abdominal CT studies, including organs, vessels, bones and also bowel, in a single examination (Fig. 4). Besides, ability of CT that scans at a shorter time greatly eliminates artifacts caused by peristaltic and respiratory movement. The results were consistent with previous studies that stated that positive oral contrast caused more streak artifacts compared to water [11]. CT images can also be reconstructed to get detail visualization of bowel wall [18].

Subtle changes in the bowel wall and its surrounding fat can be masked with the use of positive oral contrast agent like gastrografin. The reasons for this are enhanced bowel wall may have the same attenuation as the positive contrast of the lumen and high densities often occur due to heterogeneous intraluminal distribution, leading to artifacts with reduced visualization of the bowel wall and surrounding fat [16]. This may be the reason for increasing interest in the use of low attenuation contrast for a wider range of indications. Water is the primary choice; advantages include low cost, wide availability, natural and safe for anyone without any complications [7].

Water showed significantly better contrast between bowel wall and lumen and for other criteria in qualitative analysis, including homogeneity in lumen, delineation of bowel wall and overall quality image, consistent with other previous studies. Combination of water that acts as negative oral contrast agent and intravenous contrast agent that acts as positive contrast agent give a better appreciation of mural detail. Mucosal folds can be visualized clearly and actual bowel wall thickness can be determined. However, the limitation of using water as an oral contrast agent is that the patient needs to consume a large quantity of water, especially for those in-patients who are very ill. Some of them even vomit after trying to take more water. Previous study reported that there were cases of water toxicity after consuming large amount of water by patients who had chronic renal failure and congestive heart failure [7]. Water is not a suitable oral contrast for these types of patients.

In summary, this study showed that water was comparable to gastrografin as an oral contrast medium. Qualitative evaluation showed significantly superior bowel distension and contrast between bowel wall and lumen. Besides, quantitative measurements showed better distension of gaster and bowel. Water is therefore a better choice as oral contrast medium since it is inexpensive and safe to consume.

REFERENCES

1. Foley W. D. and Kerimoglu U. (2004) Abdominal MDCT; liver, pancreas, and biliary tract. *Semin Ultrasound CT MR* **25:** 122-144.
2. Horton K. M., and Fishman E. K. (2003) the current status of multidetector row CT and three-dimensional imaging of the small bowel. *Radiol Clin North Am* **41:** 199-212.
3. Raptopoulos V., Davis M. A., Davidoff A., Karellas A., Hays D., D'Orsi C. J. and Smith E. H. (1987) Fat-density oral contrast agent for abdominal CT. *Radiology* **164:** 653-656.
4. Turetschek K., Schober E., Wunderbaldinger P., Bernhard C., Schima W., Puespoek, A., Vogelsang H., Moeschl P. and Mostbeck G. (2002) Findings at Helical CT-Enteroclysis in Symptomatic Patients With Crohn Disease: Correlation With Endoscopic and Surgical Findings. *Journal of Computer Assisted Tomography* **26:** 488-492.
5. Horton K. M., and Fishman E. K. (2004) Multidetector-row computed tomography and 3-dimensional computed tomography imaging of small bowel neoplasms: current concept in diagnosis.

Journal of Computer Assisted Tomography **28:** 106-116.

6. Horton K. M., and Fishman E. K. (2001) Multidetector row CT of mesenteric ischemia: can it be done? *Radiographics* **21:** 1463-1473.
7. Winter T. C., Ager J. D., Nghiem H. V., Hill R. S., Harrison S. D. and Freeny P. C. (1996) Upper gastrointestinal tract and abdomen: water as an orally administered contrast agent for helical CT. *Radiology* **201:** 365-370.
8. Hori S., Tsuda K., Murayama S., Matsushita M., Yukawa K. and Kozuka T. (1992) CT of gastric carcinoma: preliminary results with a new scanning technique. *Radiographics* **12:** 257-268.
9. Spilde J., Lee F. T., Chosy S. G., Krupinski E. A., Kuhlman J. E. and Yandow M. R. (1999) Evaluation of an experimental low-attenuation gastrointestinal contrast agent for CT imaging of intestinal ischemia in an animal model. *Acad Radiol* **6:** 94-101.
10. Thompson S. E., Raptopoulos V., Sheiman R. L., McNicholas M. M. J. and Prassopoulos P. (1999) Abdominal helical CT: Milk as low-attenuation oral contrast agent. *Radiology* **211:** 870-875.
11. Matsuoka Y., Masumoto T., Koga H., Suzuki K., Ushimi T., Terada H., Tamura A., Yokoyama Y., Abe K. and Kamata N. (2000) Positive and negative oral contrast agents for combined abdominal and pelvic helical CT: first iodinated agent and second water. *Radiation Medicine* **18:** 213-216.
12. Berther R., Patak M. A., Eckhardt B., Erturk S. M. and Zollikofer C. L. (2008) Comparison of neutral oral contrast versus positive oral contrast medium in abdominal multidetector CT. *Eur Radiol.* **18:** 1902-1909.
13. Balfe D. M., Koehler R. E., Karstaedt N., Stanley R. J. and Sagel S. S (1981) Computed tomography of gastric neoplasm. *Radiology* **140:** 431-436.
14. Komaki S. and Toyoshima S. (1983) CT's capability in detecting advance gastric cancer. *Gasrointest Radiol* **8:** 307-313.
15. Macari M. and Balthazar E. J (2001) CT of bowel wall thickening: Significance and pitfalls of interpretation. *AJR* **176:** 1105-1116.
16. Horton K. M., Fishman E. K. (1998) The current status of multidetector row CT and three-dimensional imaging of the small bowel. *Radiol Clin North Am* **41:**199–212.
17. Halvorsen R. A. (2006) MDCT: A practical research. MDCT of *abdominal trauma.* pp. 185-195. Springer, Milan.
18. Gossios K. J., Tsianos E. V., Demou L. L., Tatsis C. K., Papakostas V. P., Masalas C. N., Merkouropoulos M. C. and Kontogiannis D.S. (1991) Use of water or air as oral contrast media for computed tomographic study of the gastric wall: comparison of two techniques. *Gastrointest Radiol.* **16:** 293-297.